The FLARE Suit: Development of a Solar Space Radiation Shielding Vest

Master Thesis in Aerospace Engineering

Margot Winters - 5805481
Prof. Alessandra Meniccucci (TU Delft supervisor)
Dr. Aidan Cowley (ESA supervisor)

European Astronaut Center (ESA), Cologne
Spaceship EAC

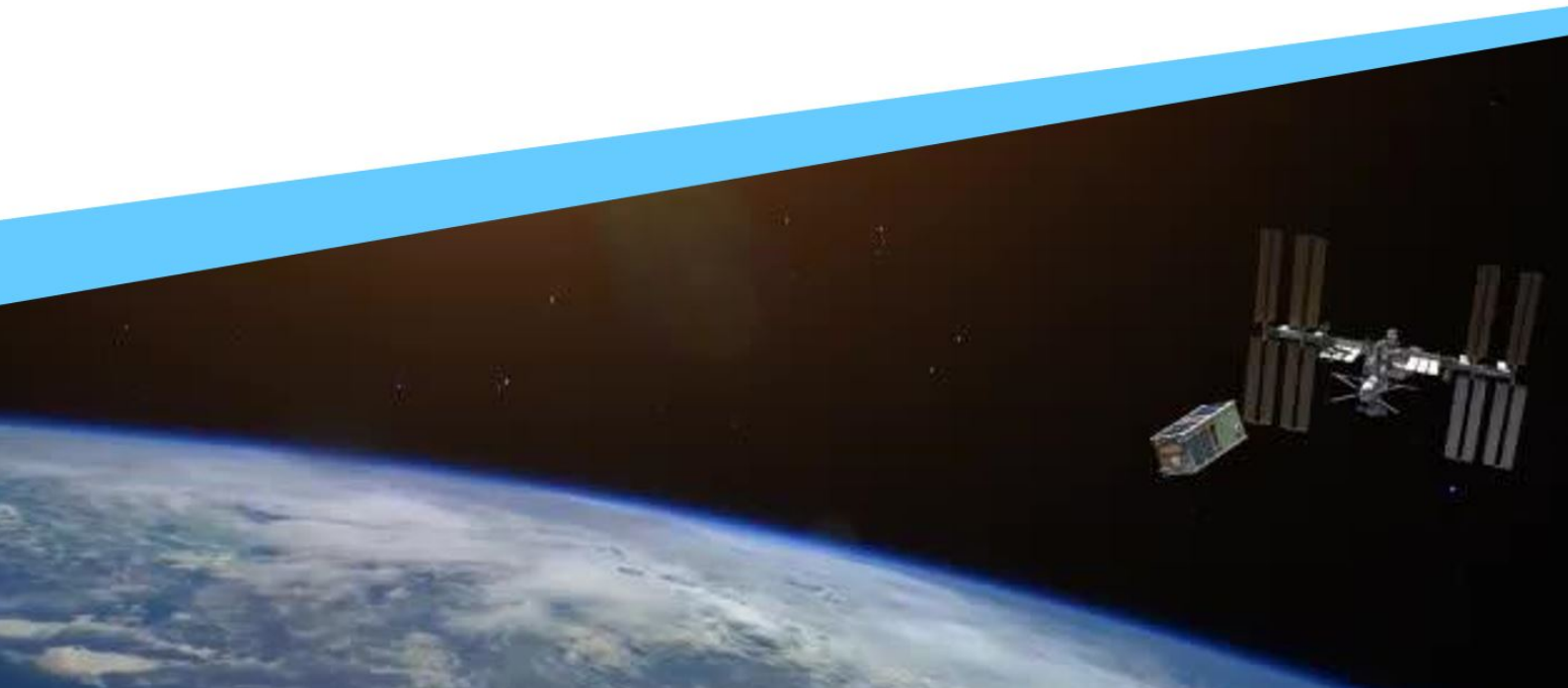

The FLARE Suit: Development of a Solar Space Radiation Shielding Vest

Margot Winters

Department of Space Engineering
Technical University of Delft

Thesis report based on the work carried out during a seven-month internship at the European Astronaut Centre in Cologne, from April to October 2024.

This thesis is submitted for the degree of
MSc in Aerospace Engineering.
to be defended publicly on 13 December 2024 at 14:00.

October 2024.

Acknowledgements

First of all, I would like to thank my thesis supervisor Prof. Alessandra Menicucci, who supported me with this thesis idea. Thank you for your belief in me on this project and making me challenge myself on a continuous basis. It has been a pleasure to work with you in every stage.

To my supervisor Dr. Aidan Cowley at the European Space Agency, I would like to express my appreciation for welcoming me within his research group at the European Astronaut Centre. The Spaceship EAC team has played an important role in the making of this thesis, and the amount of interesting and warm, supportive talks with everyone have been a true blessing. In particular, I would like to thank Sylvain Blunier for his help with the radiation shielding simulations and Noora Archer for working together on the garment design. It would not have been possible without them, and working together was a fun ride!

I am extremely grateful to Frank De Winne, who introduced me to the European Astronaut Centre before starting this master degree at TU Delft and sparked a dream which has now become reality. I remain grateful for his kindness throughout the thesis and his trust for me to present this work directly to King Philippe of Belgium and to ESA's Director General, Josef Aschbacher. I would like to thank Matthias Maurer, Samantha Cristoforetti, and John McFall for their time and input on this work. Furthermore, I'm thankful for the support of Marta Rovituso and Thomas Toet from HollandPTC in conducting proton accelerator experiments, and for the support of Roeland Van Malderen of the Royal Meteorological Institute in conducting a stratospheric balloon flight experiment in Belgium. It was wonderful to have shared this memorable progress with all of them.

Lastly, this would not have been possible without the support and love from my friends and family: thank you to my parents, my partner, and my brothers as well all other friends who supported me in any way.

Margot Winters
Cologne, October 2024

Abstract

In recent years, radiation shielding for astronauts has become an increasing priority among international space agencies, including the European Space Agency (ESA). As international efforts advance again towards exploration beyond the magnetosphere, the risks posed by Solar Particle Events (SPEs) to crew health resurface, with threats including acute radiation sickness, increased cancer risk, and damage to internal organs.

This thesis, developed at the European Astronaut Centre (EAC), presents the design of the FLARE suit, a personal radiation shielding system for astronauts in microgravity intravehicular environments. The suit uses 36 liters of on-board water and reduces the effective radiation dose by 36 $\pm$ 4.5%, with targeted protection for vital organs and a human-centered design. Simulation and accelerator testing demonstrated shielding effectiveness, while astronaut feedback refined its usability and comfort. In final review, FLARE offers a promising solution for radiation protection in future long-duration deep-space missions.

Keywords: Radiation Shielding, Solar Particle Event, Astronaut Protection Suit, Radiation Emergency Scenario, Human-Centered Space Design.

The European Astronaut Centre of ESA

The European Astronaut Centre (EAC), located near Cologne, Germany, is responsible for astronaut selection and training within the European Space Agency (ESA). Astronauts from around the world are trained here for operations on European payloads aboard the ISS, including ESA's Columbus laboratory. The EAC also hosts the space medicine office, a mission control centre, a neutral buoyancy facility for space walk exercises, and the newly established European Moon simulation facility, 'LUNA'.

This thesis is performed during a seven-month internship at the European Astronaut Centre. The research is performed within Spaceship EAC, a research team founded in 2012 and actively contributing to low-level technology development and concept demonstration for space exploration activities.

esa

SPACESHIP EAC

Table of Contents

List of Figures

List of Tables

Nomenclature

ALARA As Low As Reasonably Achievable

BFO Blood Forming Organs

CME Coronal Mass Ejection

COTS Commercial off-the-shelf

CT Computed Tomography

DLR Deutsches Zentrum für Luft- und Raumfahrt (German Space Agency)

EAC European Astronaut Centre

ESA European Space Agency

EVA Extra Vehicular Activity

FLUKA FLUktuierende KAskade (Fluctuating Cascade)

GCR Galactic Cosmic Ray

GRAS Geant4 Radiation Analysis for Space

HDPE High Density Polyethylene

HIDH Human Integration Design Handbook

HollandPTC Holland Proton Therapy Centre

ICRP International Commission for Radiation Protection

IoT Internet of Things

ISS International Space Station

IVA Intra Vehicular Activity

LEO Low Earth Orbit

LET Linear Energy Transfer

NASA National Aeronautics and Space Administration

NBP Neutral Body Posture

PERSEO PErsonal Radiation Shielding for intErplanetary missiOns

PLA PolyLactic Acid

RMI Royal Meteorological Institute of Belgium

SPE Solar Particle Event

TPU Thermoplastic PolyUrethane

TRL Technology Readiness Level

1 Introduction to the FLARE Project

1.1 Radiation Space Environment

Space is a hazardous environment. Nevertheless, throughout the last decades, technology has advanced to protect astronauts against extreme thermal conditions, vacuum environment, and micrometeoroid impacts. Protecting against the space radiation environment, at present, is much more complex [1]. On space missions beyond low Earth orbit, such as ongoing missions to Earth's moon, to Mars, or elsewhere in Deep Space, Earth's atmosphere and magnetosphere are not available to protect crew from sources of ionizing radiation. The radiation environment which astronauts and spacecraft are subsequently exposed to, can be very dynamic, harsh and unpredictable. Understanding the nature and impact of the contributing radiation sources is crucial for designing effective shielding and protective measures and to ensure the safety and success of future space missions to go beyond low Earth orbit.

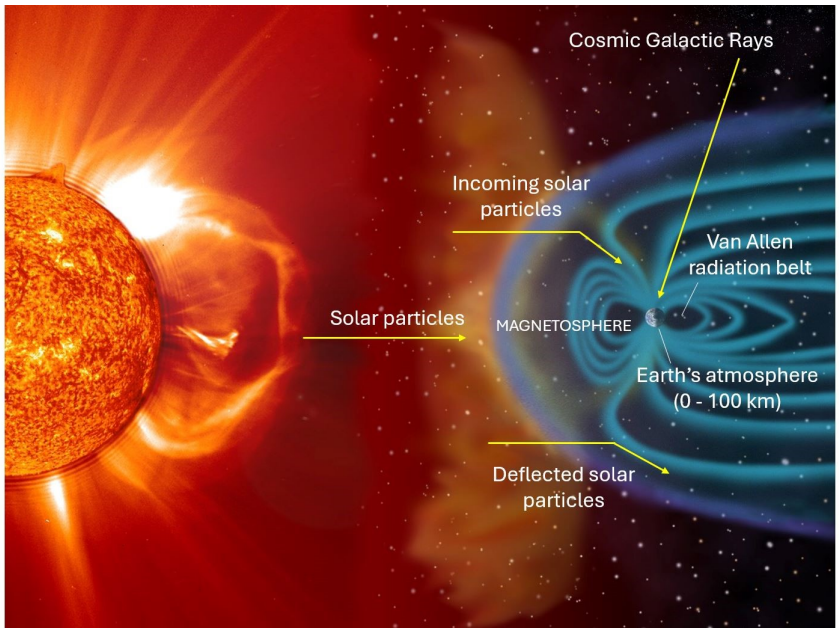

Figure 1: Illustration of the Sun-Earth system and the Earth's magnetosphere, with annotations added to indicate the components and the paths of Solar Particle Events and Galactic Cosmic Rays. Base image source: Steele Hill/NASA. Annotations by the author.

The radiation environment outside of Earth's magnetic field is characterized by incoming radiation from several sources, both inside and outside of the Solar System. Among these, the two primary sources of biological damage are called Galactic Cosmic Rays and Solar Particle Events [2]. Each poses its own unique dangers to space missions and together they form the complex and dynamic radiation environment, influenced by various factors such as the solar cycle and the interstellar medium. These primary sources are illustrated in Figure 1, which depicts their interaction with Earth's magnetosphere. The main characteristics of these two primary sources are the following:

1. **Galactic Cosmic Rays (GCRs)** constitute a continuous background of high-energy radiation. As its name suggests, these rays originate primarily from sources within our galaxy, including from supernovae remnants, active galactic nuclei, and other high-energy astrophysical processes. Exposure to the GCR radiation environment does not pose an immediate threat to an astronaut's life but raises the likelihood of developing cancer and may impact the central nervous system and cardiovascular system [3].

   The flux of Galactic Cosmic Rays is characterized by an incoming radiation spectrum of high-energy protons (about 85%), alpha particles (about 14%), and heavier atomic nuclei (about 1%), all fully ionized, and with energies ranging from a few mega-electronvolt (MeV) to several tera-electronvolt (TeV) with a peak at a few 100 MeV [4]. While highly energetic and extremely penetrating, the radiation flux is relatively low with typical values of only some particles $\mathrm{cm}^{-2}\mathrm{s}^{-1}$, due to the rarity of the aforementioned astrophysical events.

   While Galactic Cosmic Rays maintain a generally steady presence, their flux is modulated by the solar cycle. During periods of solar minimum, the reduced solar wind allows more Galactic Cosmic Rays to penetrate the solar system, leading to increased flux. Consequently, astronauts and spacecraft are subjected to increased levels of cosmic radiation. Conversely, during solar maximum, heightened solar activity and stronger solar winds deflect more Galactic Cosmic Rays, resulting in a decrease in their intensity [5].

2. **Solar Particle Events (SPEs)** are sporadic bursts of high-energy radiation, in contrast to the continuous influx of Galactic Cosmic Rays. These rays originate from either solar flares, where explosive energy releases on the Sun's surface accelerate charged particles to high energies, or from coronal mass ejections, where shock waves increase the particles' energy.

   SPEs are characterized by an intermittent flux, consisting of an incoming spectrum of high-energy protons (about 95%), electrons (about 2.5%), and heavier ions (about 2.5%), hence all charged particles. Their energies are lower compared to Galactic Cosmic Rays, typically from a MeV to several hundred MeV. While only a few SPEs occur each year, the radiation flux is characterized by a relatively high particle density, up to a few 100 000 particles $\mathrm{cm}^{-2}\mathrm{s}^{-1}$ with energies above 30 MeV, due to the proximity of the Sun compared to other galactic high-energy sources of Galactic Cosmic Rays [6].

   SPEs are mostly dominant during Solar maximum of the 11-year cycle of the Sun. With increased solar activity during this period, more sunspot activity and more frequent solar flares and coronal mass ejections are observed. As a result, astronauts and spacecraft are subjected to increased levels of solar radiation. In contrast to Galactic Cosmic Rays, the concentrated high-energy releases of SPEs can in extreme cases produce a lethal dose and pose acute radiation effects to the crew [3].

   Solar flare radiation is also often linked to telecommunication issues, as it can disrupt elec-

tronics and communication systems [7], and to other spacecraft areas, as is visualized in Figure 2. For example, historical SPEs include the infamous Carrington Event of 1859, the most powerful Solar Particle Event ever recorded, which produced auroras visible as far as tropical latitudes like Cuba and Hawaii, while setting telegraph systems on fire. In August 1972, an SPE narrowly missed the Apollo 16 mission; had it struck, it would have posed serious risks to the astronauts. Similarly, the October 1989 SPE hit Earth's magnetic field directly, causing blackouts across Montreal and Quebec, widespread power grid disruptions, satellite malfunctions, and radio communication blackouts.

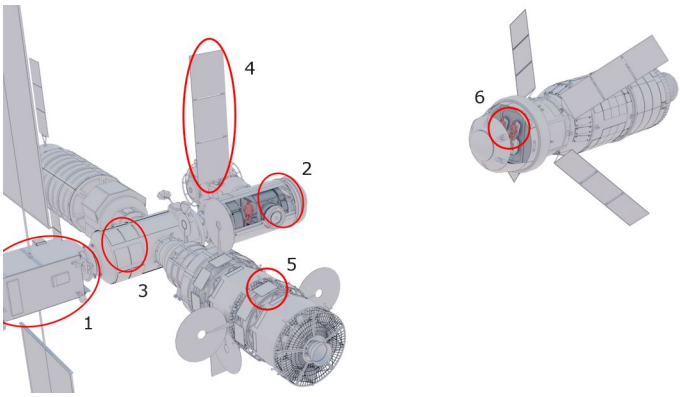

Figure 2: Areas of risk in the Lunar Gateway (left) and Orion module (right) during the strike of a Solar Particle Event. This includes sensitive electronics from the (1) propulsion module, (2) life support, and (3) communication and control systems, as well as a degradation of (4) solar arrays, (5) coatings, and (6) crew health. Due to these spacecraft components at risk, astronauts should be enabled to remain active and alert, while protected against the high-energy radiation. †

The exposure to Galactic Cosmic Rays and Solar Particle Events can cause severe limitations to the success of missions beyond Low Earth Orbit (LEO). Therefore, understanding these radiation sources is important for designing effective shielding. On one hand, Galactic Cosmic Rays originating from within our galaxy pose long-term risks, increasing the likelihood of cancer and affecting the nervous and cardiovascular systems. On the other hand, SPEs such as solar flares and coronal mass ejections have higher intensity during the solar maximum and can pose immediate dangers, potentially causing lethal doses. In the next Section 1.2, the biological effects of exposure to Galactic Cosmic Rays and Solar Particle Events will be examined more in detail in order to understand the dangers posed by each type of space radiation exposure.

1.2 Biological Effects of Space Radiation Exposure

Effects of exposure to radiation from Solar Particle Events or long-term Galactic Cosmic Ray flux could place the crew of a space mission at risk of acute **radiation sickness**, **damage to internal organs**, and increased **risk of cancer**. Esteemed experts in the field, such as Reitz et al. [8] and Durante et al. [9], have emphasized that these risks present one of the most significant challenges in space exploration, impacting not only the health and safety of the crew but also the overall success of the mission. As current radiation protection limits for Low Earth Orbit are exceeded during travel beyond Earth's magnetic field, future interplanetary missions face safety concerns and the potential for dramatically increased costs [8] [9]. Thus, understanding and mitigating the biological effects of space radiation exposure is crucial for protecting astronaut health and ensuring the success of long-duration space missions [10].

The health risks to astronauts can be categorized into short-term and long-term effects. Short-term effects are predictable and can jeopardize mission success whenever a crew member is unable to perform their duties. In such scenarios, one or more mission objectives may be compromised, and in extreme cases, the entire mission could be lost. Short-term risks pose *deterministic* effects, which means they occur when radiation exposure exceeds a specific threshold, leading to outcomes such as headaches, dizziness, nausea, fatigue, and illnesses ranging from mild to fatal. Long-term risks, which may extend beyond the mission's completion, are equally concerning. Whereas short-term effects were deterministic, long-term risks pose *stochastic* effects, which means their probability increases with exposure, but the severity of the effect does not depend on the dose. Such effects of space radiation include long-term risks such as cancer, which as probability to develop following radiation exposure [11]. Other long-term effects include cataracts [12], skin damage, heart and central nervous system damage [13], and impaired immune function. Although these effects are not immediate, they can heavily impact long-duration missions and an astronaut's health in later life [1].

Solar Particle Events are primarily linked to deterministic, short-term effects of space radiation. In particular, hazards to astronauts arise when the physical dose of incoming radiation exceeds 0.5 Gy [14]. This dose corresponds to roughly 208 years of natural background radiation a person receives on Earth (0.0024 Gr/yr), and is typically associated with the dose used in a cancer treatment session. However, while radiation therapy targets tumor cells with high precision, space radiation affects all cells throughout the body. This leads to symptoms of hematopoietic syndrome due to the destruction of hematopoietic cells in the bone marrow. The physiological consequences include nausea, vomiting, fatigue and hair loss, and death can occur within two months after exposure of space radiation. If the individual survives the acute physiological symptoms caused by radiation exposure, there is a possibility for the bone marrow to regenerate spontaneously. However, at doses higher than 8 Gy (a dose higher than any medical radiation treatment or imaging), the destruction of the hematopoietic system is complete, and death is inevitable within 60 days after exposure [14]. For immediate death, the threshold is 20 Gy, which is when breakdown of the central nervous system occurs.

As illustrated in Figure 3, Solar Particle Events between 1968 and 1969 reveal the remarkable luck of the Apollo missions, which, despite occurring during a relatively active solar period, always had the luck to avoid large Solar Particle Events. As can be seen, a major solar storm took place in August 1972, occurring between the Apollo 16 and 17 missions. Parsons and Townsend calculated an absorbed dose rate of 1.4 Gy/h during this storm [15], a number which can be compared to the previously mentioned thresholds. If a mission with astronauts had happened in August 1972, an astronaut exposed to this event would develop radiation sickness (0.5 Gy) within half an hour and, probably, neurovascular death (20 Gy) within 14 hours of exposure. Other biological risk limits are also shown as defined in the Human Integration Design Handbook, to contextualize the risks that astronauts would have faced during these historical missions.

Galactic Cosmic Rays, in contrast to Solar Particle Events, are primarily associated with the stochastic and long-term effects of space radiation. This is in contrast to the deterministic and short-term effects of Solar Particle Events, discussed above. The reason is that proton exposure from Solar Particle Events can reach dose rates as high as 1.4 Gy/hour, whereas galactic cosmic ray exposure occurs at much lower dose rates (1.3 mGy/day), though continous in time [16]. Therefore, the immediate health risks from Galactic Cosmic Rays are lower, but their chronic exposure over extended periods can significantly increase the statistical probability of stochastic effects such as cancer and other long-term health issues.

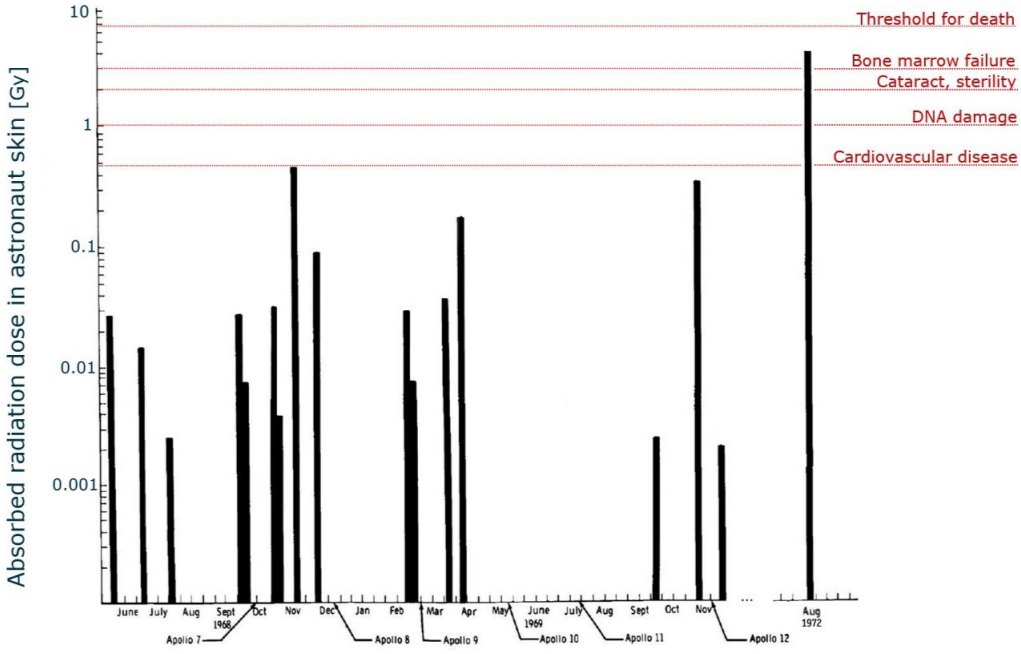

Figure 3: Estimates of radiation doses for particle events occurring from June 1968 to December 1969. Source: Adapted from the NASA Apollo Experience Report ([17]) to show biological risks according to the limits of the NASA Human Integration Design Handbook (HIDH).

1.3 Strategies for Mitigating Space Radiation Effects

Given the harsh nature of the space radiation environment and its ability to cause both short-term and long-term health effects on astronauts, it is necessary to develop strategies designed to minimize these risks for humans in space. Such strategies must address Galactic Cosmic Rays and Solar Particle Events distinctly, as both are different to such extent that they require different mitigation approaches. While heavy shielding might be most effective against the high-energy particles of Galactic Cosmic Rays, operational strategies such as avoiding missions during solar storms are most effective to avoid Solar Particle Events. Therefore, a multi-faceted approach is essential.

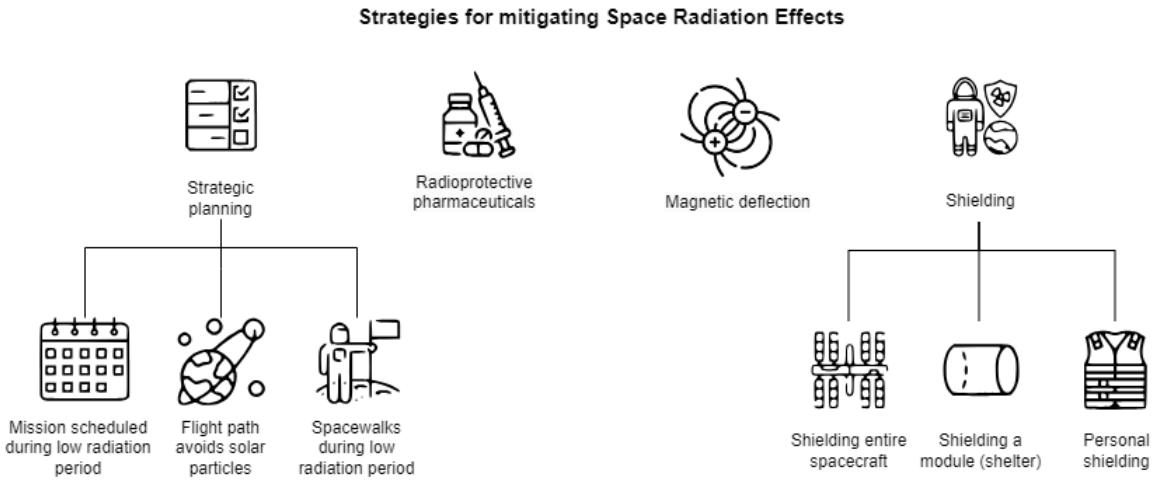

Figure 4: Overview of strategies for space radiation effect mitigation.

The most effective measures for minimizing doses are implemented before any exposure, through strategic planning of the mission, innovative biomedical countermeasures, and advanced shielding technologies (Figure 4).

Strategic mission planning involves accounting for fluctuations in radiation intensity to select optimal flight paths, mission timings, and activity schedules. Space weather plays a critical role in this process, as variations in solar activity can significantly elevate radiation levels in space. For instance, during periods of high solar activity, which are often indicated by space weather forecasts, mission planners may schedule spacewalks or other critical operations during lower radiation periods. Additionally, spacecraft trajectories can be adjusted to travel through regions of reduced radiation intensity. Real-time space weather monitoring and measurements from spacecraft instrumentation provide continuous updates, and can ensure optimal safety during solar storms [18].

Innovative **biomedical countermeasures** offer another strategy to mitigate the risks of space radiation. Researchers are developing drugs designed to mimic or enhance the body's natural

ability to repair radiation-induced damage. For instance, antioxidants like vitamin E can neutralize free radicals produced by ionizing radiation, preventing further cellular damage. However, while some progress has been made in developing drugs to counter the effects of terrestrial ionizing radiation, such as gamma radiation, advancements in countering the high-energy and massive charged particles encountered during space travel have been limited. Furthermore, if an effective drug would be developed, it would likely need to be taken several hours before exposure. This indicates another disadvantage, since Solar Particle Events cannot currently be predicted this far in advance [19].

Magnetic deflection is a third strategy for mitigating radiation exposure in space. Creating an artificial magnetosphere around a spacecraft could deflect charged particles away, much like the Earth's magnetosphere largely protects the Earth. However, generating a magnetic field of the required strength, approximately 10-20 tesla, also poses some significant challenges. In particular, the necessary equipment to obtain this field strength would add several tons to the spacecraft's mass due to the magnet size and field strength required [20]. Additionally, such intense fields are known to cause headaches and migraines in patients undergoing magnetic resonance imaging (MRI), with possible harmful long-term effects [21].

Lastly, **shielding technologies** provide a robust barrier between astronauts and space radiation. The most straightforward approach to reducing the penetration of ionizing radiation is by adding additional layers of shielding material to the spacecraft. However, shielding the entire habitable area of a spacecraft is not currently feasible due to the significant mass requirements. For instance, adding just 1 gram of extra material to every cm^2 of the Columbus module onboard the International Space Station (ISS), would require an extra weight of around 1.04 ton launched to LEO, and estimated additional costs of 52 million dollar [20]. Therefore, shielding an entire crew module would significantly increase launch costs and time. Additionally, this added mass, without a corresponding increase in spacecraft propulsion power, could prolong travel time to deep-space destinations, thereby increasing overall radiation exposure.

In line with the ALARA (As Low As Reasonably Achievable) principle, which recommends minimizing radiation exposure to the lowest possible levels without compromising the mission's practical feasibility, an alternative solution involves distributing shielding material within the habitat to create a small, protected area (shelter) [3]. However, the primary disadvantage of this method is that it confines astronauts to the shelter during radiation events, limiting their ability to perform other tasks.

It is relevant to note also that insufficient shielding can sometimes be worse than no shielding at all [22]. This is due to the interaction of primary and secondary radiation. Primary radiation consists of high-energy particles, such as protons and heavy ions, which are directly emitted from cosmic or solar sources. When these particles collide with shielding material, they can produce secondary radiation, including neutrons and gamma rays. If the shielding is too thin, it may stop some primary particles but fail to absorb the resulting secondary radiation, potentially increasing the overall radiation dose experienced by astronauts. Therefore, it is important to carefully optimize shielding thickness and material for space applications [2].

To address the limitations of shelter-based shielding, it is necessary to develop personal shielding options, such as wearable garments, to provide complementary protection alongside the shelters. Personal shielding is directly worn on the body of an astronaut and enables a reduction in the mass of shielding that is required to provide equivalent protection in other ways, such as shielding of an entire cabin or spacecraft. In addition, they provide mobility to the astronauts to perform critical tasks arising outside of the shelter during radiation events [3]. Therefore, integrating personal shielding and an onboard shelter, missions can achieve a better balance between mobility, protection, and resource efficiency.

1.4 State-of-the-Art Personal Shielding Systems

Over the past decade, two state-of-the-art vest technologies have been developed and tested to provide personal shielding for astronauts. These are the Astrorad suit, developed by the Israeli company StemRad with funding of the Israelian Space Agency, and the PERSEO suit, created by the Italian Space Agency. Prototypes of both suits were tested on board the International Space Station in 2022 and 2017, respectively.

The following provides an overview of the design and performance of each of the two existing state-of-the-art personal shielding systems:

1. The **AstroRad** vest is a solid radiation shielding vest made from Boron and high-density polyethylene, weighing 26 kg. It has low flexibility but is easy to deploy and claims to reduce the effective radiation dose approximately by half inside a spacecraft.
   The radiation shielding of Astrorad is anticipated to be limited by the thermal conductivity of the chosen materials, with an average thickness of the vest calculated to fit just within the comfortable thermal limit of clothing. The thicknesses of the vest over the torso is adapted to focus on shielding most sensitive organs, as can be seen by the line topography in Figure 5. Recent improvements have increased the vest's flexibility by incorporating layers in the vest that can slide with little friction. In addition, a pangolin scale-like structure is being studied to further enhance flexibility, as pictured in Figure 5 [23].

   The main drawbacks of AstroRad are its weight, the use of materials that cannot be re-used or created onboard through in-space manufacturing processes, limited thermal comfort, rigidity, and large required storage volume. Furthermore, StemRad's design process and R&D are costly, particularly with the development of the pangolin scales design, and the radiation shielding effectiveness is limited by a maximal vest thickness due to thermal comfort constraints.

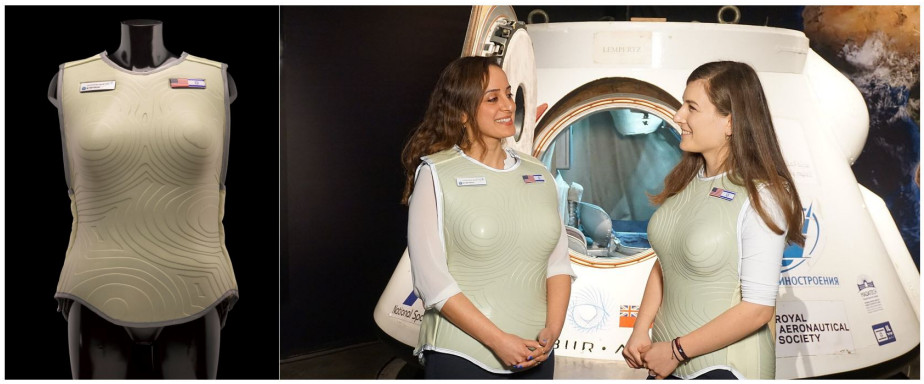

Figure 5: Left: The first prototype of the AstroRad vest, including a topographical design which shields better the tissues with higher sensitivity. Source: Lockheed Martin/Stemrad. Right: The second prototype of the Astrorad vest is expected to include materials inspired by pangolin scales. Source: Stemrad.

2. The **PERSEO** vest is a radiation shielding vest relying on four water bladders across the torso for shielding, and weighing 38 kg. The vest is slow to deploy but is flexible and reduces the effective radiation dose by half just like Astrorad.
   The radiation shielding of PERSEO is limited by the current bladder design which includes four large water bags and shields the human torso only partly, as can be seen in Figure 6. To operate the vest, the bladders need to be filled with water onboard the spaceship. Given the suit's volume and the water supply rate on the ISS, each suit would require twenty minutes to fill [24]. For a typical Orion module crew of four, this would exceed the maximum allowed deployment time. Also, the water content in its current design limits thermal comfort to be only marginally better than the AstroRad design [7].
   The main disadvantages of PERSEO's water-based design include its low thermal comfort, unoptimized radiation shielding design, and high filling time. However, the suit requires little storage space, has little weight at launch (3kg), utilizes onboard resources, and is relatively flexible.

Figure 6: The PERSEO suit for its first ISS test, aimed to assess the suit's operation time for filling and emptying, and the overall astronaut comfort. Source: [24].

1.5 Innovation Proposed by the FLARE Project

Given the harsh nature of the space radiation environment beyond Earth's magnetosphere and its ability to cause both short-term and long-term health effects on astronauts, it is important to develop the combination of radiation shelters and personal shielding systems to provide complementary protection for astronauts during solar particle emergency situations. This dual approach is key to provide operational protection when emergency tasks during a Solar Particle Event require astronauts to carry out tasks outside of the provided shelter. While the majority of research in literature has focused on advancing shielding properties of spacecraft, the development of personal shielding systems has been much less studied.

The general idea of the FLARE project is to give a preliminary conceptual design of a radiation shielding vest which can be worn by astronauts beyond the protective magnetospheric layer of low Earth orbit and in microgravity. The FLARE project therefore situates within the advancement of personal shielding systems, with the goal of reducing radiation-induced risks such as cancer and preventing Acute Radiation Syndrome caused by Solar Particle Events. Similar to competing vest concepts, the FLARE suit does not provide complete protection against the long-term effects of Galactic Cosmic Rays, only from high-intensity Solar Particle Events. However, Galactic Cosmic Rays interacting with spacecraft materials generate secondary radiation, which adds to the overall exposure. This lower-energy secondary radiation can be shielded by the FLARE vest which improves overall radiation protection.

The aim of the FLARE project is to design, develop, and test a personal shielding vest with properties superior to existing state-of-the-art concepts of PERSEO and Astrorad. In order to achieve this, the new radiation vest design had to meet the radiation shielding capabilities of these competing concepts while having better operational performance or to improve the shielding characteristics while having similar operational performance. Given the drawbacks reported for Astrorad and PERSEO situate mostly in their operational performance (flexibility, thermal comfort, ergonomics),

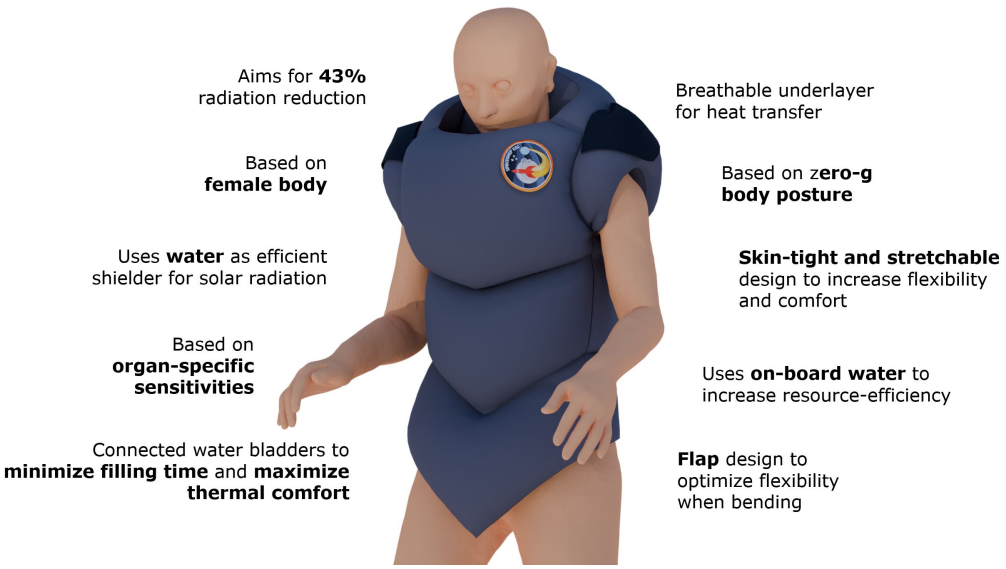

this project provides a design which meets the same state-of-the-art radiation shielding capabilities while innovating mobility, deployment time, comfort, and overall operational efficiency.

Filling an entire space suit with shielding material is not practical as it would limit the mobility of the astronaut and cause unacceptable job performance limitations. Therefore, shielding must be applied selectively, prioritizing the most radiation-sensitive areas. The FLARE suit offers targeted protection for organs and tissues that are most sensitive to radiation. This approach maximizes the biological impact of shielding while minimizing the overall mass. To achieve this, tissue weighting factors are assigned to various organs and tissues based on 3D Geant4 simulations. These factors represent the differences in radiation sensitivity, with organs such as the lungs, bone marrow, colon, stomach, breasts and ovaries known to be particularly vulnerable. Selective protection of these organs was achieved by creating a suit with adjustable shielding thickness to complement different body parts. As a result, this approach provides a suit with an intriguing, technically innovative topographic structure.

Aside its optimized topographic design, the FLARE suit is characterized by its default female model and the use of flexibly attached water shielding as the basis of its construction.
The FLARE suit design starts from a female model as women are generally more susceptible to radiation-induced cancers, such as breast, lung, thyroid, and ovarian cancers, and therefore have stricter limits on time spent in space. For example, during solar maximum, a 45-year-old man has a 344-day limit on the ISS versus a 187-day limit for a woman. Designing a suit for the female physiology ensures optimal protection for the most at-risk group, and provides a standard from which the male version suit will be developed during future iterations of the project [25].
Additionally, water is used as principal shielding material of FLARE as it is a known effective shielder against high-energy protons and as it allows for the use of on-board water supply, limiting launch mass and storage volume in compact new generation spacecraft. Additionally, water circulation and its inherent mobility due to being a liquid will serve the aims of advancing (thermal) comfort and flexibility in the FLARE suit [3].

In summary, the FLARE suit is able to combine radiation protection, flexibility, comfort, and mission support for astronauts beyond Earth's magnetosphere, with key features listed below:

1. Deployable alone or in combination with on-board storm shelter;
2. Targeted radiation protection for sensitive organs;
3. Enhanced thermal comfort and ergonomics in microgravity;
4. Full mobility using water shielding;
5. Based on the female body as default model;
6. Lightweight and highly foldable construction for efficient storage.

2 Definition of the Design Concept

2.1 Need & Mission Statement

In the first chapter, the FLARE project was introduced by identifying the problem to be addressed and the need to be fulfilled by the system. From this context, the need and mission statements for the FLARE vest were formulated.

Whereas the need and mission statement in systems engineering are typically concise, here more detailed statements are intentionally used. Since this thesis is conducted within the Spaceship EAC team, this clarity ensures that any future students following up on the project will have an unambiguous understanding of its fundamental objectives and that the project is easily transferable.

The need statement, which identifies the problem to be addressed and serves as the basis for the system's functional requirements, is formulated as follows.

Need Statement:

Future deep-space missions will expose astronauts to elevated radiation levels beyond the protective magnetosphere of Low Earth Orbit. To address the increased risks to crew health, a radiation shielding solution is needed that offers individual protection to astronauts, complementing the spacecraft's existing shielding. This solution must be lightweight, flexible, thermally comfortable, and capable of rapid deployment in emergency situations.

The mission statement, which describes how the system's need will be addressed through the capabilities of the FLARE vest, is formulated as follows.

Mission Statement:

The FLARE vest will provide astronauts with effective intravehicular personal radiation protection by reducing the received effective dose from Solar Particle Events during deep-space missions. To this aim, the system will deliver targeted protection to vital organs and ensure continued operational performance of the astronaut in the suit.

2.2 Identified Research Questions

From the mission statement, five research questions were derived for the FLARE project. The first four research questions each focus on a systems engineering need on the FLARE design: radiation protection, flexibility, thermal comfort, and deployment time. A fifth question addresses the need for improved human-centered design features, derived from analysis of the challenges from the two current state-of-the-art radiation protection vests Astrorad and PERSEO (Section 1.4).

1. **Radiation protection:** How effective is the FLARE design in reducing radiation exposure compared to alternative designs?

2. **Flexibility:** What are the most effective methods for integrating flexibility into astronaut suits to enhance mobility?

3. **Thermal comfort:** How can thermal regulation systems in personal protective equipment be optimized to maintain astronaut thermal comfort during extended use?

4. **Deployment time:** How can the FLARE vest improve deployment time and ease of use compared to the PERSEO vest?

5. **Human-centered design:** How can a human-centered focus within the FLARE design improve astronaut operational performance and comfort?

2.3 Use-Case Scenario: a Solar Proton Event Emergency

This section outlines the general use-case of the FLARE vest during a Solar Particle Event. It describes how the FLARE vest is designed to function during SPE emergencies to mitigate radiation exposure. Insights into this scenario were obtained through discussion with Alex Karl, EUROCOM & Crew Support Engineer for Space Applications Services at the European Astronaut Centre.

Use-Case Scenario:

Four astronauts are on board of the Lunar Gateway orbiting the Moon, when **a Solar Particle Event is detected by Earth-based satellites**. The event, caused by a coronal mass ejection (CME) or solar flare, is quickly identified by ground control as an SPE. The charged particles are moving toward Earth at high speed and are expected to reach the Lunar Gateway in about two to five hours.

Upon receiving the warning, **ground control provides astronauts with an early indication of the event's intensity and expected duration**. Based on this information, the astronauts plan their stay in the Orion shelter and manage their food, water, and ventilation needs accordingly. Supplies are either pre-positioned in the Orion shelter or added during this preparation period.

The ground station instructs one astronaut to prepare the FLARE vests, while the other three astronauts reorganize supplies inside the Orion module to establish a radiation shielding shelter. The astronauts **take shelter in the Orion module**, **don their FLARE vests**, and **align their orientation** relative to a quasi-unidirectional incoming radiation to maximize shielding effectiveness. They remain inside the shelter until an all-clear signal is given by ground control.

In **a worst-case scenario**, a critical emergency arises inside the the Lunar Gateway that requires immediate attention, such as a fire or a leak. In this case, an astronaut may be required to exit the shelter. In the case of a fire or ammonia leak, astronauts are to be equipped with protective breathing equipment, including most importantly an oxygen mask. The FLARE vest is designed to not restrict the astronauts' ability to put on this mask or perform tasks any other tasks for fire suppression, which can be done while wearing the suit.
In case of a severe leak, astronauts are to follow the usual protocol to identify the affected module, which involves iteratively closing hatches, identifying from which side the leak comes, and in the end performing necessary actions like tilting racks and removing equipment to find the hole. Tasks require a large range of motion in the case of a leak, including arm and torso movements. The FLARE vest is designed to not restrict necessary mobility to perform these tasks.

Astronauts are expected to remain in the shelter until radiation levels drop to acceptable limits, which typically occurs within a couple of hours, depending on the intensity of the solar storm. In the meanwhile, ground control continuously monitors radiation levels through the personal dosimeters integrated onto the FLARE vests. The acceptable limits for radiation exposure are determined by NASA and ESA guidelines.

In crewed spacecraft such as at the ISS, two major emergency scenarios exist which typically require immediate attention: on-board fires and atmospheric leaks. While other emergency cases can occur, these two are the two cases which may require immediate intervention, even during a Solar Particle Event. In contrast, other issues such as life support system failures are often mitigated by built-in redundancies, allowing the system to be repaired after the SPE has ended. The scenarios of a fire and atmospheric leak emergency are discussed in detail in the following subsections.

2.3.1 Double Failure Scenario: Fire Emergency

In the case of fire, astronauts need to be able to put on protective breathing equipment, which consists of a mask connected to an O2 bottle for clean air. Samantha Christoforetti, middle person in the right image of Figure 7, is wearing an oxygen mask with a 7-minute supply of oxygen. During an emergency, this mask is worn for the first response. Afterwards, the mask is exchanged for the mask worn by Butch Wilmore and Kjell Lindgren in Figure 7. In case of fire, red cartridges are used as displayed by Butch Wilmore in the right image. In case of an ammonia leak, as will be discussed

Figure 7: Left: NASA astronaut Kjell Lindgren wears protective breathing equipment, which would be used in the unlikely case of a fire or leak within the International Space Station. Right: From left to right Butch Wilmore, Samantha Cristoforetti, and Terry Virts. Display of available protective breathing equipment in the ISS. Source: ESA/NASA.

in the next section, pink cartridges are used as displayed by Kjell Lindgren in the left image. The act of **donning the mask** should not be limited by the vest design.

All three aids during a fire emergency (mask, bottle, extinguisher) are available in almost every module on board the ISS and can normally be easily retrieved. This retrieval poses no constraint on the FLARE design. The movements necessary for **extinguishing the fire** should, however, not be restricted by the FLARE suit.

2.3.2 Double Failure Scenario: Leak Emergency

During a leak, the emergency procedure for a loss of atmosphere is more complicated than that for a fire. Depending on the severity, protective breathing equipment may be required. The first step is to determine where the leak is coming from. To this aim, the hatch in between the American and the Russian part of the ISS is closed for a few minutes. It is expected that the part which contains the leak, will depressurize slightly in this time frame. This depressurization is recorded through sensors which inform the crew about which of the two parts contains the leak. This operation of opening and closing hatches continues iteratively until the module/node with leak is identified. The necessary movements for **hatch opening** are shown in Figure 8. Astronaut Don Pettit can be seen to perform arm movements with wide range of motion, as well as torso rotations.

After having identified the module containing the leak, it is possible that racks need to be temporarily removed in order to find and close the leak. Therefore, racks may need to be tilted. The images in Figure 9 show the **rack tilting** process. They give an indication of the body movement required during tilting, including hip and arm movement. Removing a fridge-sized rack, such as the storage rack and European Drawer Rack as shown in Figure 9, requires from the FLARE vest either the ability to maneuver carefully in a limited space or the ability to be doffed quickly during this temporary process.

Figure 8: NASA astronaut Don Pettit opens the hatch from the ISS to SpaceX's Dragon cargo craft. Source: NASA.

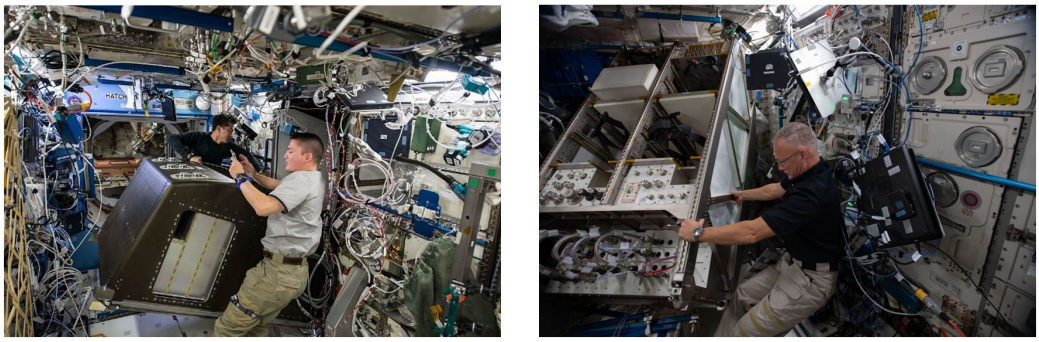

Figure 9: Left: Japanese astronaut Kimiya Yui (left) and NASA astronaut Kjell Lindgren (right) are seen removing items from a storage rack inside the Destiny laboratory of the International Space Station. Right: NASA astronaut Doug Hurley manoeuvres the European Drawer Rack Mark 2 to its new position. Source: ESA/NASA.

2.4 Stakeholders of the FLARE Suit

A list of system stakeholders is shown in Table 1. These stakeholders have been classified into active and passive categories, depending on the nature of their involvement in the FLARE project. In a further development, ESA would be the primary customer for the FLARE suit. This list is developed on the rationale that ESA defines the mission objectives, provides funding, and ensures that the FLARE suit meets the required specifications to be included on a deep-space mission.

Table 1: Active and Passive Stakeholders of the FLARE Suit.

Active Stakeholders	**Rationale/Motivation**
Astronauts	Primary users of the FLARE suit. Responsible for wearing and operating. Directly impacted by the vest's performance, comfort, and effectiveness in radiation protection.
ESA	Oversees the mission, sets requirements, and funds the project. Ensures the vest meets mission objectives and safety standards for deep-space exploration. Ensures that the project has the necessary budget for development, testing, and production.
Spacecraft Engineers	Design the spacecraft systems with which the FLARE suit will be used. Ensures that the FLARE suit integrates well with on board systems and meets mission requirements.
Medical Experts	Assess health risks and benefits of the FLARE suit for astronauts. Evaluate the effectiveness of the suit in preventing radiation-related health issues.
Radiation Protection Scientists	Research and test the effectiveness of the FLARE suit's radiation shielding capabilities. Ensure the vest provides adequate protection against solar and cosmic radiation.
Manufacturers	Produce the FLARE suit according to design specifications and quality standards. Convert the design into a physical product.
Testing Engineers	Conduct tests to validate the FLARE suit's performance under simulated conditions. Verify the FLARE suit functions as intended and meets all performance and safety requirements.
Regulatory Bodies	Set and enforce safety and quality regulations for the FLARE suit. Ensure that the FLARE suit complies with space safety regulations and standards.
Astronaut Trainers	Train astronauts on the use and maintenance of the FLARE suit.
Passive Stakeholders	**Rationale/Motivation**
Public	General interest in the outcomes of the FLARE suit project. Interested in the success of space exploration missions and the technologies developed for astronaut safety.
Media	Shares information with the public about the FLARE suit project's achievements and challenges.

2.5 Quantification of the FLARE Design Needs

Based on the mission statement and use-case scenario presented in Section 2.1 and Section 2.3, four key design needs have been identified for the FLARE radiation vest. The following fundamental needs should be addressed by the FLARE suit for it to achieve its intended functionality:

1. Radiation protection
2. Flexibility
3. Quick integration
4. Thermal comfort

These needs were quantified through literature review and conversations with subject-matter experts. The following sections present the specific values and criteria associated to each of these four identified needs.

2.5.1 Radiation Protection

As mentioned in Section 1.2, the health risks of Solar Particle Events to astronauts can be categorized into short-term and long-term effects. Short-term effects are responses to radiation exposure that develop within weeks or months after the initial exposure. Long-term effects develop over a period of years to decades.

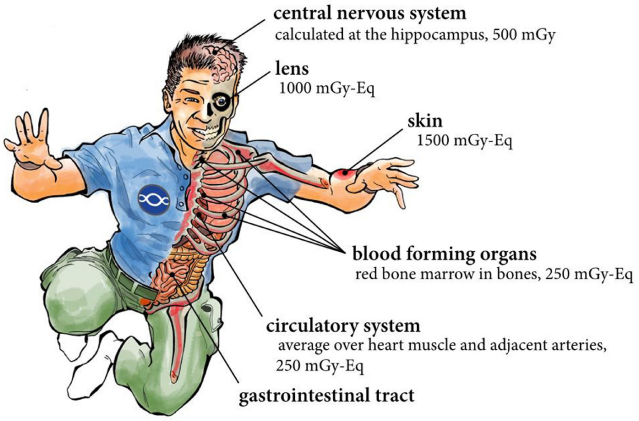

Figure 10: Equivalent dose of incoming radiation which for each organ group triggers the particular radiation sickness effects. Source: [24].

1. **Short-term effects** are responses to radiation exposure that develop within weeks to months after exposure. A summary of the dose levels that a human body and its organs can endure is given in Figure 10 and in Table 2 and Table 3.

   In Table 2, the dose thresholds for various early effects are specified. A significant fraction of tissue loss is expected if the body is exposed above these thresholds. In general, it can be deduced from this table that maintaining the cumulative radiation dose below 0.5 to 1.0 Gy limits the most detrimental effects when exposed to Solar Particle Events.

Table 2: Dose Thresholds for Various Early Effects. Adapted from [14] and [26].

Effect	Threshold
Blood count changes	0.5 Gy
Loss of appetite	1.0 Gy
Threshold for vomiting	1.0 Gy
Nausea	1.5 Gy
Fatigue	1.5 Gy
Threshold for mortality	1.5 Gy
Bone marrow significant harm	1.5 Gy
Bone marrow failure	3.0 Gy
$LD^{*}_{50/60}$ (if minimal care available)	3.2-3.6 Gy
Skin damage	5.0 Gy
$LD_{50/60}$ (with best medical treatment)	4.8-5.4 Gy
$LD_{100/60}$ (with best medical treatment)	8 Gy
Guaranteed mortality due to breakdown of central nervous system	20 Gy

* $LD_{50/60}$ is the dose at which 50% of the population will die within 60 days due to exposure at this threshold.

In Table 3, dose limits are specified which have been set for astronauts in the International Space Station (ISS). These limits consider the type of radiation field, the biological effect reported, the duration of exposure, and the tissue involved. Currently, limits are determined by applying Earth-based limits to the space environment and by ignoring variation among individuals. Establishing appropriate limits is difficult because of the lack of human data in space, which leads to the use of extrapolated animal models and a lack of study on the variability of health effects between individuals (especially between sexes). As a result, it is commonly believed that these estimates do not offer adequate protection, and further data in these areas is necessary [14][25].

Traditionally, the blood-forming organs (BFO) are used for dose computations of short-term effects [3]. This is because the BFO are present in extensive areas of the body, and radiation exposure on these tissues typically have large biological consequences across the body. Bone marrow cells can be sensitive to radiation doses as low as 0.5 to 0.9 Gy. If exposed to higher doses, primary effects are the killing of platelets and white blood cells. While some of its cells are sensitive to 0.5 Gy, for significant effects the threshold is about 1.5 Gy. As specified in Table 3, the 30-day dose limit set for blood-forming organs of ISS astronauts has been set at 0.25 Gy, which is well below this threshold [14].

2. **Long-term effects** are responses to radiation exposure that develop within years to decades after exposure. Therefore, late effects are those that would occur usually only after the mission has ended and over the further lifetime of the astronaut. A summary of the dose levels that a human body can endure for certain long-term effects is given in Table 4.

Table 3: Career Exposure Limits for Non-Cancer Health Effects. Adapted from [14].

Organ	30-Day Limit (mGy)	1-Year Limit (mGy)	Career Limit (mGy)
Lens of the eye*	1000	2000	4000
Skin	1500	3000	6000
Blood-forming organs	250	600	n/a
Circulatory system**	250	500	1000
Central nervous system***	500	1000	1500
Central nervous system*** (heavy particles Z$\geq$10)	n/a	100	250

* Lens dose limit to prevent early cataracts ($<$5 yr).
** Dose limit calculated as average over heart muscle and arteries.
*** Dose limit calculated at the hippocampus.

The development of radiation-induced cancer is one of the most critical long-term risks associated with space radiation exposure [22]. The threshold for cancer is variable due to there being different factors that influence how ionizing radiation interacts with biological tissues and the what its biological response is. Firstly, the type of radiation plays a significant role, with high-LET (Linear Energy Transfer) radiation, such as heavy ions from Galactic Cosmic Rays, known to cause more severe DNA damage compared to low-LET radiation, such as protons from Solar Particle Events. Additionally, the dose and dose rate affect cancer risk: while high doses delivered over a short period can overwhelm repair mechanisms, chronic exposure at low dose rates may allow cells to repair some of the damage, and thereby reduce cancer risk [11]. Lastly, individual variability influences greatly the susceptibility to cancer, with factors such as genetics, age, and sex playing important roles. For instance, younger astronauts whose cells are dividing more frequently, are more vulnerable to cancerous mutations, while female astronauts are more vulnerable to certain cancers, such as breast cancer [25].

For the human eye, the most reported effect of space radiation exposure is the induction of cataract. This is because cataract radiation damage is easy to detect and its threshold of induction is about 2 Gy, which is lower than all other observed consequences to the eye. However, the induction of cataracts is not likely to have a direct impact on the mission. Another late effect of radiation exposure concerns the cardiovascular system. Studies on animals have shown changes in vascular beginning at 0.5 Gy [14].

Thresholds for radiation exposure levels, particularly in space, are subject to significant uncertainty and large error margins due to the limitations of current research. A key limitation is that the assessment of short-term and long-term health risks associated with space radiation exposure relies primarily on research with animal models [27]. In contrast, the main human model which is taken into consideration stems from research on atomic bomb survivors, which were exposed to much different types and higher doses of ionizing radiation compared to astronauts in space. As a result, the biological effects of low doses of space radiation may differ from those of typical low doses of ionizing radiation encountered on Earth. Another main

limitation particularly about cancer thresholds comes from the latency period of such long-term effects and the cumulative nature of exposure. This means that risks may only manifest decades after the initial exposure, which adds complexity to the definition of appropriate dose level thresholds for cancer.

Table 4: Dose Levels for Various Late Effects. Adapted from [14].

Effect	Threshold
Induction of eye cataract	2.0 Gy
Threshold for cardiovascular disease	0.5 Gy
Temporary sterility	0.5-1.0 Gy
Threshold for permanent sterility (female)	1.5 Gy
Threshold for permanent sterility (male)	6.0 Gy
Cancer	variable
Genetic detriment (due to protons)	1.0 Gy

2.5.2 Flexibility

The FLARE vest should not restrict any necessary movements during emergency operations. To achieve this, it is best to include functional mobility into the design requirements rather than maximum ranges of motion. Where the latter refers to the absolute limit of joint movement a person can achieve, functional mobility is the range of motion required to perform everyday tasks or mission-critical actions. This concept, visualized in Figure 11, shows that functional range of motion is typically less than the maximum range of motion [29]. Therefore, designing based on functional mobility typically results in more relaxed suit and vehicle design requirements [28]. The functional mobility limits for relevant body joints are summarized in Table 5. These limits are derived from experimental data presented in NASA's Human Integration Design Handbook (movements marked with * in Table 5) and Functional Mobility Testing (movements not marked with *), which involved 20 adult test subjects (10 male, 10 female) [14, 28].

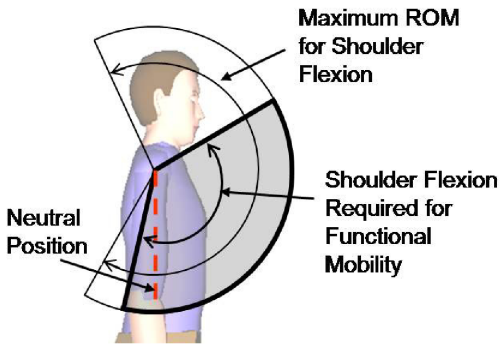

Figure 11: Theoretical Visualization of Maximum Shoulder Flexion and Shoulder Flexion Required for Functional Mobility. Source: [28]

Table 5: Average Joint Movement Limits in Unsuited Conditions. Adapted from [14] and [28]

Relevent joint movements		Limit
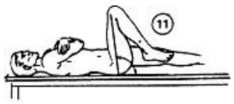	Hip flexion*	165°
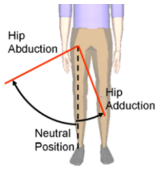	Hip abduction (B)	25°
	Hip adduction (A)	15°
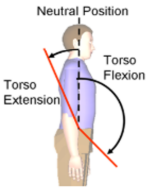	Torso flexion	-165°
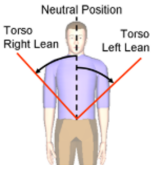	Torso left/right lean	25°
Figure 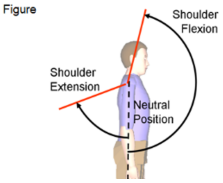	Shoulder extension	-70°
	Shoulder flexion	145°
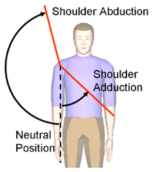	Shoulder abduction	-105°
	Shoulder adduction	35°
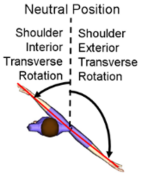	Shoulder interior traverse rotation	46°
	Shoulder exterior traverse rotation	-121°
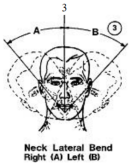	Neck lateral bend*	35°

2.5.3 Quick integration

The filling of a FLARE suit should take less than 30 minutes. This is the NASA/ESA allowable time for all the donning of personal protective equipment during a Solar Particle Event onboard the Lunar Gateway. Ideally, the donning time is shorter than 30 minutes.

2.5.4 Thermal Comfort

Maintaining an appropriate atmospheric temperature is important for astronauts to maintain a safe core body temperature and for user comfort. In general, humans can endure a wide spectrum of atmospheric temperatures for varying durations. Specifically, in the Space Shuttle, the temperature could be regulated within the range of 18℃ to 27℃. [14].

In contrast to this wide range of atmospheric temperatures, human comfort requires a fairly narrow skin temperature range. Figure 12 shows the Wissler Model (1986) which gives the time allowed in a suit without active cooling, as limited by the temperature in that suit and the activity level of the astronaut. Note that 60℉ = 15.5℃ and 100℉ = 38℃ and that 350 Bth/hr can be expected for a normal person seated at rest, compared to 512 BTU/hr for walking, 750 BTU/hr for light work such as mechanical production, and 1466 BTU/hr for heavy work such as athletics [30] [14].

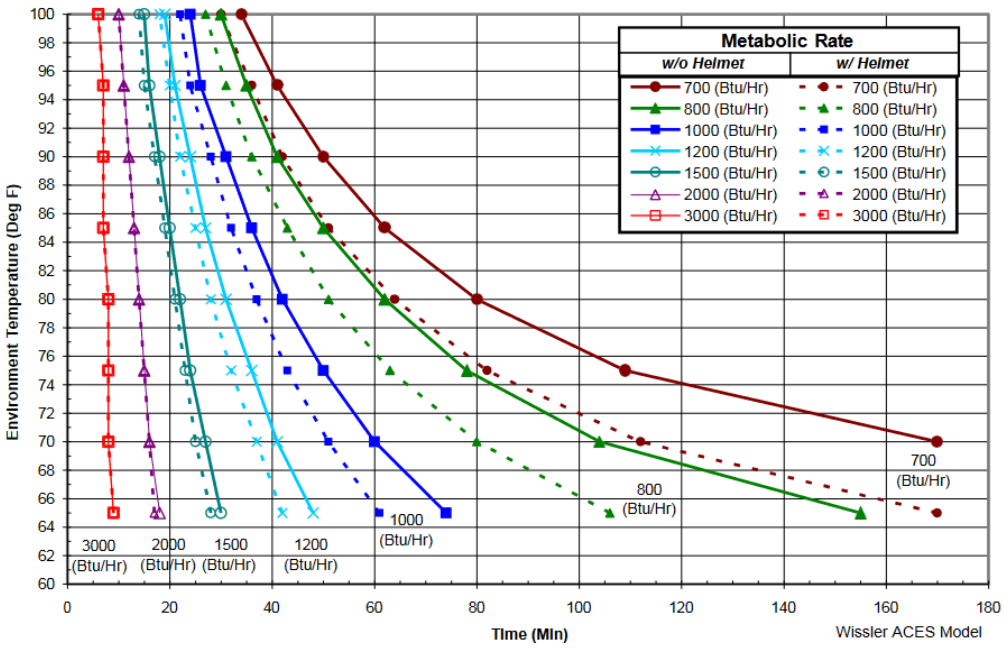

Figure 12: Time allowed in pressure suit. Source: [14]

2.6 Preliminary System Requirements

Upon analysis of the FLARE mission definition and stakeholder inputs, a set of preliminary technical system requirements was developed. These requirements are intended to guide the definition, design, and verification of the FLARE vest and are summarized in Table 6. The table includes the ID label, category, method of verification, and current status of each requirement.

The labeling convention follows the structure: FL - [REQ TYPE] - [REQ NUMBER], where ”REQ TYPE” corresponds to the requirement category. Requirements are organized into six categories:

- Functional: Define the core capabilities and operations of the system.
- Design: Specify physical and structural attributes.
- Performance: Focus on quantitative metrics the system must meet.
- Interface: Cover compatibility with other systems and components.
- RAMS (Reliability, Availability, Maintainability & Safety): Address system dependability and safety criteria.
- Operational: Specify requirements for use in the intended environment.

To ensure compliance with ECSS standards [31][32], each requirement is also given a specific verification method: Review of Design, Analysis, Inspection, or Testing. The selected verification method is chosen based on the nature of the requirement and the most efficient step of demonstrating its fulfillment.

The requirements presented in Table 6 represent the first iteration of a coherent requirements set for the FLARE vest. These requirements are expected to evolve as the project progresses, led by stakeholder feedback, additional analysis, and updated mission needs. Therefore, the status of each requirement in Table 6 represents the latest developments at the time of writing. Future iterations should follow control practices, such as those described in [33], to ensure consistency.

Table 6: FLARE System Requirements

Label	Category	Requirement	Verification Method
Radiation Shielding Requirements			
FL-RAD-01	Performance	The FLARE suit shall limit astronauts' exposure to Solar Particle Events to doses below 1 Gy.	Test: Testing under simulated Solar Particle Events in a controlled environment. Can be guided by radiation modeling with Geant4 software and proton accelerator testing.
FL-RAD-02	Performance	The shielding effectiveness of the FLARE suit shall be optimized for protecting against Solar Particle Events with energies depositing between 100-200 keV per micrometer (LET values).	Review of Design: radiation modeling, examination of the design documents for materials used, thicknesses, and radiation shielding calculations.
Flexibility Requirement			
FL-FLEX-01	Functional	The FLARE suit shall allow astronauts to perform a range of functional movements and emergency tasks without significant restriction, based on the functional range of motion criteria outlined in NASA's Human-Systems Integration Requirements.	Test: Testing with human subjects or realistic mannequins.
Integration Time Requirement			
FL-TIME-01	Functional	The FLARE suit shall be deployable within 30 minutes.	Test: Timed deployment exercises.
FL-TIME-02	Functional	The FLARE suit shall be deployable by a single astronaut.	Test: Deployment exercises.
Thermal Comfort Requirement			
FL-TEMP-01	Performance	The FLARE suit shall maintain the microclimate temperature within the range [18℃, 27℃].	Review of Design: Thermal modeling to simulate the suit's performance in various temperature scenarios.
Other Preliminary System Requirements			
FL-INT-01	Interface	The FLARE suit shall seamlessly integrate with the spacecraft's water supply system.	Inspection: Inspection of the interface connections and integration points.
FL-DUR-01	RAMS	The FLARE suit shall withstand at least 10 cycles of simulated space travel conditions without significant degradation in performance to ensure reliability and durability in long-duration missions.	Test: Repeated testing under simulated space travel conditions (e.g., vacuum, thermal cycling, radiation).
FL-LEAK-01	RAMS	The FLARE suit shall demonstrate water leak resistance to prevent loss of the shielding medium.	Test: Water leak testing under operational conditions.

2.7 Outline of the FLARE Development Process

The mission statement in Section 2.1 and use-case scenario in Section 2.3 formed the basis for defining the design needs of the FLARE vest in Section 2.5. These needs on radiation protection, flexibility, thermal comfort, and operational efficiency, guided the further development process which is followed in the rest of this thesis.

The choice of a water-based shielding system naturally followed from the need to balance radiation protection with flexibility and thermal comfort. Additionally, the importance placed on resource efficiency in future missions beyond Low Earth Orbit led to the implementation of targeted shielding for the most sensitive organs. To this aim, radiation simulations were performed to develop this topographically optimized design. The following outlines the step-by-step development and testing process of this topographical design:

1. The thickness of the suit at each location of the body is optimizable. Simulations were performed in Geant4 to measure the radiation doses absorbed in every organ of the human body using a simplified ellipsoid-vest around the body of 12 different uniform water thicknesses.

2. For every organ separately, these simulations allowed to make an exponential curve fit describing how much each water thickness decreases the radiation doses which are absorbed in the phantom body. The result is a clear estimation for each organ of the absorbed dose and dose reduction compared to an unshielded (no vest) scenario.

3. The aim of FLARE is to design and develop a personal shielding vest with properties superior to existing concepts such as PERSEO and Astrorad. In order to achieve this, the new radiation vest design had to meet the radiation shielding capabilities of these competing concepts while having better operational performance *or* to improve the shielding characteristics while having similar operational performance. Given the drawbacks reported for Astrorad and PERSEO are mostly operational and not in terms of radiation shielding, this project aims to provide a design with similar radiation shielding capabilities while improving mobility, deployment time, comfort, and operational efficiency. The PERSEO and Astrorad vests both aim for 50% dose reduction, and therefore the aiming point of FLARE is also a dose reduction of 50%. It is to be noted, however, that PERSEO's flight design reached significantly less reduction, and that no quantifiable radiation shielding performance has been published for the Astrorad vest).

4. A Python optimization algorithm was developed to calculates the optimal thickness of water for each individual organ, in order to have an effective total dose reduction at the body of up to 50%. The effective dose is a weighted sum of all the doses received for each organ, taking into account weighting factors proportionate to how affected the health of an organ is by the incoming radiation. By using effective dose instead of dose, FLARE will shield the more sensitive organs better than less-sensitive organs. The optimal thicknesses for each organ are those that make the suit the lightest and the smallest. Therefore, the algorithm optimizes the set of organ thicknesses in such way that the sum of its squares is as low as possible. As the radiation vest focuses on the most critical organs which lie in the human torso, all organs

outside of the torso (limbs, head, etc.) have their thickness set at 0 cm within the algorithm. As a last step within the algorithm, an upper limit is placed on the allowed thicknesses of the suit. Three designs were made using these the following upper limits: 7cm, 11cm, 15cm. The upper limit of 7cm means that the suit will not be thicker than 7cm at any place around the body. This corresponds to a maximal effective dose shielding calculated at 34%. For the upper limit of 11cm, the calculated shielding is 43%, and 46% for 15cm.

5. Using these thicknesses, the desired suit topography can be constructed and visualized. The visualization is performed in Blender, an open-source 3D computer graphics software used for creating a wide range of digital content, including 3D models [34]. The construction of the suit topography is performed through an expansion process for all organs. This means that if, for instance, the kidney has a calculated optimal thickness of 4.3 cm from the simulations, then in this visualization the kidney is expanded in volume so that a 3D layer of 4.3 cm is added to its shape. The resulting expanded organ model shows the shape which is a first iteration shape of the vest, to be filled in such shape with water.

6. The topographical 3D model allowed to inspect and alter the design to add flexibility, (thermal) comfort, and other functionalities in the design. According to human-centered design principles, users (astronauts) and other stakeholders were involved to give feedback in this design process (participatory design).

7. The resulting design is simulated in Geant4 to calculate the final effective dose reduction performance. The results of this step will give the necessary information for creating an improved second iteration prototype.

8. Proton accelerator testing further quantified radiation properties of materials to be used in the FLARE suit, with the goal of underpinning past design decisions as well as serve as the basis for future design decisions.

2.8 Human-Centered Design: Definition and Core Principles

Human Centered Design in the systems engineering of the FLARE project focused on improving comfort and operationability, addressing the limitations of state-of-the-art vests PERSEO and Astrorad. The following insights on human-centered design were obtained through the experiences during FLARE suit development as well as conversations with Guy André Boy, Chief Scientist for Human-Centered Design at NASA Kennedy Space Center (KSC) from 2010 to 2016, and Fellow of the International Council on Systems Engineering (INCOSE). These insights were key guiding principles throughout the FLARE design process.

Human-centered design (HCD) is an approach to problem-solving that is applicable in engineering, including systems engineering, and prioritizes the needs, preferences, and limitations of the end-users throughout the design process. The aim is to create solutions that are highly usable, effective, and satisfying for the people who will ultimately use them (the 'user').

The core principles of human-centered design are contextual consideration (*scenario-based* design), user insight and involvement, multidisciplinary collaboration (*participatory* design), and more generally ensuring system reliability. Characteristic to systems engineering in general, but especially to human-centered design, is also the use of iterative design processes.

Contextual consideration (*scenario-based* design)

Contextual consideration in design refers to the process of understanding and incorporating the specific circumstances, environments, and conditions in which a product or system will be used. The goal is to create designs that are not only functional but also intuitive for users within their specific contexts. As part of contextual consideration, scenario-based design is a user-centered design approach that formulates realistic scenarios of the system to be designed. Scenarios help envision how users will interact with a product in real-life contexts, and ensures designers that the design addresses the user needs effectively.

An example of the importance of scenario-based testing can be found in the Apollo 11 mission. In this mission, Buzz Aldrin and Neil Armstrong were tasked to take home Moon rock samples. However, on the Moon it became quickly clear that after making a fist or grasping objects, the lunar regolith could enter the joints and articulations of the gloves, which created immediate resistance and made it difficult for astronauts to straighten their fingers or release objects again after gripping them. As a consequence, the gloves' performance was compromised, despite the task of grasping objects being a primary design requirement. This historical example shows the importance of anticipating real-world conditions in the design process: Testing the gloves in environments that simulate lunar conditions would have helped identify these practical issues before the suits were ever used in an actual mission.

This example also highlights the important distinction between tasks and activities in human-

centered design. While tasks are the intended actions described during the planning phase (grabbing rocks effectively on the Moon), activities are the actual actions performed in practice. In this case, the activity was a poor execution of the intended goal. This distinction is important as real-world execution often deviates from theoretical plans, and the testing of the system should therefore model real-world conditions as well as possible in order to assess the extent to which the activity deviates from the task.

In the FLARE development process, the principle of contextual consideration was applied through scenario definition (Section 2.3) and a focus on scenario-based questions during the end-user testing phase (Section 4.2), where realistic mission scenarios were simulated to understand how astronauts would interact with the FLARE vest in an actual deep-space environment.

User insight and involvement

In order to design these effective contextual scenarios, a designer must deeply understand the users of the system to be designed. In human-centered design, such foundational user understanding guides the design process and ensures a final product that aligns with user requirements. A simple example can be drawn with anthropologists: in order to understand the tribe, it is effective to go live with the tribe and learn immersively. While it is not necessary as a designer to become one of your end-users (nor as an anthropologist, for that matter), gaining a deep understanding of their experiences, their 'language', and behaviors is essential when creating system scenarios that are realistic and relevant to the users' actual conditions and needs.

In order to gain user insight, it is valuable to actively involve users in the design process through participatory design and during most of its iterative feedback loops. Indeed, both during design, development and testing, it is important for a designer to include user testing. Since individual competencies can vary greatly, and the competencies of the group of users may not correspond to the competencies of a designer, frequent and early-on testing on the intended user during the iterative process can reveal a lot of insights that are not always obtainable when testing the system on designers.

For instance, during the 1987 development of the robotic arm for the European space plane Hermes, the design team under Guy André Boy at CNES invested one year on developing a complex control algorithm. However, when the system was tested by an astronaut with background as experienced air combat pilot, the astronaut quickly succeeded in controlling the arm without using the intricate algorithm at all. This example shows that having only designers as test subjects during development did not capture the competencies and real-world skills of the actual users. Instead, it is essential to test early-on with the end users who will operate the system to make sure the design meets their requirements effectively.

In the context of designing a FLARE space radiation shielding vest for astronauts, meetings with astronauts are invaluable. Asking astronauts directly about what they need from the suit provides insights that only an end-user can offer. Also after prototyping, it remains extremely valuable to

observe their interactions with the prototype in certain test scenarios to uncover flaws early in the design process and avoid situations similar to the Hermes control algorithm example. Astronauts might provide critical feedback such as ”this is a good idea, but it might not be useful in a certain situation,” which can then be seriously considered by the designer. In cooperating with users, it is important to try to team up with them as partners in the design process, rather than treating users as test subjects (‘guinea pigs’). This fosters a sense of commitment to the success of the project and allows them to become active participants in the design process. It is equally important to remember that astronauts are not professional designers, and a designer is eventually responsible to integrate any information using their expertise. During feedback loops and testing, it can prove valuable to explain practical and technical constraints to the astronauts to increase transparency and involvement and enable more informed and relevant feedback. Lastly, it is good to keep in mind that astronauts' experiences with past suits will condition their practices and expectations. This means that they might not always articulate what can change in a new design, as their feedback is influenced by their experiences with different types of previous suits. Recognizing these subtleties can require a higher level of understanding from the designer.

Multidisciplinary collaboration (*participatory* design)

Human-centered design is inherently participatory, involving a design approach that actively engages all stakeholders (e.g., engineers, customers, regulatory bodies, end-users, etc.) throughout the design process to ensure the outcome addresses their needs and remains practical. The cooperation between designers and users covered in the previous paragraphs is a very important element of participatory design. On the other hand, the design approach also includes the multidisciplinarity of the design team, where team members bring together diverse skills to create the best possible solution. In space design, this is especially true and most smaller or large space system projects will generally integrate expertise from multiple backgrounds.

For example, when the Lunar Electric Rover was designed at NASA in 2006 [35], the design team consisted of several type engineers and scientists, as well as an astronaut, geologist, and two cartoonists for visualization. This is a very good example of the participatory approach to ensure the final design is both functional and intuitive for the astronauts who would rely on it.

In the case of FLARE, collaboration included experts like Sylvain Blunier, a radiation simulation specialist, whose experience in setting up and executing Geant4 simulations significantly accelerated the FLARE development process. Noora Archer, a virtual designer with a background in fashion, created several quick and effective visualizations of the FLARE suit.

Beyond these core team members, a wide range of experts lent their knowledge at key stages. These included Marco Schena, an expert in Lunar Gateway logistics; Anna Fogtman, who specializes in space radiation; Alex Karl, with expertise in astronaut operations; Frank De Winne, knowledgeable in ESA regulations; and Giorgio Baiocco, the principal investigator of the state-of-the-art PERSEO vest. While these experts were not actively involved in the day-to-day project work, their insights were invaluable during consultative meetings.

System reliability

Reliability is an important characteristic in human-centered design and involves more than preventing failures; it is about creating a system that ensures safety, efficiency, and comfort under all conditions. In the context of the FLARE vest, there are three key considerations to reliability: these are efficiency, comfort, and safety.
Efficiency indicates that the vest should not hinder the astronaut's ability to perform tasks efficiently. This includes minimizing the time and effort required for donning, doffing, and maintaining the vest. In addition, the vest should be comfortable to wear, as discomfort can lead to fatigue and decreased performance over long periods. Lastly, safety refers to the assurance that the vest will protect astronauts from harm and operate reliably under all expected conditions. It is the primary concern in space and the ability to quickly implement solutions is vital. For the FLARE project, safety includes for example the prevention and reparation of a puncturing of the water bladders.

No design is perfect, and unforeseen situations can arise. Therefore, designing with recovery in mind means having contingency plans and procedures ready. For instance, when the Apollo 13 crew faced with a CO2 issue, the team on ground was only able to quickly devise a solution to save the crew because of NASA's well-performing recovery strategy. The approach included a combination of technology, organizational coordination, and people (astronauts and engineers), and can be encapsulated into the TOP-Model (Figure 13) [36]. TOP stands for Technology, Organization, and People:

1. Technology: Because of the use of adaptable technological materials on board Lunar Module, engineers on the ground were able to quickly devise a makeshift CO2 scrubber using the onboard available materials.
2. Organization: Good coordination was vital to discover and implement the solution within a limited timeframe. The team on Earth was enabled to communicate, simulate the problem, develop a solution, and communicate the precise instructions to the astronauts.
3. People: The astronauts' expertise and calm under pressure played a crucial role in executing the recovery plan. Simultaneously, the engineers on ground had advanced problem-solving skills and creativity.

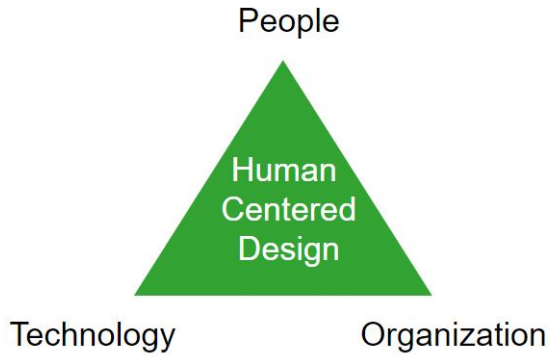

Figure 13: Illustration of the TOP model for Human-Centered Design. Source: [36].

For the FLARE project, in order to achieve a reliable design, a TOP-Model for reliable design should be integrated into the design process:

1. Technology-Driven Strategies: Incorporate advanced materials and engineering practices to minimize the risk of failures, such as leaks in the water bladders.
2. Organizational Strategies: Establish protocols for communication and problem-solving in case of a failure scenario. Simulate the potential failure scenarios during training sessions to prepare both astronauts and ground crew for an effective response.
3. People-Centered Strategies: Involve astronauts in the design and testing phases. Gather their feedback to understand potential issues and improve the design. Equip astronauts with the skills to perform emergency repairs and troubleshooting.

3 Construction of Prototypes

3.1 Geant4 Simulation

Radiation simulations have been performed for the FLARE project to develop a topographically optimized design for the suit, which has targeted shielding for the most radiosensitive organs. This section provides background information on radiation quantities which are used, and gives overview of the 1D- and 3D-simulations which have been conducted.

3.1.1 ICRP Radiation Protection Quantities

Simulations for the FLARE project yield data on the absorbed dose, equivalent dose, and effective dose. This section provides a brief overview of the definitions of each of these three quantities. These definitions were chosen according to the recommendations by the International Commission on Radiological Protection (ICRP) [37], which sets internationally recognized standards for radiation protection, including how doses should be measured, calculated, and interpreted to ensure safety and compliance.

3.1.1.1 Mean Absorbed Dose of an Organ In radiological protection, the focus is primarily on the absorbed dose averaged across the volume of a tissue or organ, rather than the dose at a specific point within the body. This average is referred to as the mean absorbed dose, D_T, for a particular tissue T. In environments with mixed radiation fields, the mean absorbed dose D_T for an organ or tissue T is calculated as the sum of the mean absorbed doses contributed by each radiation type R:

$$D_T = \sum_R D_{T,R}$$

The gray (Gy) is the SI unit used for measuring absorbed dose, defined as J kg^{-1}. For strongly penetrating radiation, the absorbed dose tends to be relatively uniform within most organs, which makes the mean absorbed dose an appropriate metric for assessing the dose within an entire organ or tissue.

3.1.1.2 Dose Equivalent in an Organ The protection quantity known as equivalent dose, H_T, for a specific organ or tissue, incorporates the mean absorbed dose, $D_{T,R}$, and adjusts it using a radiation weighting factor. This accounts for the differences in biological impact among various radiation types. While D_T quantifies the energy absorbed by tissue T, the equivalent dose H_T quantifies the potential risk of tissue damage and radiation-induced effects, such as cancer, resulting from the exposure. The dose equivalent can be calculated using the following formula:

$$H_T = \int_L Q(L) D_{T,L} dL$$

The quality factor (Q) is a dimensionless number used to express how biologically harmful radiation is, based on the type of radiation. It specifically helps compare how much damage high-LET (Linear Energy Transfer, L) radiation, such as alpha particles, can cause in biological tissues compared to low-LET radiation, like X-rays or gamma rays. Here, LET refers to how much energy a particle deposits into a material (like biological tissue) as it travels through. High-LET radiation such as alpha particles deposits more energy per unit of distance, which usually makes it more damaging to tissues compared to low-LET radiation such as gamma rays. The formula for H_T integrates over all the different LET values, hence over all particles with increasing biological effect.

3.1.1.3 Effective Dose

The effective dose is defined as:

$$E = \sum_T w_T H_T$$

Here, w_T represents the tissue weighting factor for a specific organ or tissue T, indicating its relative contribution to the overall health detriment. It applies that $\sum_T w_T = 1$. The effective dose was first introduced by the ICRP in their *Publication 60* [38] and redefined in *Publication 103* [39]. The total sum is calculated over 14 individual organs and tissues of the human body, as specified in the definition of E, with corresponding w_T values applied as specified in Table 7. These weighting factors are based on the detriment from stochastic effects due to radiation exposure and are averaged across all ages and genders to provide representative mean values for humans. The SI unit for effective dose, like that for equivalent dose, is J kg^{-1}, commonly referred to as the sievert (Sv). Effective dose is particularly valuable in radiation research because it provides a single, comprehensive measure that can be used to set exposure limits, including for astronauts.

The effective dose is calculated using the mean value of the equivalent dose H_T, averaged over the male and female organ/tissue: $H_T = 0.5(H_T^M + H_T^F)$. Since this research focuses on developing a radiation shielding suit prototype for a female physiology, $H_T = H_T^F$.

Different parts of the body have different sensitivities to radiation and require more/less protection. In the table below, the sensitivity of different tissues is expressed with their weighting factor

Table 7: Tissue (w_T) Weighting Factors of ICRP-103 Report ([39]).

Organ/tissue	w_T	Total contribution
Lung, stomach, colon*, bone marrow, breast, remainder**	0.12	72 %
Gonads***	0.08	8 %
Thyroid, oesophagus, bladder, liver	0.04	16 %
Bone surface, skin, brain, salivary glands	0.01	4 %

** The specified remainder tissues (14 in total, 13 for each sex) are: adrenals, extrathoracic tissue, gallbladder, heart, kidneys, lymphatic nodes, muscle, oral mucosa, pancreas, prostate, small intestine, spleen, thymus, and uterus/cervix.
*** The w_T for gonads is applied to the mean of the doses to testes and ovaries.

w_T. Radiation hitting the lungs ($w_T = 0.12$) carries three times more risk as radiation hitting the liver ($w_T = 0.04$) [14].

3.1.1.4 Normalized (Equivalent) Dose

In order to quantify radiation shielding effectiveness of a certain material, the radiation dosage for each organ can be compared to the unshielded case, i.e. comparing the amount of incoming dose when there is shielding to when there is not. In general, this comparison is done with the equivalent dose H_T. The quantity obtained after normalization with the no-shielding case, is referred to as normalized (equivalent) dose, which is defined as:

$$\text{NormDose. [\%]} = \text{Dose}_{\text{shielded}}/\text{Dose}_{\text{unshielded}}$$

Using mathematical notation with the equivalent dose H_T for a certain water thickness d, this definition can be translated to:

$$\delta H_T(d) = \frac{H_T(d)}{H_T(0)}$$

3.1.2 1D-Simulations

To quickly estimate the thickness of a suit needed for a specific level of radiation protection, preliminary results from 1D simulations can be used. Using a 1D-environment serves to accelerate the 3D simulation process.

Simulations in 1D were performed in 2019 by KTH-student Sébastien Ruhlmann during his internship in the Spaceship EAC team, whose work is reported in earlier work [7]. In the used test configuration, protons were beamed from a single point and directed onto layers of material representative of the Columbus module's structure, before reaching a varying thickness of water and finally a skin sample. The water layer varies between thicknesses of zero to twenty centimeters and is at all times adjacent to the skin, which is at two meters distance with respect to the Columbus' structure. Furthermore, the thickness and surface area of the skin was chosen arbitrarily as the radiation dose measurements are to be normalized. Altogether, the 1D-simulation setup is visualized in Figure 14. Using this setup, comparative results were obtained between a shielded astronaut and an unshielded one.

For this 1D-experiment, incoming solar particles followed Spenvis' Xapsos 2000 model of October 1989 [40]. These particles were then randomized five times, after which a million of these randomized particles were beamed onto the simulation setup for each water thickness.

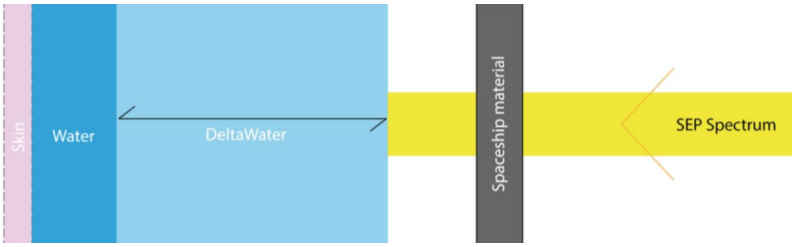

Figure 14: 1D simulation setup, including Columbus module material (gray), variable water layer (with thickness between the dark blue and light blue region), and skin (pink). In practice, the beam has no physical thickness, and the particles originate from a single entry point. Source: [7].

The findings of these 1D-simulations are displayed in Figure 15, showing a reduction in equivalent radiation dose with a steep decline for small water thicknesses and a longer slope attenuation as the thickness increases. This dose reduction attenuation corresponds directly to the physics of energy deposition within a water layer: as the water layer becomes thicker, particles have more opportunity to deposit energy, resulting in fewer particles escaping. Ruhlmann's graph shows directly that a small increase in water thickness has greatest impact on the radiation dose within the first few centimetres. Furthermore, it can be seen that a water layer with a thickness of four centimeters is estimated to achieve the dose reduction goal targeted by AstroRad and PERSEO, which is providing approximately double the level of protection. This result is to be taken as a valuable but preliminary indication of the necessary water shielding thickness, given the limitations of the 1D model and the simplification of the human body to a mere 'skin' layer.

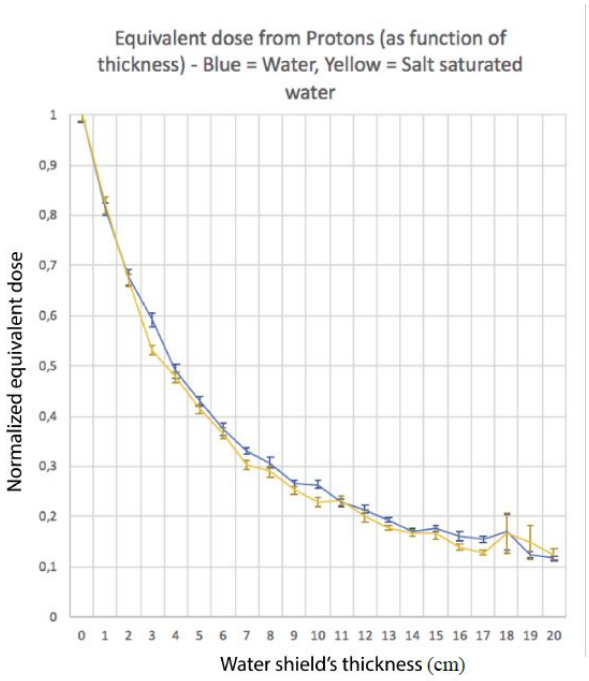

Figure 15: 1D-simulation results of the normalized equivalent dose as function of the suit's water thickness. Results for pure water in blue and for salt-saturated water in yellow. Source: [7].

3.1.3 3D Simulations

3.1.3.1 Definition of the Geant4 Simulated Setup

Within the FLARE project, simulations of different suit thicknesses were performed using the Geant4 v11.1.1 framework [41], and realized by physicist Dr. Sylvain Blunier at ESA, specialized in space radiation simulations. Geant4 is a Monte Carlo simulation framework used to model the transportation of particles through matter, taking into account various interactions and physical processes. These physical processes include: ionization, bremsstrahlung, photoelectric effect, Compton scattering, elastic and inelastic hadronic interaction, nuclear capture, and particle decay [42]. The simulation setup is described below.

The simulated environment consisted of a simplified Lunar Gateway I-HAB module, in the center of which a human phantom is placed wearing a vest of specific water thickness.
The human phantom chosen for these 3D-simulations is the polygon-mesh version of the ICRP-145 voxel phantom, which consists of 188 distinct organs and tissues. This phantom choice further explained in its dedicated Section 3.1.3.2 [43]. The I-HAB module inside the Lunar Gateway was chosen as spacecraft environment as it is ESA-built and has a large habitable volume, implying ESA astronauts will spend considerable time there. Additionally, it has a cylinder-shaped geometry (unlike Orion), which is easily simulated as an Aluminum cylinder of external diameter 3.350m, length 5.9m and thickness 4mm. In the simulations, a 1/3-scaled module was used for the purpose of computing resource efficiency, since radiation results are minimally impacted by this scale change. Therefore, the I-HAB module was finally simulated as an aluminum cylinder with external diameter of 1.1 meters, length of 2 meters, and a thickness of 4 mm.
Lastly, the human phantom wears a vest of certain uniform water thickness which is simulated as an ellipsoid segment. The water thicknesses which were simulated are: 0 mm, 1 mm, 2 mm, 5 mm, 10 mm, 20 mm, 30 mm, 40 mm, 50 mm, 70 mm, 100 mm, 150 mm. This range of thicknesses allows to evaluate the shielding effectiveness of a wide range of suits, by comparing the equivalent radiation doses in all 188 tissues and organs of the human phantom for each thickness. Altogether, the 3D-simulation setup is visualized in Figure 46.

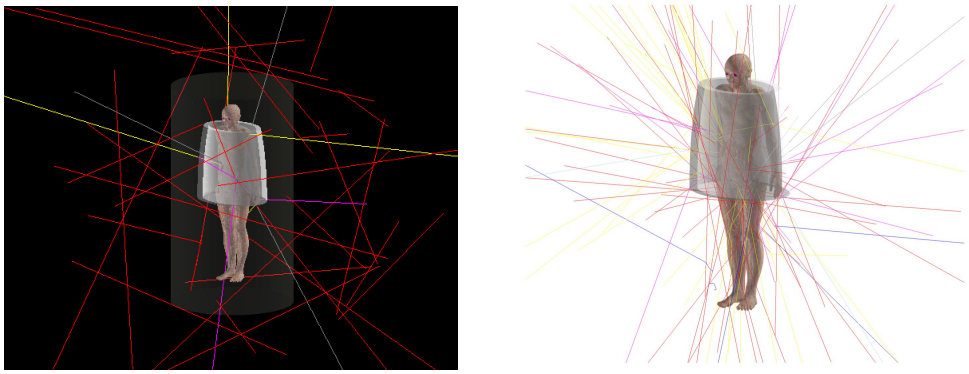

Figure 16: 3D simulation setup. On the left is shown the I-HAB module (dark grey), ellipsoid segment simulated vest (light grey), and human phantom (cyan). On the right is shown a close-up of the ICRP voxel phantom with ellipsoid vest.

3.1.3.2 Choice of the Computational Human Phantom

Good models of the human body, also refered to as computational phantoms, are important in radiation simulation. Of the two previously developed radiation shielding suits, PERSEO and AstroRad, only PERSEO has shared details about their radiation simulations and the phantom that was used in those simulations. As described in their initial publication [3], the simulations used the ORNL stylized phantom within the Geant4 radiation simulation framework, which is shown on the left of Figure 17. These stylized phantoms are based on simplistic 3D geometries, such as spheres, cones, and cylinders, to represent organs or larger body sections. While functional, this approach is naturally constrained by a lack of precision in capturing the complexity of human anatomy.

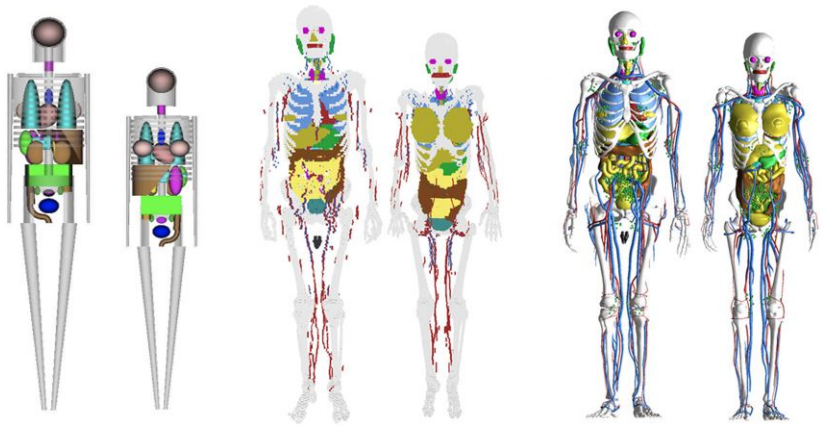

Figure 17: Illustration of three different types of adult male and female mathematical phantoms. Stylized phantom developed at the Oak Ridge National Laboratory in the late 1970's (left), voxel phantom published in ICRP-110 in 2009 (center), and polygon-mesh ICRP-145 phantom (right). Figure constructed from [44] and [45].

Using a phantom that offers more realistic anatomy is a desired step to further the development of the FLARE vest, as it allows more accurate modeling. While the stylized phantom has been used in previous simulations of PERSEO, the *ICRP 145* phantom has been selected for this research.

Advances in computing and medical imaging, such as CT scanning, enabled the development of voxel phantoms—digital models composed of cubic volumetric elements (voxels) derived from CT images. These phantoms provide a detailed anatomical representation based on three-dimensional scans. The International Commission on Radiological Protection (ICRP) utilized voxel phantoms to construct the adult Reference Male and Reference Female models described in ICRP Publication 110 [37], which include detailed organ definitions and properties from ICRP 89.

While voxel phantoms offer a significantly better anatomical representation compared to stylized phantoms, they consist of volumetric pixels which have limited resolution compared to the smooth mathematical shapes of stylized phantoms. This causes smaller tissues, such as the skin and lens of the eye to not be segmented properly. For this reason, phantoms have been developed that can combine the realism of patient-based voxel phantoms with the flexibility of mathematical phantoms. These are called 'boundary representation' (BREP) phantoms, and they are produced by creating

a polygon mesh format of the voxalised phantoms [46]. In this context, the ICRP Committee started a research project to produce replicas of the ICRP Publication 110 voxel phantoms in this polygon mesh format. The resulting adult reference computational BREP phantom is displayed in the left image of Figure 17.

3.1.3.3 Definition of the Geant4 Simulation Environment

The test configuration used for FLARE's 3D simulations includes protons which are beamed isotropically (modeled as a sphere around the habitat) and directed onto the previously described habitat environment. In total, between $6 \cdot 10^7$ and $3.2 \cdot 10^8$ protons of different energies were beamed, the number depending on the simulation scenario.

Modeling the radiation environment requires the choice of a suitable solar proton model to describe the energy spectrum and the fluence of particles. The energy spectrum was instead built using the Xapsos et al. (2000) model present on the ESA SPENVIS website using the October 22th 1989 flare flux and mean/worst-case composition for protons only and without considering the Earth magnetic shielding [47]. This model is used in ECSS standards and its averaged spectrum is shown in Figure 18 through both the energy differential flux [#/(m² MeV sr s)] (right axis) and the integral flux [#/(m² sr s)] (left axis).

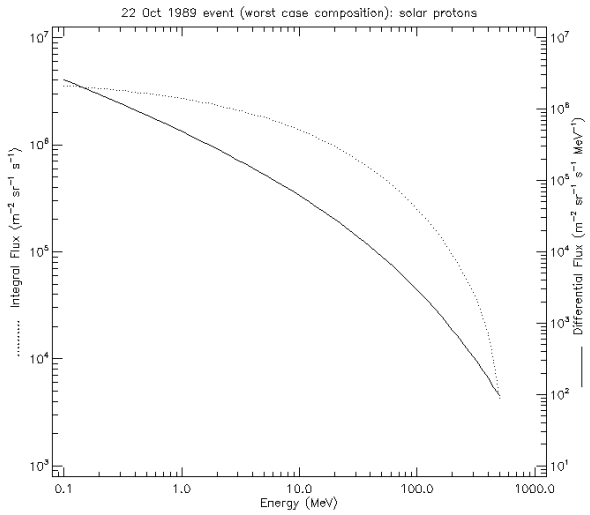

Figure 18: Differential energy fluence [#/(cm² MeV s)] and integral energy fluence [#/(cm² s)] using the Xapsos et al. (2000) model from the ESA SPENVIS website.

3.1.3.4 3D Simulation Results

Geant4 simulations provided the dose equivalent and its standard deviation for each of the 188 organs and tissues of the ICRP 110 human phantom and for 12 thicknesses of the water vest, including a zero thickness which represents the unshielded case. The effective doses measured in the human phantom for each of the 12 ellipsoid vest thicknesses is shown in Figure 19. A reduction is observed which is steeper for small added thicknesses and reaches 49.8 % $\pm$ 4.7 % of the initial dose for a vest thickness of 15 cm.

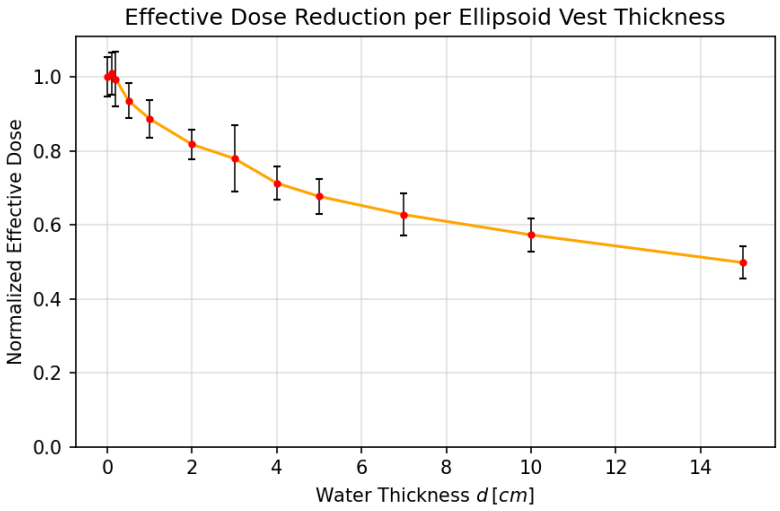

Figure 19: Effective dose reduction as function of the thickness of the simulated ellipsoid water vest.

For all organs and tissues, the normalized dose was calculated for each water thickness according to the definition in Section 3.1.1.4, i.e. by dividing the equivalent dose of the shielded case to the equivalent dose of the unshielded case. By this means, 188 plots were constructed, one for each considered organ in this study. For the humeri spongiosa tissue, which represents the shoulder bones, the normalized dose plot is shown in Figure 20.

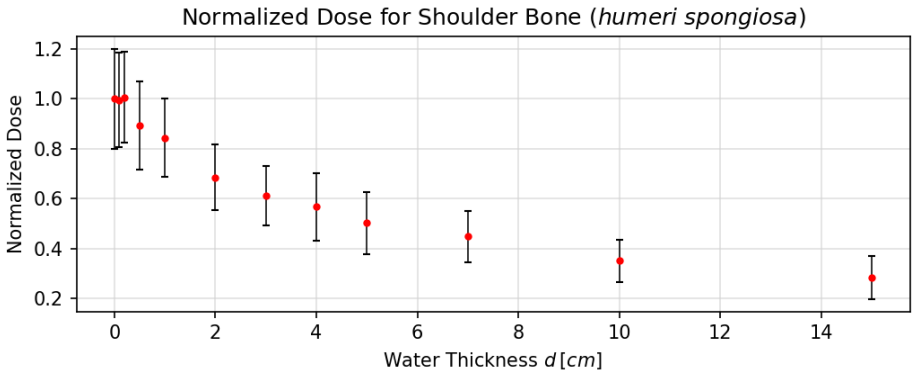

Figure 20: Normalized dose with uncertainty given as function of water shielding thickness for the humeri spongiosa (shoulder) tissue.

An exponential decay curve was fitted for the 188 organs and tissues involved in the simulations, according to the fitting function:

$$f(d) = a \cdot e^{-\mu d}$$

Here, $f : \mathbb{R}^+ \to [0, 1] : d \mapsto f(d)$ is a function that projects the suit's water thickness $d \in \mathbb{R}^+$ onto the normalized dose $\delta D_T \in [0, 1]$. The curve fit thereby describes how quickly the equivalent dose absorbed by the human body decreases for increasing water shielding thickness. For example, in the humeri spongiosa tissue of Figure 20, the curve fit was calculated as $f(d) = 0.92 \cdot e^{-0.0982d}$. This curve fit is displayed in Figure 21. For the humeri spongiosa tissue, it can be deduced that a water layer of six centimeters is needed to reach the dose reduction targeted by FLARE, i.e. double protection (indicated by the green cross).

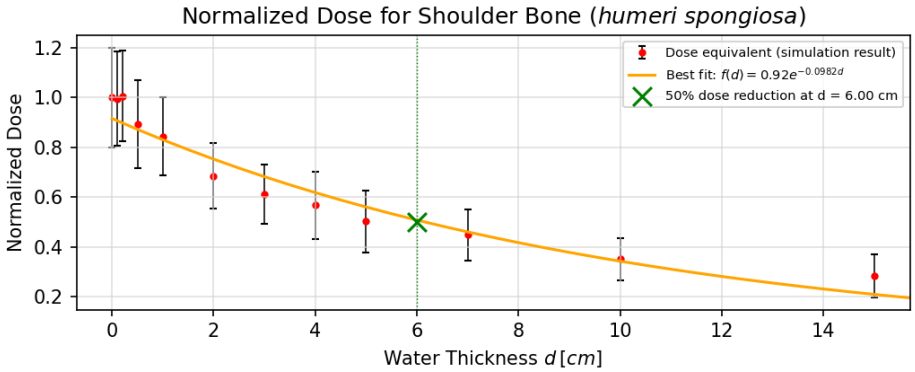

Figure 21: Curve fit of the exponential decay function $f(d) = a \cdot e^{-\mu d}$ on normalized dose data as function of water shielding thickness for the Humari spongiosa (shoulder) tissue.

3.2 Prototype Design

3.2.1 Optimization of the Suit Topography

The aim of FLARE is to design and develop a personal shielding vest design with the same radiation shielding capabilities of PERSEO and Astrorad while improving mobility, deployment time, comfort, and operational efficiency. The PERSEO and Astrorad vests both aim for 50% effective dose reduction, and therefore the aiming point of FLARE is also a dose reduction of 50%. An appropriate note to make on this number, is that PERSEO's ISS flight prototype has been much simplified from their original aim and reached less dose reduction. In addition, the about the Astrorad's design no quantifiable radiation capability has been published to date.

In order to reach a dose reduction of 50%, two approaches can be followed: in the most straightforward approach, the equivalent dose received in every of the 188 organs and tissues is halved. This means, for every tissue is calculated at what thickness d the dose reduction is exactly 50%. For the humeri spongiosa, as directly shown in Figure 21, this is at approximately 6 cm. A problem that occurs when using this approach, is that the necessary shielding thickness for some organs is exceedingly high, up to 2 meters. This can be interpreted as being a tissue for which adding shielding material has low impact. And yet, such tissues would require the largest amount of resources and shielding. In order to remove this problem and optimize water resources, a second approach is used as an alternative where resources are allocated in a topography where they are enabled to have most impact. This is done by looking into a 50% dose reduction of the total effective dose (Section 3.1.1.3) instead of the equivalent dose in each organ. This means that instead of requesting 50% dose-reducing shielding for each organ and tissue individually, a 50% dose-reduction over the entire body is obtained by varying percentages of dose-reducing shielding. Hence, less sensitive organs will be shielded less than 50%, and more sensitive organs will be shielded more.

In using the effective dose, weighting factors are assigned to each organ and tissue of the ICRP 110 human phantom, which indicate their sensitivity to radiation doses. Next, an optimization algorithm was constructed and applied. The aim of this algorithm is to find thickness d_i for each of the 188 organs and tissues i such that the effective dose reduction is equal to $Q = \frac{1}{2}$, where:

$$Q = \frac{\text{Eff. Dose shielded}}{\text{Eff. Dose unshielded}} = \frac{H_{T_{1,S}} w_{T_1} + H_{T_{2,S}} w_{T_2} + ... + H_{T_{187,S}} w_{T_{187}}}{H_{T_{1,U}} w_{T_1} + H_{T_{2,U}} w_{T_2} + ... + H_{T_{187,U}} w_{T_{187}}}$$

The curve fit that was performed for each of the tissues and organs allows to be implemented in this equation. The curve fit is given by $\frac{H_{T_{i,S}}}{H_{T_{i,U}}} = a_i \cdot e^{-\mu_i d_{T_i}}$, written differently $H_{T_{i,S}} = H_{T_{i,U}} \cdot a_i \cdot e^{-\mu_i d_{T_i}}$. In this equality, w_{T_i} are the weighting factors per organ as given by standard ICRP values, and $H_{T_{i,U}}$, a_i and μ_i were calculated through a the curve Least Square fit of the simulation data. Hence the equality $Q = \frac{1}{2}$ can be written as a function with as variables only the thicknesses $d_1, d_2, ..., d_{188}$ of water required for each organ i.

$$Q = \frac{1}{2} = f(d_1, d_2, ..., d_{188})$$

This equality is the 'constraint function' of the optimization algorithm. The algorithm will aim to solve for values of $d_1, d_2, ..., d_{188}$ such that this equality is true. Since there are many such possible configurations of $d_1, d_2, ..., d_{188}$, the following 'objective function' is applied as the quantity which should be minimized:

$$\sum_{i=1}^{188} d_i^2$$

The minimization of this quantity will ensure that the shielding thicknesses for each organ remain preferably small, which is beneficial for the resource-efficiency, thermal comfort, and flexibility of the FLARE suit.

This mathematical optimization problem has been solved numerically with Sympy and Numpy (Python). The resulting shielding thicknesses are displayed for a selection of organs and tissue in Figure 22. In this image, it can for instance be seen that the thyroid, which is an important hormone-producing organ, requires the vest to have shielding around the neck. This is displayed by the pink sphere in the figure, which sits partially inside the human body. Similarly, the shoulder bones (humeri spongiosa) require about 4 cm of shielding around the shoulder tips, as shown by the orange spheres in Figure 22.

In the case all 188 organs and tissues are included in the optimization problem, the resulting

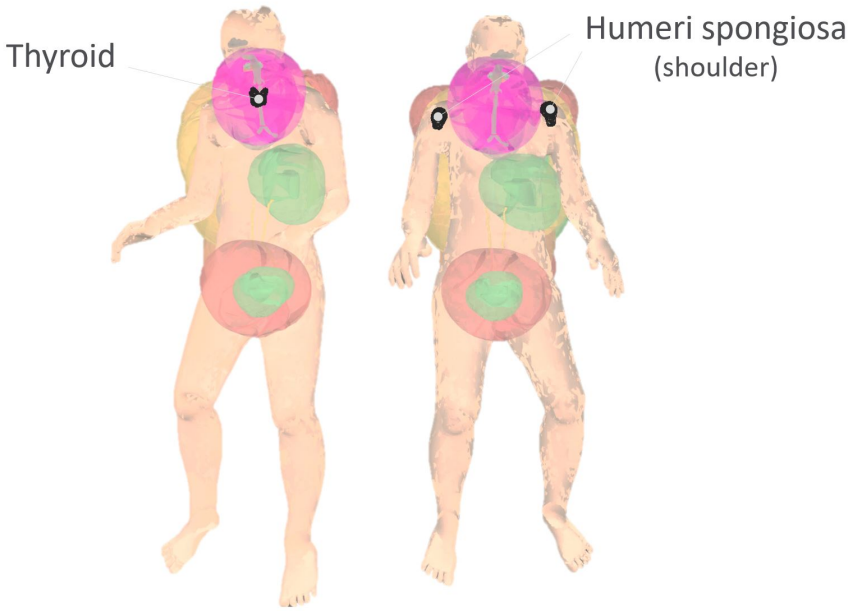

Figure 22: Thyroid and humeri spongiosa (shoulder bone) tissues and their necessary shielding thickness displayed in pink and orange, respectively. †

Figure 23: Visualization of the optimization case scenario where also tissues outside of the torso area would be allowed coverage by the suit. As the FLARE suit aims for torso coverage only, it is necessary to set suit thickness $d = 0$ for all such organs in the optimization algorithm, so that they do not add inaccurately to the effective dose reduction. †

shielding distribution after optimization is visualized in Figure 23. It shows an image from which this method's signature as the 'Frankenstein' method seems not far-fetched. The figure shows visually very well why all organs outside of the torso (limbs, head, etc.) had their thickness set at 0 cm within the algorithm. This is because the radiation vest focuses on the most critical blood-forming organs of the human body, which lie in the human torso.

As a last step within the algorithm, an upper limit is placed on the allowed thicknesses of the suit. Three designs were made using these the following upper limits: 7 cm, 11 cm, 15 cm. Particularly, an upper limit of 7 cm means that the suit will not be thicker than 7 cm at any place around the body. The resulting 'Frankenstein' models are displayed in Figure 24. It was calculated that an upper limit of 7 cm corresponds to a maximal effective dose shielding of 34%. For the upper limit of 11 cm, the calculated shielding is 43%, and 46% for 15 cm.

An upper limit of 11 cm was selected for the design as it provides 43% radiation shielding while keeping the suit practical and comfortable. This thickness prevents the suit from becoming too bulky, so that astronauts can still move freely and stay thermally comfortable.

In contrast, a 15 cm limit would make the suit significantly bulkier, even potentially shifting the

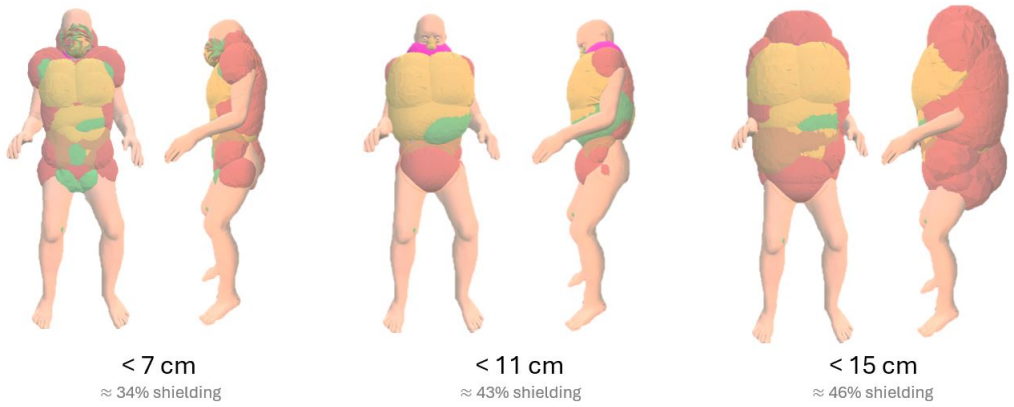

Figure 24: Visualization of the shielding thicknesses required in the case of 7cm, 11cm, and 15cm maximal shielding thickness. †

astronaut's center of mass to an inconvenient extent. As shown in Figure 24, this thicker design covers the head and upper arms completely, which is an undoubted restriction of operational movement of the astronauts. Since extra bulk of a 15 cm suit limits range of motion, and the small increase in radiation protection is only 3% more than with an 11 cm thickness suit, the benefit in this case does not outweigh the drawbacks and the 15 cm upper limit has been discarded.

On the other hand, the 11 cm limit provides more protection than a 7 cm suit, increasing shielding by around 11%. The added bulkiness to the suit is also rather limited and does not seem to significantly reduce flexibility, as is seen in Figure 24. In this configuration, the suit with an 11 cm limit allows similar freedom of movement in the upper arms compared to the 7 cm version, and even improves leg mobility by reducing pelvis shielding. Therefore, the range of motion of the astronaut does not seem notably more restricted for a limit of 11 cm. Though the 11 cm thickness slightly affects downward visibility due to a bulkier chest area, this drawback is minor compared to the increased radiation protection in light of the gravity of health effects due to Solar Particle Events.

The optimization code with 11 cm upper limit produces a set of desired water thicknesses, one for each of the 188 major human tissues. Figure 25 presents the optimized suit thicknesses from various angles, noting which organs contribute to the suit's external shape. Out of all the organs and tissues considered, this external shape turns out to be the combination of only 11 contributing tissues. This means that while other organs do require shielding, their needs are fully covered by the water thickness required for these 11 key organs. This visualization serves as the technical basis of the first FLARE prototype, which guided the subsequent stages of design in the rest of this section. The optimized shape of the FLARE suit will be further also referred to as the suit "topography", which describes the surface contours and varying thicknesses of the suit that result from the shielding needs of different organs.

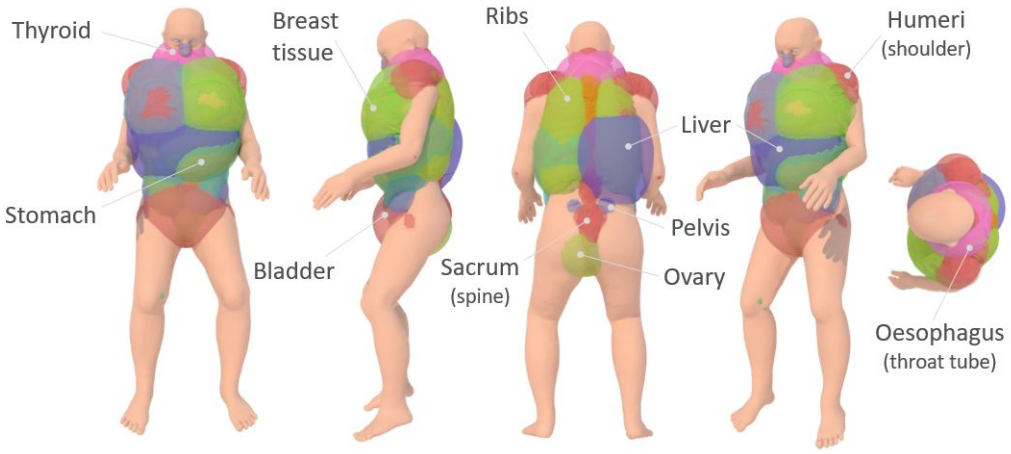

Figure 25: Closer look into the ”Frankenstein” visualization of all blown-up organs to the size of the shielding they require as output of the shielding optimization algorithm. This visualization is a good indication of where in the vest what shielding thickness is desired in further design.†

3.2.2 Considerations for Functional Clothing

The nature of the FLARE project requires to consider a vest or suit as a **functional clothing** tailored to the specific context of a space radiation environment. In general, functional clothing is defined as a garment with features to provide performance, comfort and protection from external conditions. For instance, a moisture-wicking shirt is a functional garment that provides protection from sweat and heat in sports environments. Depending on the intended use, functional clothing can have various purposes: to retain or release the accumulated body heat, allow freedom of movement, offer a pleasant tactile experience, be durable, resistant to wear, or environmentally friendly. Some garments may also be recyclable or biodegradable, while others can have more extreme functions, such as protection from fire or microbes.

As a functional suit, FLARE should protect astronauts from space radiation while ensuring comfort and mobility. The primary function of the FLARE suit is to shield astronauts from harmful radiation in space. This requires materials that effectively absorb radiation. The suit should also be able to manage heat and moisture, preventing overheating or excessive cooling of the body as was experienced with the Astrorad vest. The suit must furthermore allow for an operational range of motion, and be durable enough to withstand several Solar Particle Events.

The purposes of FLARE are such that the functional vest can be specifically categorized as a survival garment. Similar to survival clothing in polar navigation, medieval armor or deep sea exploration, it is expected to combine technology and design. In order to transition from the conceptual suit topography of FLARE to a functional and wearable survival prototype, this means that additional design considerations have to be taken into account. The remainder of this section discusses several key design elements which were integrated in the final prototype design, which were based on FLARE’s functional purpose as survival garment.

3.2.2.1 Segmented Design for Increased Joint Mobility

The FLARE suit should be design to keep the arms and legs as free as possible, in order not to affect the astronaut's mobility and range of motion in the suit. This mobility is already partially achieved by the choice of limiting the water shielding to the radiation-sensitive torso. In addition, segmented designs similar to those found in advanced sports gear, such as the flexible panels in high-performance climbing suits, can allow for larger freedom of movement without sacrificing radiation protection.

3.2.2.2 Flaps for Increased Joint Mobility

Flaps have historically been used in various types of armor to improve mobility while protecting the human body. For instance, 15th-century plate armor used overlapping metal segments, known as lamellar armor, to improve mobility at the joints, such as hips and shoulders [48]. This design allowed knights to move more freely in the otherwise constraining armor. The design principles of medieval armor were themselves influenced by earlier Roman armor such as the lorica segmentata, and are still used at present in for example the shoulder pads of American football players [49]. In the context of the FLARE suit, flaps could serve two critical purposes: enhancing visibility by allowing parts of the suit to bend and shift away, and improving mobility. For example, by incorporating flaps at the shoulders and hips, the FLARE suit can improve arm and leg mobility without compromising on shielding. Flap design can be implemented in the FLARE vest by using water-bladder segments that are attached to the rest of the suit with only one attachment point. Additionally, areas where multiple attachment points are needed, slightly overlapping bladder segments can be used.

3.2.2.3 Scaled Outer Layer for Increased Flexibility

Another historical design for flexibility is scale armor, for example used in ancient Chinese and Roman armors, as well as observed in the natural world in creatures like the pangolin and certain species of fish [50][51]. These armors consist of overlapping scales that are flexible while also still providing robust protection. Testing in Spaceship EAC's laboratory has confirmed the feasibility of 3D-printing small scales onto a fabric layer. This opens up the possibility to include a hard outer layer in the suit without compromising on flexibility, which is advantageous for reducing puncture risks as well as for increasing the amount of possible material choices. When implementing scale designs on the suit, the flexural limitation should be taken into account when bending in concave areas of the body.

3.2.2.4 Second-Skin Fit for Increased Comfort

The FLARE suit should aim to feel like a second skin, moving smoothly with the body instead of feeling like a rigid external layer. Existing examples of athletic wear, such as Nike Pro Compression gear and Zoot triathlon suits, show that fabric technologies can achieve this type of fit by providing muscle support and reducing drag [52][53]. As the FLARE suit is bulkier than the typical athletic wear or wetsuit, the same snugly fit is much harder to achieve. Rather than that, the suit can be interpreted to feel more like an additional layer of mass, similar to extra body fat. This "second-skin" fit can be incorporated into the FLARE design in multiple ways. Firstly, stretchable fabrics such as Lycra or Spandex can be used to reduce drag with the body and provide muscle support. Additionally, elastic strap attachment is used instead of commonly-used rigid Velcro fastenings in order for the suit to fit a wider array of physiologies while keeping the suit snug to the body. Lastly, features such as flatlock seams can reduce chafing

and enhance comfort. Flatlock seams are flatly finished seams common in athletic wear and which reduce friction and irritation during movement.

3.2.2.5 Neutral Body Posture for Increased Ergonomics The neutral body posture (NBP) is the natural position the human body adopts in microgravity, where any other posture would require muscular effort.

Although most spacesuit designs are not based on a microgravity-based posture [3] [54] [55], the FLARE project adopts the NBP for several reasons. Primarily, FLARE suit's design toward enhancing ergonomics and comfort is driven by the limited flexibility of state-of-the-art vests PERSEO and Astrorad. This focus on posture allows astronauts to conserve energy, and reduces wearer's fatigue. In particular, during a Solar Particle Event, when astronauts might need to wear the FLARE suit for days, the importance of small ergonomic adjustments becomes increasingly important.

While adopting the neutral body posture is a logical choice, its practical application in the design process is not straightforward. Research on NBP is scarce, leaving the definition of a universal "neutral body posture" somewhat elusive. Over the past fifty years, only three major studies have been conducted, namely during the Skylab-4 mission (1973) [56], the Space Shuttle STS-57 mission (1993) [57], and an ISS mission (2019) [58]. Combined, these studies provided posture data for just nine astronauts (seven men and two women).

The most influential of these studies, Skylab-4 in 1973, recorded the NBP of three male astronauts, and the averaged results continue to inform space community designs today. These measurements shown in Figure 26 are the only ones to have been integrated into NASA's Human Factors and Health Technical Standards (NASA STD3000 & STD-3001) and the Human Integration Design Handbook (HIDH). However, this heavy reliance on a minimal dataset has led to a broad use of statistically insignificant results in applications from ISS workstations to car seats on Earth. For female astronauts, only a projected female neutral body posture was published in the Skylab report, derived from the male data. Since, no female NBP model has been developed.

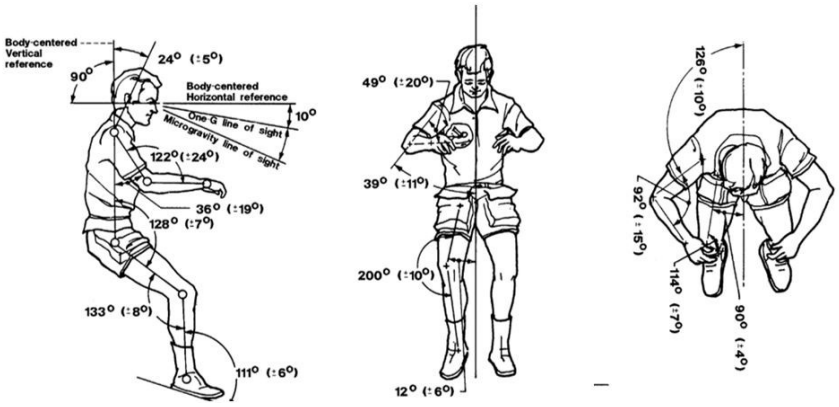

Figure 26: Schematic of the averaged neutral body posture as defined in NASA's Human Factors and Health Technical Standards (NASA STD3000 & STD-3001) and the Human Integration Design Handbook (HIDH). Data taken from 3 male astronauts on board the Skylab-4 mission (1973). Source: [56]

Table 8: Averaged Female Neutral Body Posture (N=2).

	Mean	Standard Deviation
Hip flexion	20.5°	8.5°
Hip abduction	5.25°	2.19°
Knee flexion	27.75°	16.25°
Ankle plantar extension	26.5°	11.5°
Neck flexion	11.5°	4.5°
Shoulder flexion	47.25°	11.25°
Shoulder abduction	32°	2.5°
Medial shoulder rotation	37.5°	11.5°
Elbow flexion	68.25°	10.75°

The lack of NBP data is particularly concerning given its widespread use in both space and terrestrial design over the past decades. The problem is worsened by findings from the 1993 STS-57 mission, which revealed significant variability in NBP between individuals [57]. This variability complicates the reliance on the 1973 male-only average as the basis for international standards.

A reliable female NBP model needed to developed for this thesis, as the male-averaged Skylab standard does not adequately represent female astronauts. This is important because the FLARE vest is designed for a female physiology, which is more sensitive to the effects of space radiation. Since no female NBP standard has been reported in the literature, this model was created using NBP measurements from the Space Shuttle STS-57 mission, which provides the only existing two female data points. The resulting body posture angles are presented in Table 8 and schematically represented in Figure 27. This female model allowed to create a virtual twin in the Blender software to base the FLARE suit design on.

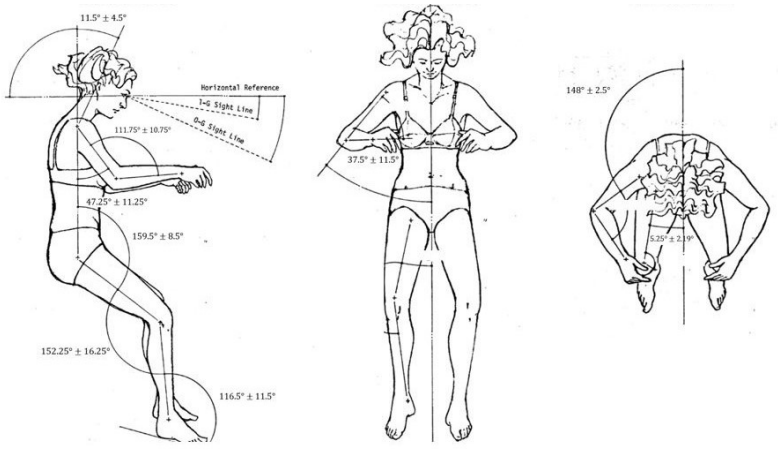

Figure 27: Schematic of an averaged female neutral body posture, calculated from the Space Shuttle STS-57 mission.

3.2.3 Outcome of the Prototype Design

Within the FLARE project, the initial prototype design was created virtually using the Marvelous Designer application, with the experience of Noora Archer at ESA, a visual artist at ESA specialized in fashion design. Marvelous Designer is a 3D computer graphics application used primarily for creating digital garments in the fashion industry. This software allows to experiment with digital garment design without the need for physical materials and provides a realistic preview of how the suit will look and move. Access to the software for the FLARE design was provided via Noora, who enabled the translation of the technical basis provided by the Frankenstein model to a feasible design using the design considerations in Section 3.2.2. The prototype design that resulted from this work is shown in Figure 28.

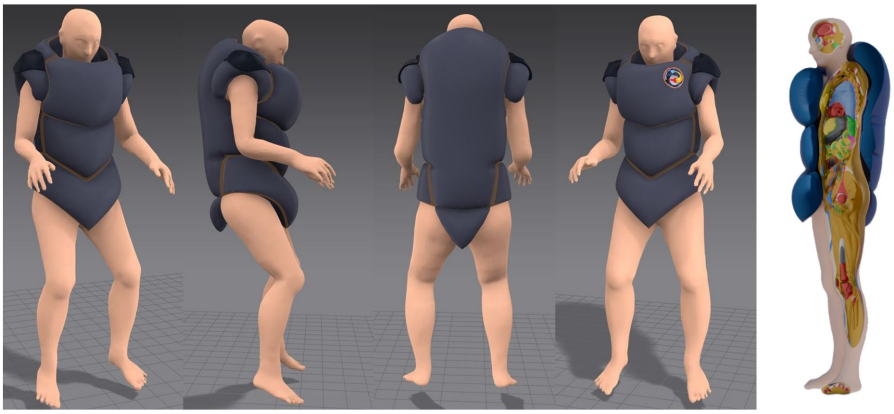

Figure 28: The first prototype design with ”Frankenstein” model of upper limit 11 cm as technical basis. On the right is displayed a vertical cross section of the design. †

Key design considerations discussed in Section 3.2.2 have been implemented into this first prototype design. First, the design is based on a female in zero-gravity neutral body posture: this means that the upper and lower legs and arms are bent inward, and the head and ankle are tilted downward. Next, the suit is segmented into smaller separate water bladders, each with adjustable valves to regulate water flow between sections. During filling, all valves are to be open which allows the suit to fill through one water entry point. During donning and wearing the suit, the valves are to be closed in order to avoid excessive water leaks in the case of puncturing of the suit. In the astronaut's front, the three main separate bladders have been created by horizontal division of the simulation-based optimization outcome. A horizontal division allows for increased bending mobility compared to any other segmentation, which is useful when bending the torso and legs closer together. Furthermore, flaps were introduced at the shoulders and pelvis. Flaps serve a similar aim as the segmented design does, namely increased joint mobility. Yet while the segmented design improves general flexibility throughout the suit by using movable bladders, flaps target mobility at specific arm and leg joints. For the shoulders, a system similar to the cantilever shoulder pad system in American football is used.

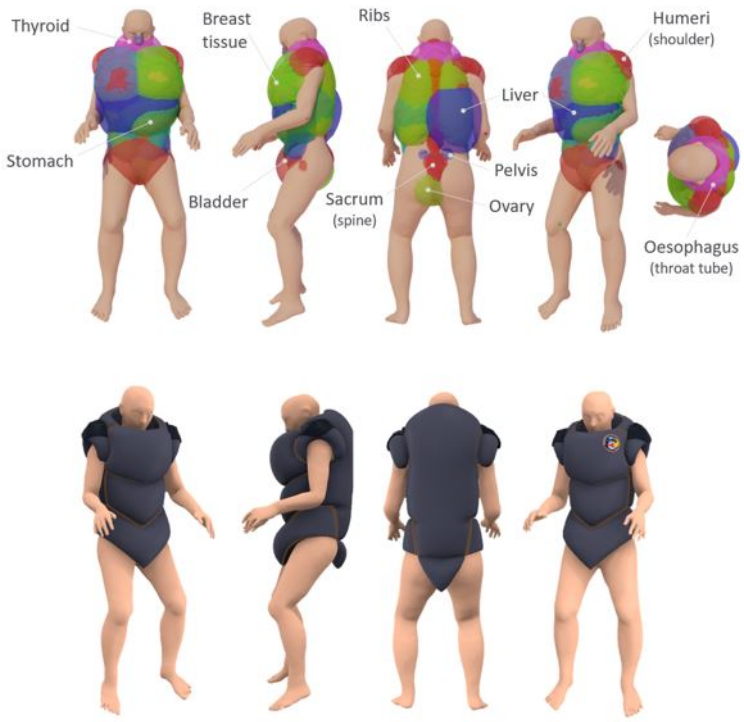

Figure 29: Comparison between the simulation-based results for the optimized suit topography (top) and the final design on FLARE's first prototype which has been derived from it. †

Lastly, additional bulk was added to the upper back torso region of the suit, as can be seen from the comparative visualization in Figure 29. The reason for this design choice is the concentrated nature of incoming Solar Particle Event radiation, which can be simplified as having a dominant angle of incidence. While the actual radiation pattern can be more complex, this assumption allows for practical optimization of shielding. In microgravity, astronauts can adjust their orientation relative to the incoming radiation, enabling precise control over their exposure angle. The preferred orientation is shown in Figure 30, where the astronaut positions their upper back torso at a 45° angle toward the assumed incoming radiation direction. This orientation is advantageous for two reasons: (1) placing the additional water bulk on the upper back avoids obstructing the astronaut's visibility and range of motion, and (2) minimizing the body's cross-section along the beam path allows internal tissues to act as additional shielding for deeper tissues.

The FLARE suit was calculated using Geant4 modelling software to be launchable as a compact 964g folded garment stored in a sealed transport bag. During use, the garment is unfolded, and the astronaut makes sure all interconnecting valves between the bladder segments are opened. The suit is then connected to the spacecraft's water supply, allowing it to be filled entirely up to a target volume of 36 liters. Once this amount of water is reached, the flow is stopped and the suit is disconnected from the on-board water source, after which all valves are carefully closed to prevent unintended water movement and to provide a countermeasure against severe water leak in the case of puncturing of the suit.

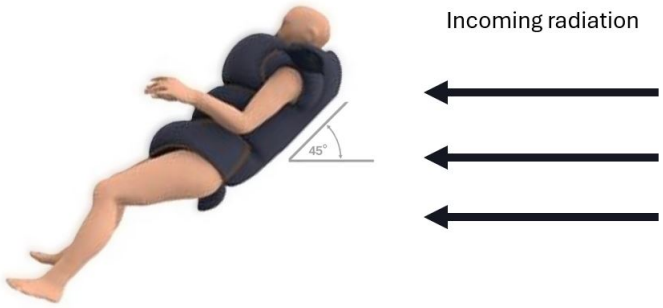

Figure 30: The astronaut is instructed to orient themselves in the FLARE suit at a 45° angle relative to the primary direction of incoming SPE radiation. Although the actual radiation pattern of SPEs is typically more complex, assuming a single dominant direction simplifies the scenario for practical implementation in this first iteration of the FLARE design.†

3.3 Suit Materials

The prototype design of the FLARE suit includes a multi-layer system, consisting of the functional layers listed below. In this section, the materials and implementation of each layer of the FLARE suit is further discussed.

1. Base Layer: Closest to the skin, this layer should manage moisture and support thermoregulation. Its primary function is to keep the astronaut's skin dry by moving sweat away from the body and towards outer layers.
2. Middle Layer: This layer contains water and is the primary layer aimed at shielding in the suit. To the extent possible, it should support flexibility and help regulate body heat using the natural water circulation.
3. Outer Layer: This layer serves as a protective barrier, shielding the astronaut from external hazards and wear-and-tear.

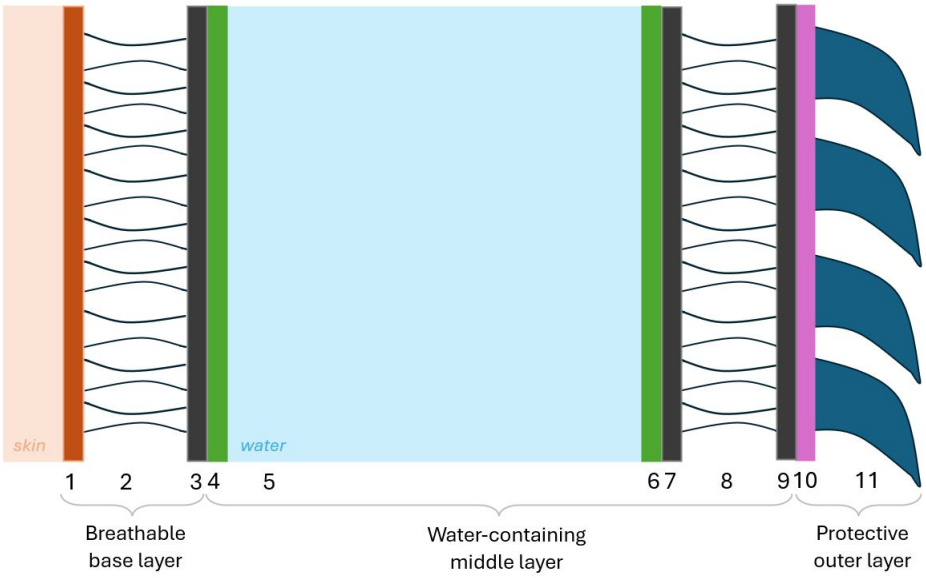

Figure 31: Visualization of the different layers of the FLARE suit prototype. Indicated are in the breathable base layer the (1) skin-adjacent hydrophilic supporting layer, (2) intermediate Spacer layer, and (3) hydrophobic supporting layer. In the water-containing middle layer are indicated the (4) TPU bladder layer, (5) water, (6) TPU bladder layer, (7) hydrophobic supporting layer, (8) intermediate spacer layer, and (9) hydrophobic supporting layer. In the protective outer layer, indicated are the (10) outer durable nylon layer and (11) a layer of hardened scales. For simplicity, the visualization is shown for uniform suit thickness.

3.3.1 Breathable Base Layer

A breathable underlayer is important for comfort, especially because the water bladders that form the primary shielding component of the FLARE suit are naturally constraining to the human body. An ideal undergarment material should maintain a dry and room-temperature environment on the skin while also act as barrier to the water within the suit. In addition, the vest contact layer should be flexible to follow the movements of the human body. Lastly, the undergarment should provide comfort to the astronaut by reducing friction with the suit [59].

Advanced materials are able to be integrated in the FLARE undergarment to achieve optimal comfort and flexibility. Currently, many Commercial off-the-shelf (COTS) available breathable fabrics still have limitations, including low integrity, insufficient air permeability, and limited water vapor transmission [60]. Therefore, a breathable undergarment using a three-layer spacer fabric structure is proposed for the FLARE suit. Spacer fabrics are a type of three-dimensional textile construction, where two outer layers of fabric are linked by a layer of spacer yarns [61] [62]. The spacer yarns of this intermediate layer consist of thousands of threads looped and bonded in-between the two surface fabric layers.

A schematic of the FLARE undergarment with spacer fabric is shown in Figure 32. The undergarment consists of an initial layer for moisture and heat release, an interior spacer layer for air flow, and a third outer layer which is adjacent to the water bladders. The skin-adjacent surface layer of the spacer fabric is made from hydrophilic yearn, able to attract and move moisture away from the skin. The interior spacer layer uses polyester monofilaments which are designed for cushioning and air-flow. This choice of polyester, compared to alternatives such as polypropylene and polyamide (nylon), is because it provides a balance between breathability, flexibility, and thermal resistance without compromising the structural integrity of the suit over time [63]. Polyamide and polypropylene would offer improved breathability and flexibility, but less durability which is prioritized for the FLARE suit.

The FLARE suit undergarment can be further improved with advanced materials. First, breathable fabrics like Polartec Alpha, which are known to enable airflow while providing insulation [64][65]. Hence, Polartec Alpha could be layered into the spacer fabric's outer layer to improve breathability. In addition, the skin-adjacent layer could incorporate materials such as Coolmax or Cocona, known for their cell-like air pocket structures that facilitate ventilation. Therefore, these materials will help in moisture control and friction removal of the FLARE suit [66]. Localized patches of D3O, a shock-absorbing material, could be added to high-impact areas such as the shoulders and knees. This will provide an extra layer of protection against any impacts [67]. Finally, phase-change materials like Outlast could be embedded within the middle layer of the spacer fabric to further optimize the thermal balance [68][69]. These materials can absorb excess heat generated during intense physical activity and release it when the astronaut cools down, keeping the wearer comfortable and thermally stable throughout their mission.

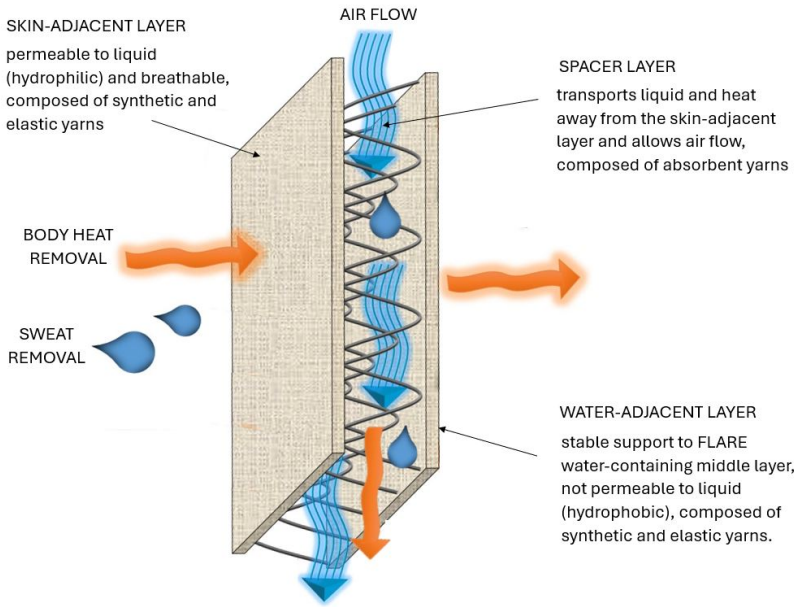

Figure 32: Schematic of the FLARE undergarment three-dimensional Spacer fabric textile structure, comprising of an initial skin-adjacent layer for moisture and heat release, an interior Spacer layer for air flow, and a third layer adjacent to the suit water bladders. Adapted from [70] with annotations by the author.

3.3.2 Water-Containing Middle Layer

The water-containing middle layer is the primary layer for radiation shielding in the FLARE suit, in addition to the protective outer layer which also has shielding capability. The design of the middle layer is built on several constraints: it must securely hold the water, prevent contamination, allow operational movement. The materials selected for the middle layer were chosen to balance these functional requirements.

To contain the water effectively, the inner component of the middle layer is made of thermoplastic polyurethane (TPU) [71] [72]. TPU is a suitable material because it is both waterproof and highly durable, meaning that the water remains contained with small leak probability, even under the physical stresses of space travel. Additionally, TPU's stretchability allows it to adapt to the dynamic movement of the astronaut, compressing and expanding with body movement without damaging the structural integrity of the bladders. A third advantage of TPU is its resistance to microbial growth, which prevents contamination of the water and the suit and is important for the repotability of the on-board water.

To prevent the water from pooling unevenly, the water bladders are divided into segmented compartments so that the water remains evenly distributed, adjusting to an astronaut's posture and movements. However, while TPU is ideal for containing the water, it alone does not provide this flexibility for ease of movement. Spacer fabrics can provide a solution instead.

Spacer fabrics, composed of two outer layers connected by a network of spacer yarns, will be integrated around the water bladders to improve the suit's flexibility. The 3D structure of spacer fabrics allows them to compress and expand with movement, to ensure the suit moves smoothly with the astronaut [73]. The material is also known to be breathable and lightweight, as discussed in Section 3.3.1. These characteristics are advantageous in terms of comfort, but the primary reason for being included in the FLARE suit is their ability to maintain the suit's shape while allowing for fluid redistribution within the bladders. Hence, the spacer fabric provides a *cushioning* effect, and is able to absorb stresses exerted on the bladders during movement, ensuring the water remains evenly spread across the suit. This will also reduce the likelihood of pressure points or rigid areas. However, spacer fabrics are not used for directly containing the water, as their breathability is incompatible with holding liquids. Instead, they serve as a supporting structure around the TPU water bladders to promote flexibility and cushioning.

In previous work of EAC-intern Sebastian Ruhlmann, the addition of salt within the water bladders was studied as a means to enhance protection against secondary neutron radiation [7]. It was found that salt-saturated water improves the efficiency of the water shield, offering an average increase in water layer thickness of five millimeters compared to pure water while providing the same protection. Ruhlmann calculated that this would reduce the FLARE suit's volume by 12.5%, but increase its weight by 43% due to the added salt. As a result, the addition of salt is currenlty considered inefficient: the suit becomes heavier, with only a slight reduction in thickness. In addition, there would be increased challenges in water recycling after use due to salt contamination of the pipes and recycling system. As such, the use of salt in the water bladders has been discarded for the FLARE suit.

The overall structure of the middle layer thus comprises two key elements: the inner TPU water bladders, and the intermediate spacer fabric for flexibility and support. Together, these materials form a system that will effectively contain and manage the water used for radiation shielding in FLARE, while also ensuring that the astronaut can move as freely and comfortably as possible given the constraints.

3.3.3 Protective Outer Layer

The protective outer layer of the FLARE suit is to provide shielding against punctures and abrasions, ensuring the integrity of the water-based radiation shielding system. This layer is composed of two key components: a durable fabric exterior and a layer of hardened scales, both working together as protective interface between the water bladders and its external spacecraft environment.

The outer fabric of the FLARE suit will be made from nylon ripstop or polyester, materials known for their durability and lightweight properties. Nylon ripstop consists of a reinforced grid pattern that prevents small tears from spreading, which makes it particularly effective for withstanding abrasions and impacts in the FLARE suit. For polyester can be expected a similar performance. Both fabrics give extra resilience to external wear and tear.

Figure 33: 3D-printed PLA scales on a fabric layer. The left image displays a fabric with PLA scales printed on its surface, while the right image shows the same fabric with scales bent to demonstrate flexibility of a hard material through considerate design. Produced in the Spaceship EAC laboratory with the help of fellow intern Louis Quinot.

The second protective component is a layer of hardened scales. This design takes inspiration from ancient armors, such as those used by Roman and Chinese warriors, as well as from natural protective mechanisms found in animals like the pangolin and certain species of fish. The bio-inspired scales are constructed from a solid material which is resistant to punctures and abrasions, in order to provide a robust barrier against sharp objects that astronauts might encounter when moving inside the spacecraft. By using overlapping scales instead of a rigid outer layer, the design preserves mobility, especially in convex body areas. While rigid, the scales do not inhibit movement because they are arranged to allow for flexion at the joints. This means that the scales can move as the astronaut bends or twists, and still maintain an effective protective layer against potential punctures that could damage the water bladders beneath. The concave insides of joints do not include scales when limiting to the astronaut's functional range of motion.

The hardened scales are primarily designed to offer flexible protection against puncturing; however, within this choice their material can also be selected for radiation shielding properties. Two main competing materials are considered for the FLARE suit. Firstly, the scales can be 3D printed from high-density polyethylene directly onto the nylon ripstop. This option would be easy to produce and testing in Spaceship EAC's laboratory has confirmed the feasibility of 3D printing small PLA scales onto a fabric layer, as shown in Figure 33. Iternatively, scales can be constructed from a composite material produced by Genevation Aircraft Ltd. This composite material is an epoxy resin-based carbon fiber prepreg composite (160 g/m², 50% epoxy ratio) that has come out as successful in FLARE's literature study. The carbon fibers are known for their exceptional strength-to-weight ratio, yet its production process is complex and costly, which may limit its applicability in broader contexts.

The overall structure of the protective outer layer thus comprises two key elements: a durable fabric exterior and a bio-inspired layer of hardened scales. The use of nylon ripstop for the outer fabric provides resilience against abrasions, whereas the hardened scales provide protection against sharp objects. During the testing phase in the HollandPTC accelerator (Section 4.1), the radiation shielding effectiveness of both potential scale materials is evaluated, leading to a decision on the most suitable option for the scale material based on their protective capabilities and usability.

3.4 Prototype Manufacturing

The construction of a physical prototype is an important step in the FLARE suit's design process, providing insights into its functionality and ergonomics of the suit before a full-scale production.

A physical prototype was manufactured in order to gather practical design feedback for the FLARE suit design. The resulting 1/4-scale FLARE prototype shown in Figure 34 was presented to four astronauts, together with two other 1/4-scaled designs using different attachment styles. This feedback loop is a vital part of the human-centered design process applied in the project. To this extent, the astronaut end-users were invited to provide feedback on key design elements such as the suit's water volume, mobility, and attachment points. The results of this testing phase are discussed in Section 4.2.

Figure 34: 1/4-scale FLARE suit prototype on displayed on a mannequin from multiple angles. Upper left: angled view showing the suit's overall structure and proportions. Upper right: front view. Lower left: side view. Lower right: shot of the partial donning process, showing the back section secured with a belt at the midsection, which is to be followed by the front flap closure.

A 1/4 scale model provides a useful approximation of the final suit's appearance and functionality, with the advantage of fast iteration and adjustments due to its scale. This is especially useful during the early engineering design process. However, while it offers a general sense of the suit's proportions and attachment mechanisms, some features — such as the bulk and weight distribution of the suit — cannot be fully anticipated at a smaller size. Additionally, the ability to evaluate certain aspects of mobility and comfort is somewhat constrained when working with a scaled-down version. Therefore, as the project progresses, full-scale prototypes will be required to assess feedback regarding fit and flexibility and refine the design further.

The 1/4-scale prototype was constructed using black cotton fabric, with foam material inserted as stand-ins for the more advanced material layers described in Section 3.3. While the cotton and foam do not replicate the complex water-containing layers and spacer fabrics of the final suit, they allow to focus on key mechanical and ergonomic questions without the added complexity of using the actual composite and water-based materials. In particular, they are sufficient for evaluating attachment points, openings, and overall fit. In addition, the foam allows to evaluate how the suit might drape and move with the astronaut's body. The cotton outer fabric of the prototype, while much simpler than the nylon ripstop and scaled materials planned for the final suit, gives a rough sense of how the suit might interface with the external environment and maintain the overall structure. The decision to use simulant materials is mostly a pragmatic one, as it allows to rapidly prototype and test without the need for complex and lengthy manufacturing processes. Once the attachment mechanisms and overall form are refined, future iterations of the prototype will incorporate more realistic materials, including water bladders and advanced fabric layers, to test the full functionality of the suit.

Moving forward, the prototype will need to evolve beyond its current 1/4-scale form and current stand-in materials. This will allow for more realistic testing of the suit's performance in terms of radiation shielding, thermal comfort, puncture resistance, and mobility. Future testing phases will also involve more extensive feedback from astronauts under realistic conditions, such as simulated space activities in microgravity environment (through a parabolic flight campaign), to ensure that the suit functions effectively in the space environment.

4 Testing

The FLARE project followed a phased testing approach, focusing in each phase on one or more key performances of the suit, including radiation shielding, astronaut functionality, and operational effectiveness. The testing has been performed in four distinct phases: proton accelerator testing, astronaut feedback testing, radiation simulation testing, and stratospheric balloon testing.

Proton accelerator testing

Stratospheric balloon testing

Radiation simulation testing

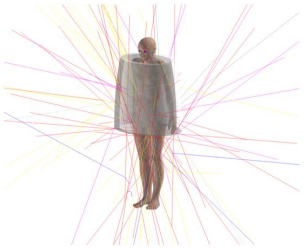

Astronaut feedback testing

1. **Proton Accelerator Testing**: The first testing phase evaluated several materials for their radiation shielding effectiveness. Six multi-layer samples, produced by Genevation Aircraft Ltd. in Hungary, were exposed to a low-energy proton beam at the Holland Proton Therapy Center. The goal of this phase was to characterize the dose deposition within materials and assess their potential for integration into the FLARE vest.

2. **Astronaut Feedback Testing**: The second phase of testing came forward from the project's focus on human-centered design, which draws attention to the importance of early and frequent user testing. Astronaut feedback was gathered during a series of focused one-on-one interviews to provide feedback with a focus on comfort, safety, and ease of movement. Astronauts included Matthias Maurer, Samantha Cristoforetti, John McFall, and Frank De Winne.

3. **Radiation Simulation Testing**: In the third testing phase, Geant4 simulations were conducted to assess the radiation shielding performance of the first FLARE vest prototype. This phase built logically on initial simulations conducted earlier in the design process, using a consistent environmental setup. Results are used to ensur the FLARE suit can meet the necessary standards for space missions.

4. **Stratospheric Balloon Testing**: During the final phase of testing, a stratospheric balloon flight was conducted to test the SensorConfetti device, an IoT sensor designed for real-time environmental data collection and data transmission. While the FLARE suit was not tested directly during this phase, the demonstration of successful communication of environmental data via SensorConfetti serves as an important step towards future stratospheric missions where the FLARE prototype is to be tested alongside a dosimeter and the SensorConfetti device, to simulate the complex mixed-field radiation environment of space.

4.1 Proton Accelerator Testing

4.1.1 The Aim of FLARE Accelerator Testing

Radiation testing was performed to assess the radiation shielding capability of a candidate material for the FLARE project, produced by Genevation Aircraft Ltd. in Hungary. Six multi-layer samples, considered for use in the radiation-protective FLARE suit, were exposed to a low-energy proton beam to characterize their radiation dose deposition. The interaction of these materials with proton beams was analyzed using dosimetric equipment typically used in medical radiation applications.

The experiments took place at the cyclotron-based **Holland Proton Therapy Center (HollandPTC)** in the Netherlands, which features a fixed horizontal proton beamline capable of delivering therapeutic proton beams ranging from 70 MeV to 250 MeV. A proportional counter system (PTWDosimetry) was set up downstream of the samples to measure the Bragg curves for appropriate FLARE suit thicknesses and compare them to the same setup without any material present. Water and PLA served as reference materials, and the normalized doses of the candidate materials were compared against these benchmarks.

The points of contact during the arrangement and execution of the proton accelerator testing were Marta Rovituso and Thomas Toet, R&D Beam Line Coordinator and Physics Technician at HollandPTC, respectively.

Figure 35: View of the R&D bunker at HollandPTC, featuring a fixed horizontal proton beamline from the ProBeam superconductive cyclotron for radiobiological applications. Source: HollandPTC.

4.1.2 Materials and Methods

4.1.2.1 Selection of the Candidate Materials The choice of candidate materials for this study was driven by a collaboration with Genevation Aircraft Ltd., who developed a composite material with enhanced radiation shielding properties under ESA contract (No. 4000135471/21/NL/CBi). Cooperation for radiation testing at HollandPTC was initiated following a literature review that highlighted the material's potential in the FLARE radiation shielding vest. Genevation's composite is based on an epoxy-carbon fiber structure, with several options for shielding-specific additives. As a hard material, it could complement the more flexible, water-based inner layers of the FLARE suit.

The selection of additives for testing was based on the principles of particle interaction physics. Unlike gamma or X-rays, protons primarily lose energy through inelastic interactions with atomic electrons, resulting in a rapid increase in energy deposition near their stopping point, known as the Bragg peak [74]. To optimize shielding, additives were chosen for their lighter nuclei and high density of free electrons, which enhance inelastic collisions while minimizing neutron production. For example, hydrogen would be a good additive as it has no neutrons, and also oxygen and carbon are prone to break down into helium nuclei without producing neutrons [75]. Finally, the choice of materials also factored in safety, cost, and availability in the trade-off for composite additives. The selected additives include Bismuth Oxide (Bi_2O_3) and High-Density PolyEthylene (HDPE). All selected samples for this study are listed in Table 9.

Table 9: List of Composite Materials Selected for Testing

Sample Number	Thickness [mm]	Sample weight [g]	Carbon weight* [wt%]	Epoxy resin* [wt%]	Additive B2O3* [wt%]	Additive HDPE* [wt%]
1	2.55	138	50	32	18	0
2	7.55	165	50	32	18	0
3	15.7	830	50	35	15	0
4	23.25	995	50	32	18	0
5	22.5	848	55	45	0	0
6	23.3	1000	50	30	0	20

In order to evaluate the shielding capability of the composite material provided by Genevation Aircraft Ltd., it is compared to well-known reference materials. As suggested by Kuess et al. [76], a material with a cross section similar to that of current space suit materials should be considered as a reference. Key examples include polylactic acid (PLA) and polyethylene, both organic polymers primarily composed of carbon and hydrogen atoms. Both materials have relatively low atomic numbers, which helps to minimize the production of secondary radiation. Given its potential for in-space additive manufacturing, PLA was selected as a reference in this test campaign (Table 10).

Table 10: List of All PLA Material Thicknesses Selected for this Study

Sample Number	Thickness [mm]
7	2.55
8	7.55
9	15.7
10	23.25
11	54.5

The thicknesses of the PLA and composite material samples were selected to provide nearly uniform spacing, giving similar intervals between the different layers. The selection is visualized in Figure 36, with alternative thicknesses offered by Genevation Aircraft Ltd. shown in grey.

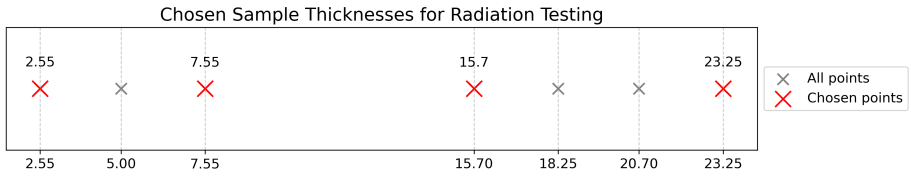

Figure 36: Visualization of the selected thicknesses for composite material testing.

4.1.2.2 Experimental Setup The effectiveness of the sample materials listed in Tables 9 and 10 to shield against high-energy charged particles was assessed by measuring their dose reduction. The proton beam characteristics used in this test campaign where chosen to serve as proxy for the radiation encountered during Solar Particle Events (SPEs). The chosen beam energies and their respective ranges in water are shown in Table 11.

Table 11: Selected Beams for Testing

Beam	Energy [MeV]	Range in water [cm]
Proton beam	120	11-12
	200	26-27

The experiments were carried out at the Holland Proton Therapy Centre [77], which specializes in cancer treatment. Beyond patient care, HollandPTC also serves as a research and educational institution. The ProBeam superconductive cyclotron at HollandPTC was used to irradiate the candidate material samples with protons at varying energies. Capable of producing proton beams with energies ranging from 70 to 250 MeV, the HollandPTC cyclotron is an ideal setup for simulating Solar Particle Events, as these bursts of high-energy radiation consist primarily of protons (95%) within this energy range.

The setup for an experimental campaign on radiation shielding needs to be well-considered. A diagram of the experimental setup used in this study is shown in Figure 37. From right to left, are represented: (1) the vacuum pipe exit window, (2) scattering foil, (3) beam monitor, (4) dual ring, (5) water sample, (6) composite material sample, and (7) Bragg peak chamber. In the configuration, a beam monitor chamber with an active area exceeding the beam profile (20 × 20 cm²) was placed upstream of the samples to quantify the flux of the incoming beam. The dose behind the shielding was measured using a Bragg peak chamber (type 34070 produced by PTWDosimetry), positioned as close as possible to the target, within a 1 cm distance. A scattering foil and dual ring were employed to achieve the desired pencil beam shape and profile. To facilitate measurements, samples were exposed to a pencil beam irradiation field. Statistical fluctuations were minimized by ensuring the pre-set threshold of 800.000 incoming protons was counted at the beam end.

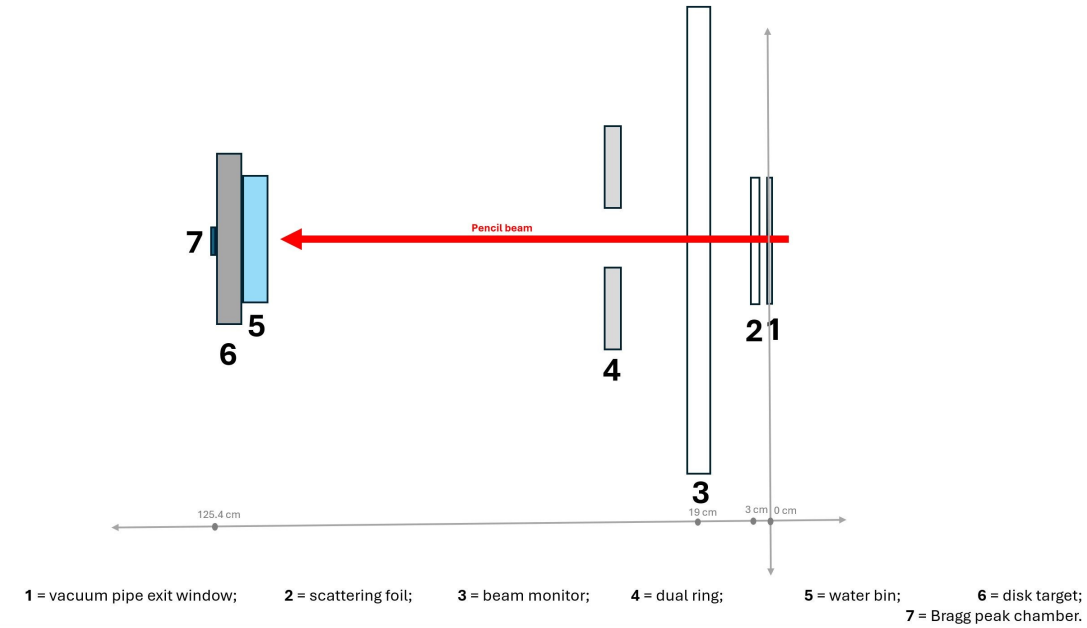

Figure 37: Illustration of the beam-line configuration and test setup for radiation experiments.

In the test campaign, no-target measurements were used to normalize the dose reduction measured for each sample. The experimental configuration was selected to measure the dose deposition of protons in the sample while reducing the influence of neutrons, which have a minimal interaction in the monitor chamber and proportional counter. Each test run was limited to approximately 12 minutes due to safety restrictions related to the cyclotron.

4.1.2.3 Data Analysis To evaluate the shielding effectiveness of a material target, normalized dose was measured as follows [75]:

$$\delta D = \frac{(D_{out}/D_{in})_T}{(D_{out}/D_{in})_0}$$

In this equation, D is the doses measured outgoing (out) and incoming (in) of the target material. The ratios D_{out}/D_{in} with the subscript T represent the values obtained with the target in place, and are normalized against data collected without the target (noted with subscript 0). This normalization aims to account for variations in dose caused by the experimental setup. A Bragg curve is obtained by plotting normalized dose against the thickness of the material.

Given that multiple target thicknesses were tested in this study, it is preferred to present the results in a depth-independent way. One approach is to express dose as a function of area density, where:

$$\text{area density } [g/cm^2] = \text{thickness } [cm] \times \text{density } [g/cm^3]$$

The characterization of the radiation shielding capability of a thin suit material is complex. Ideally, space suits should sufficiently reduce the dose to the body. However, protons do not lose energy gradually; instead, they release the majority of their energy near the end of their travel path, creating a Bragg peak. Since suit materials are often not thick enough to fully contain the Bragg peak, introducing any suit material into the beam path shifts the peak's location within the body rather than remove it. As a consequence, a poorly selected material thickness could move the Bragg peak toward sensitive tissues or organs, potentially causing more damage than if no shielding material were used.

The complexity of analyzing radiation properties of suit materials leads naturally an the implementation of experimental methods typical to (medical) particle therapy dosimetry. While a classical shielding dosimetry approach would focus on quantifying dose reduction at each given thickness, a more relevant measure for space suit materials can be the water equivalent thickness (WET). WET refers to the thickness of water that would cause protons to lose the same average amount of energy as they would when passing through the material being evaluated [78] [79]. The Water Equivalent Thickness (WET) is calculated by:

$$WET = d \times \frac{S_{material}}{S_{water}}$$

where d is the physical thickness and S is the stopping power of the material, defined as:

$$S(E) = -\frac{dE}{dx}$$

In this context, $S(E)$ represents how much energy E is lost per unit distance x as a proton travels through the material. The ratio of stopping powers indicates how the material compares to water in terms of energy loss.

By characterizing the WET for target space suit materials, they are essentially considered as a bolus in radiation oncology. A bolus is a material placed on a patient's skin to move the Bragg peak closer to the skin's surface during particle therapy, improving the treatment for superficial tumors [80]. In radiation oncology, the WET of various materials is determined to characterize which bolus is able to shift the Bragg peak in the most beneficial way for the patient. Similarly, the WET of the space suit target materials in this radiation test campaign is determined in order to optimize the Bragg peak shift inside the astronaut during a space radiation event.

4.1.3 Experimental Results

The normalized Bragg curves for water target material in 120 MeV and 200 MeV proton beams are shown in Figure 38 and Figure 39, plotted as a function of water thickness (mm). These curves were obtained through simulation using the Geant4 Monte Carlo code with water phantom [81]. Measurements obtained at the HollandPTC facility were placed on the graphs using an error-minimizing normalization to the Bragg peak dose.

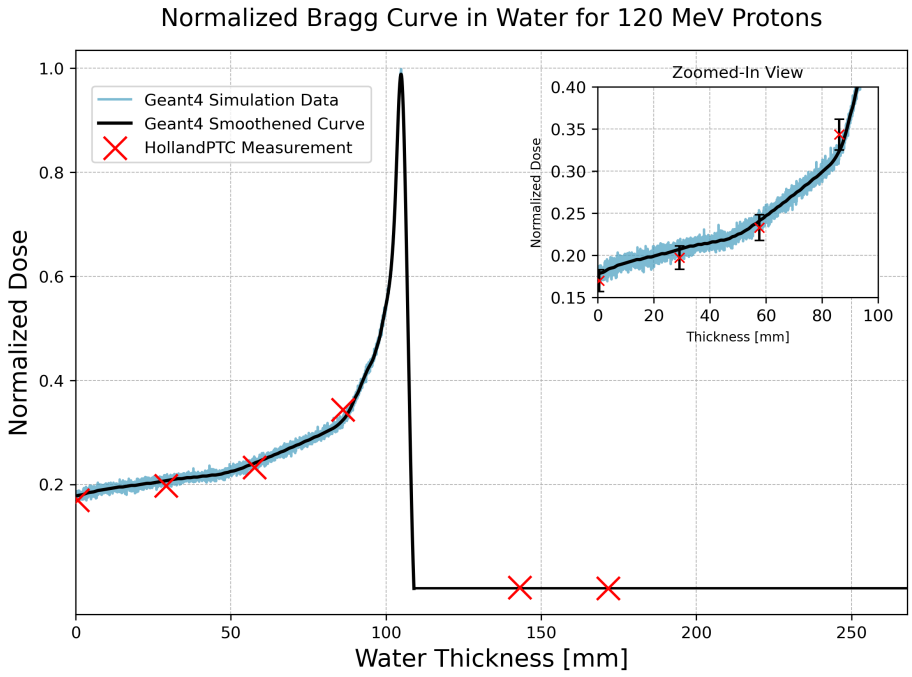

Figure 38: HollandPTC measurements compared to full Bragg peak curves for a 120 MeV proton beam in water, based on Geant4 Monte Carlo simulation. The upper plot magnifies the dataset up to a depth of 100 mm, for comparison of dose deposition in the initial stages.

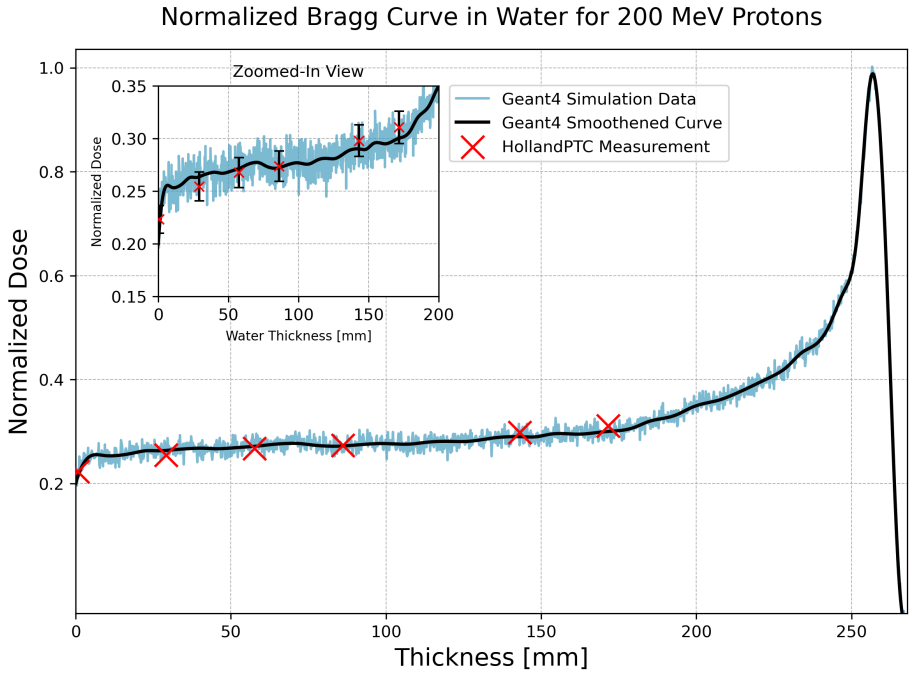

Figure 39: HollandPTC measurements compared to full Bragg peak curves for a 200 MeV proton beam in water, based on Geant4 Monte Carlo simulation. The upper plot magnifies the dataset up to a depth of 100 mm, for comparison of dose deposition in the initial stages.

The partial Bragg curves for various target materials are shown in Figure 40, plotted as a function of thickness in g/cm². Measurements for greater thicknesses were not conducted, as the test campaign focuses on assessing materials for the FLARE suit, where larger thicknesses are impractical for operational use.

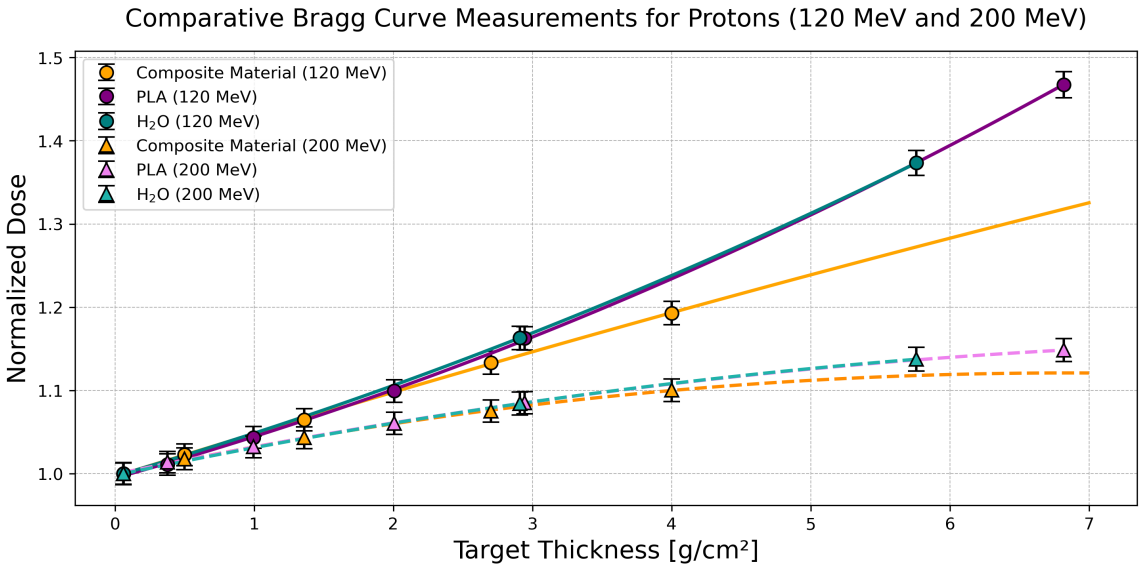

Figure 40: Partial Bragg curves of 120 MeV and 200 MeV protons in the composite material, PLA and water.

The differences in dose reduction among the additives are illustrated in Figure 41.

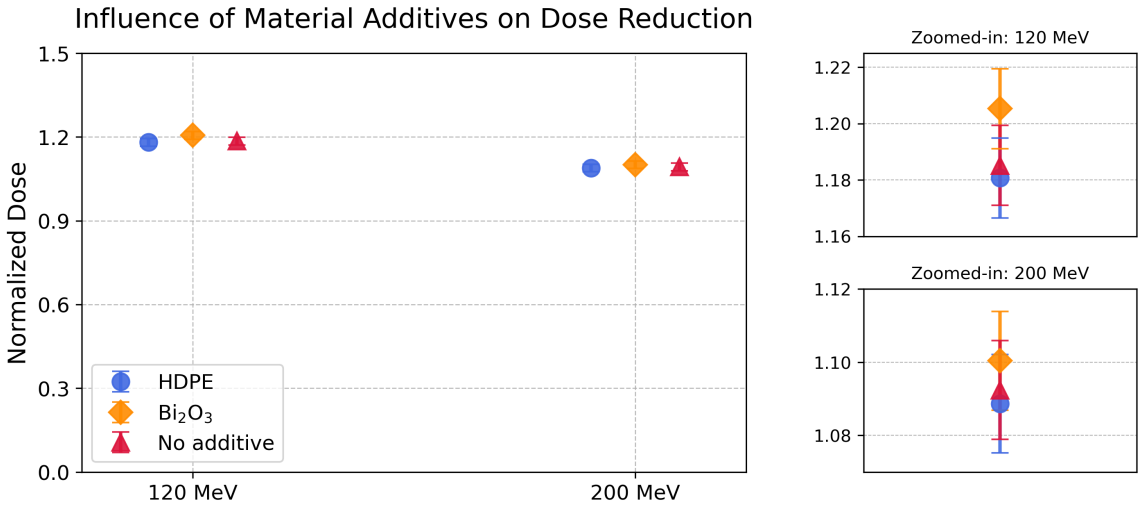

Figure 41: Normalized dose reduction for a 120 MeV and 200 MeV proton beam of the composite material with HDPE additive (blue), Bi2O3 additive (orange), and without additive (red). The precise dose reduction values and their error are shown in the zoomed-in side graphs (right).

Figure 42 displays the impact of reversing suit materials on dose reduction for 120 MeV and 200 MeV proton beams. In the “normal order,” the proton beam first passes through the composite material, followed by 5.8 cm of water, representing the design scenario of the water-filled FLARE suit with hardened shielding as the outer layer. In the “inverted” configuration the proton beam passes the water first, followed by the composite material.

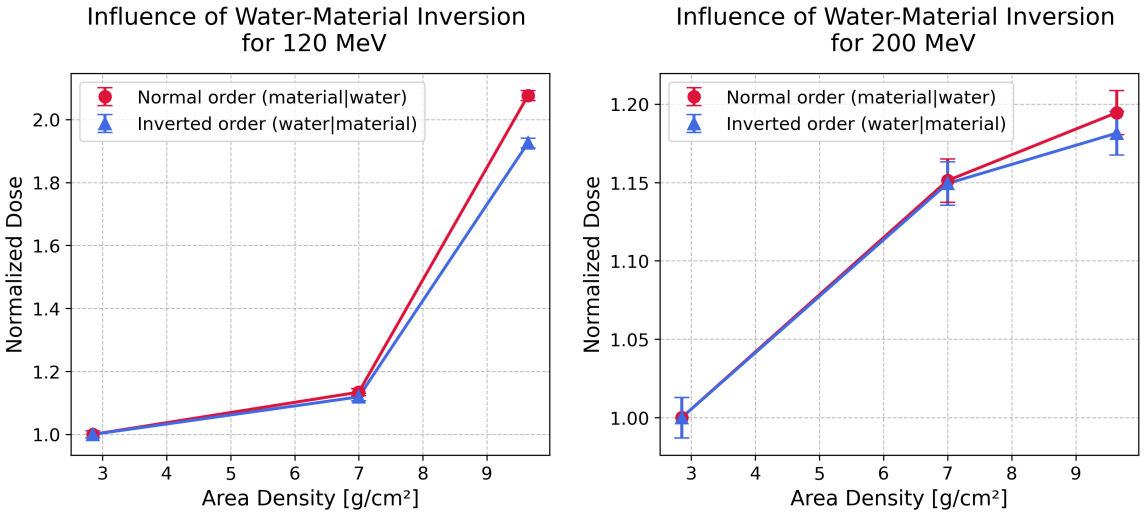

Figure 42: Dose Reduction of inverted configurations of composite material and water when exposed to a 120 MeV (left) and 200 MeV (right) proton beam.

4.1.4 Analysis of Experimental Results

4.1.4.1 Water Target: Conformity with Theory The Bragg curve measurements with water target (Figure 38 and Figure 39) give a general indication of the correspondence of the experimental measurements at HollandPTC with simulated results by the Geant4 toolkit [81] and with available data by the United States National Institute of Standards and Technologies (NIST). As seen in the figure, there is generally a strong agreement between the experimental and simulated values. This good correspondence means the integration of the radiation campaign in the existing research landscape is justified.

4.1.4.2 Composite Material Targets: Characterization of Shielding Capability The Depth Dose Profiles (partial Bragg curves, Figure 40) measured with proton particles at 120 MeV and 200 MeV give insight into the radiation shielding properties of the target material. The composite material has a comparable trend in the plateau region, with values that are near those of the reference materials PLA and water at a given depth. The Bragg curve of the composite material has a slight tendency towards lower dosages as in the other materials, which can be seen for both 120 MeV and 200 MeV proton beams. This indicates energy depositions deeper in the body when compared with water and PLA. This characteristic of the composite material suggests that the radiation shielding capability for water and PLA is better than for the composite material, though the difference is minimal for small composite material thicknesses relevant to the FLARE suit.

For a proton beam at 120 MeV and 200 MeV, inelastic processes dominate: the Bragg peak is primarily driven by the increasing energy loss due to ionization and excitation as the protons slow down, with limited contribution from nuclear interactions. In the plateau region of Figure 40, the slope of the curve is influenced by the material's effectiveness in interacting with atomic electrons; the greater the interaction, the more noticeable the increase in dose. The trend indicates that in the composite material less inelastic interactions occur between the proton beam and the material's atomic electrons, through the difference with the reference materials PLA and water is minimal.

The Depth Dose profiles allow to conclude that all considered shielding materials behave in a similar way, although some slight differences are found. This corresponds to a similar trend which is visible from the material ranking in Figure 43 computed by Vuolo et al. [3]. The material ranking shows the classification of classical shielding materials based on the dose equivalent reduction after a thickness of 5 and 11 g/cm² of material. Polyethylene ranks first due to its high hydrogen content (approximately 14%) and the lack of heavy atomic elements, with only carbon making up around 86% of its composition [82]. The shielding capability of PLA in this test campaign is slightly less effective for radiation shielding compared to polyethylene, due to its lower hydrogen content. The shielding classification of PLA is instead comparable to water, which ranks third in the classification after polyethylene (in first position) and the fatty acids (in second position). The classification of the composite material can be induced based on the other available materials in this list. The material is composed of 50% carbon fiber, 30% epoxy resin, and 20% Bi_2O_3 or HDPE. While its carbon fiber and epoxy components provide structural integrity, their radiation shielding capabilities are comparable to materials like Kevlar and Nomex, which are ranked lower in shielding efficiency due to their limited hydrogen content and lack of heavy elements. However, the inclusion of bismuth oxide significantly enhances its performance, particularly against high-energy gamma radiation. Therefore, the material is estimated to be ranked between Kevlar+Epoxy(20%) and Epoxy in the classification displayed in Figure 43.

Data collected for different variants of the composite material provide an indication of the material behaviour with different additives, as shown in Figure 41. The results for the HDPE additive, Bi_2O_3 additive, and the no additive case present similar depth dose characteristics for both 120 MeV and 200 MeV proton beam energies, with only a slight increase in dose for the Bi_2O_3 additive.

Data shown in Figure 40 were used to calculate the WET of the composite material for a 120 MeV and 200 MeV proton beam (Table 12). As specified in Materials & Methods, the characterization of these WET values allows the usage of design processes that are well-defined in medical particle therapy, for the choice of suit material and thickness in radiation shielding solutions such as FLARE. Indeed, space suits can be compared to the bolus in radiotherapy, as they do not fully block dose deposition but instead strategically shift the depth at which the highest dose is delivered. In radiotherapy, the thickness and material of each bolus is carefully designed for a patient's dose plan in order to obtain a water equivalent thickness which positions the Bragg peak in the preferred place inside the patient's body. Similarly, the composite material's WET values allow for a quantified analysis of the suit thickness for different body parts, given a more elaborate Bragg peak data acquisition.

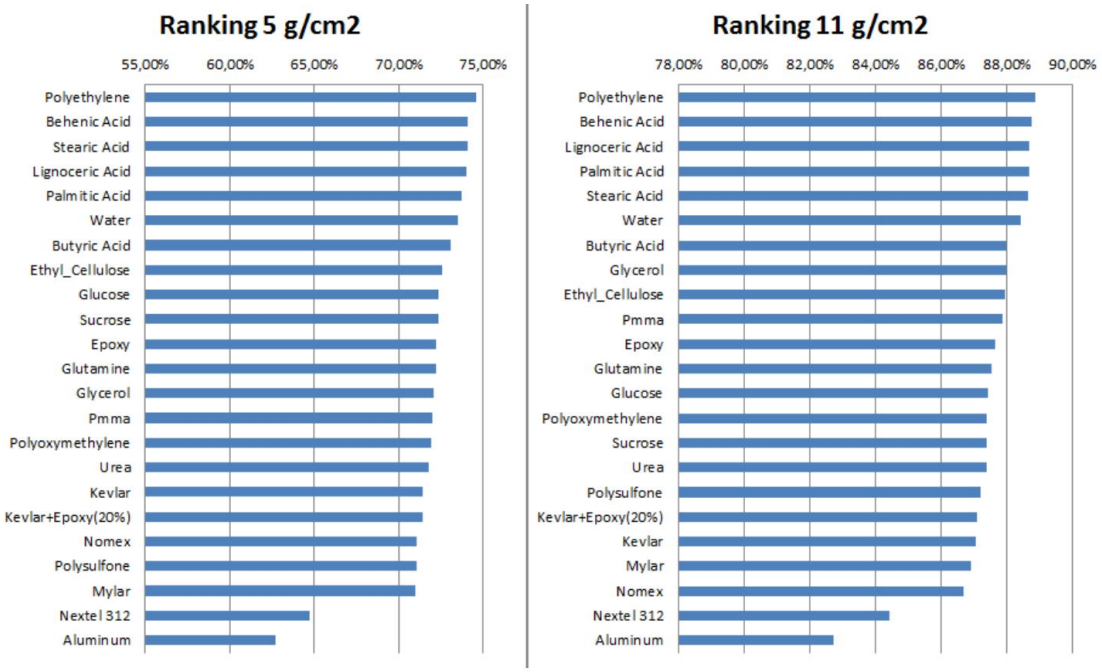

Figure 43: Material ranking based on dose equivalent reduction for two fixed shielding layer masses (5 g/cm² and 11 g/cm²). Source: [3].

Table 12: Water Equivalent Thickness of the Composite Material and Water/PLA References

	WET (120 MeV) [cm]	WET (200 MeV) [cm]
Water	1	1
Composite material	0.88	0.9
PLA	0.97	0.98

The WET of the composite material, measured at 120 MeV and 200 MeV proton beam energies, is approximately equal to that of water, with minimal differences (0.88 cm vs. 1 cm at 120 MeV and 0.9 cm vs. 1 cm at 200 MeV). This similarity suggests that, for the thicknesses considered in the FLARE suit design, water and the composite material can be used interchangeably. Given that the suit is composed of water bladders of organ-specific thickness, the established simulations for determining the optimal thickness for each organ can remain valid. The composite material can be integrated as part of the shielding, allowing flexibility in the design by substituting water with the composite material where necessary. For example, water, being more flexible, could be preferred in areas requiring flexibility, while the composite material could be utilized in areas prone to puncture risk due to its rigidity and structural strength.

Since the composite material shows comparable proton shielding to references PLA and water at the studied thicknesses, other considerations important in suit design naturally come to the forefront. Of the studied materials, water offers clear advantages due to its availability on human spacecraft and the flexibility it provides to the wearer. PLA and polyethylene, on the other hand, can be 3D-printed into complex shapes like pangolin scales to enhance flexibility in otherwise stiff areas of the suit. Additionally, the ability to be 3D-printed makes them practical for on-board repairs

or repurposing when suit pieces are degraded or broken. In contrast, the composite material lacks this adaptability and does not offer the same ease of integration into suit designs which require mobility.

While the composite material has promising characteristics for space radiation shielding purposes [83], it cannot be concluded that the material outperforms the chosen reference materials in their radiation shielding capability. Furthermore, its limited flexibility and adaptability compared to materials such as polyethylene make it less suitable for the FLARE suit, where water and 3D-printed polymers offer superior performance. Based on the outcome of this test campaign, and for the FLARE suit, it can be concluded that water and PLA/polyethylene are preferred as suit materials over the studied composite material.

4.1.4.3 Combined Water and Composite Material Target: Influence of Configuration Inversion

When the two configurations representing a normal and inverted suit (Figure 42) were exposed to a proton beam of 120 MeV and 200 MeV, they showed similar shielding effectiveness. A decrease in dose is observed when the composite material is substituted behind the water sample, which corresponds to the material being positioned as inner layer of the suit, instead of as outer layer. This result implies that energy depositions of the proton beam may occur slightly deeper in the body for an inverted configuration. This characteristic of the inversed configuration suggests that the radiation shielding capability is not improved when the composite material serves as inside later of the FLARE suit rather than as outside layer.

4.1.5 Key Takeaways from Accelerator Testing

The assessment of the composite material developed by Genevation Aircraft Ltd. has concluded that, despite its innovative design and the incorporation of potential radiation-shielding additives, it is not the most suitable candidate for implementation into the FLARE astronaut suit.

The radiation campaign conducted at HollandPTC demonstrated that the shielding effectiveness of this composite material is generally comparable to existing materials such as PLA and polyethylene, which are already utilized in space applications. However, the composite material exhibits a slight tendency for lower energy deposition compared to the water and PLA reference materials, indicating that more energy deposition occurs deeper within biological tissues.

In general, an inward shift of the Bragg peak towards more critical organs can pose significant risk and should be avoided. In order to quantify this potential risk, a Bragg curve analysis is advised for candidate suit materials, allowing for a careful characterization of their induced radiation dose deposition within the human body. This analysis can be performed through experimental or simulation-driven testing. During this analysis, it is important to note that generalizations of the observed effects of proton irradiation must be made reasonably, as body proportions can vary significantly among individuals.

Furthermore, the experimental data indicates that the composite material facilitated fewer inelastic interactions between incoming high-energy protons and atomic electrons compared to PLA and water. This outcome aligns with expectations based on the composite's formulation, which consists of 50% carbon fiber, 30% epoxy resin, and 20% bismuth oxide/HDPE. While the carbon fiber and epoxy contribute to the material's structural integrity, their low hydrogen content results in reduced effectiveness in minimizing proton energy deposition compared to materials like polyethylene and PLA, which have a higher hydrogen content.

Overall, complete protection from proton bombardment in free space cannot be expected from these or similar materials due to a thickness limitation for operational mobility in FLARE. This is also in agreement with previous measurements on space suit designs [76]. It is important to note that the primary consideration when choosing materials for space suits is not always their radiation shielding effectiveness, as effects can be minimal between the materials compared to vastly different material properties. As such, studies on IVA space suit design should instead prioritize the material's ability to improve operational mobility, logistical considerations, and space readiness. Nevertheless, quantifying the performance of materials under the experimental influence of Solar Particle Event proton radiation will remain a central focus of the post-thesis continuation of this project.

4.2 Astronaut Feedback Testing

4.2.1 The Aim of FLARE User Feedback Testing

User testing allows for direct input from astronauts, who are the intended end-users of the system. It provides insights into practical considerations that may not naturally be evident for a designer or engineer during the design phase.

For the FLARE project, user feedback was obtained from several astronauts with diverse experiences and expertise. These included **Matthias Maurer**, who had worn the competitor AstroRad suit and brought relevant insights from his work at ESA's LUNA facility for FLARE suit maneuverability; **Samantha Cristoforetti**, whose perspective as sole female astronaut was important for evaluating the suit's requirements, particularly since the design process prioritized a model tailored for female astronauts before considering male models; **Frank De Winne**, astronaut and head of the European Astronaut Center (EAC), whose regulatory and logistical knowledge provided an overview of what is required to make the suit flight-ready; and **John McFall**, the first parastronaut candidate, who has experience as an orthopedic surgeon and a unique perspective on adaptive design.

The feedback of the astronauts is important in a high-stakes project like FLARE, because it ensures that the suit is not only functional and comfortable but also meets other specific needs of astronauts. By adopting this user-centered approach early in the development process, risks further down the process are minimized and the suit is more likely to meet astronauts' needs.

4.2.2 Testing Protocols

Structured discussions with the four astronauts were conducted in a series of focused one-on-one interviews, lasting approximately an hour each. The sessions began with a brief overview of the FLARE project and the suit's conceptual design, followed by a guided discussion on specific aspects of the suit. Each session included tactile and visual aids, such as the 1/4-scale prototypes and design sketches, to facilitate feedback as is shown in Figure 44.

Human-centered design principles were applied during these discussions based on specific recommendations provided for the FLARE project by Guy André Boy, former Chief Scientist for Human-Centered Design at NASA Kennedy Space Center. Human-centered principles in the discussion included collaborating with astronauts as active rather than passive partners in the design process, which meant that astronauts were not just providing feedback after being posed a question; they were involved in the brainstorming and helped identify potential usability issues, such as comfort, range of motion, and overall functionality. Additionally, attention was paid to how they interacted with the 1/4-scale prototypes. It was also recognized that astronauts' past experiences with other suits would shape their expectations, making it extra valuable to understand their previous experiences thoroughly. A detailed overview of these recommendations is given in Section 2.8.

Three key aspects of the FLARE suit were emphasized during these discussions:

- **Comfort**: Astronauts shared their experiences with previous suits, providing insights into how materials, fit, and weight distribution affect overall comfort during extended wear.
- **Safety**: The astronauts discussed safety features that would be important in emergencies, such as quick-release mechanisms and the ability to remove the vest rapidly. Insights into the visibility and access to emergency equipment while wearing the suit were also considered.
- **Maneuverability**: The suit's design was evaluated for ease of movement and donning/doffing in confined spaces of the ISS and Lunar Gateway architecture.

Figure 44: On the left, astronaut Samantha Cristoforetti is shown the 1/4-scale FLARE suit prototypes during a feedback session, where she was able to closely observe the features and provide insights based on the physical models. On the right, parastronaut candidate and orthopedic surgeon John McFall reviews the "Frankenstein Model" visualizations, which show the Geant4 simulation outcomes for radiation effects on organs.

All feedback from the end-user discussions was temporarily recorded with permission of the individual and carefully documented after the sessions. Detailed notes were made to capture clearly the key points from each conversation. After gathering the feedback from each of the four sessions, each session was analyzed deeper to identify common themes. In cases of differing opinions, sometimes further discussions were held to better understand the different views and find a balanced approach to the design suggestions that were made.

4.2.3 Astronaut Feedback on FLARE Prototypes

This section presents a summary of common themes and areas where astronauts expressed suggestions or concerns about the FLARE prototype. This includes areas where astronauts expressed similar opinions as well as themes with differing viewpoints.

In alignment with the General Data Protection Regulation (GDPR) requirements established by ESA, measures are implemented to protect the personal data of the astronauts involved in this study. In the remainder of this section, feedback is attributed to anonymous identifiers "Astronaut A," "Astronaut B," and so forth, so that no identifiable personal information is disclosed.

4.2.3.1 A Moisture and Heat Removing Undergarment The FLARE undergarment is a base layer to be worn under the FLARE suit, which wicks moisture and heat away from the skin. All astronauts agreed with the need of a breathable inner layer to manage moisture effectively. Astronauts A and Astronaut C specifically noted that moisture buildup can lead to discomfort and temperature fluctuations, reinforcing the need for materials that wick moisture away from the skin. Astronaut A noted that plastic-like materials in the AstroRad suit led to sweat accumulation, causing coldness when stationary and overheating during movement. Astronaut C recommended materials like Merino wool, which absorbs moisture while remaining breathable, and neoprene, often used in wetsuits. He advised against materials with high polyester or nylon content due to their potential to trap moisture and create a damp environment against the skin, which can lead to skin irritation.

4.2.3.2 A One-Size-Fits-All Vest? The idea of a one-size-fits-all design for the FLARE vest has received mixed feedback from astronauts. Astronaut A supports the idea of a one-size-fits-all baseline FLARE vest that comes with adjustable water bags that can be added on top, which would allow it to be used by all astronauts. He thinks this layering approach, similar to layering clothes, would work well for different body types and different emergency scenarios. He recommends that in case of a modular design, the add-on bladders should be designed for attachment while in the Orion shelter during the SPE storm, when the base layer of the suit has already been assembled. This approach would streamline the process of donning in the limited time between alarming of the SPE and its arrival at the spacecraft. Astronaut B also disagrees with the one-size-fits-all concept, though for another reason. She points out that the Russian Orlan space suit is the only example she knows of, and she finds it uncomfortable and not well-suited for astronauts. She also mentions that many existing space suits do not fit typical female sizes, especially for smaller astronauts. This poor fit can limit movement and visibility. Astronaut B believes that newer space suits are being

designed with a wider range of sizes in mind, which is a positive change. Astronaut D suggests offering the vest in three sizes: Small, Medium, and Large, though he is unsure if the adjustable pieces will also come in different sizes.

4.2.3.3 Water Supply of the FLARE Suit Two astronauts highlighted the need for the FLARE suit to be able to reclaim and purify water after use in the suit, especially since the Lunar Gateway will lack filtration systems in its early stages. Astronaut A emphasized the need for the suit to reclaim and purify water so that it can be made drinkable. This is particularly important because the Orion module on the Lunar Gateway doesn't have a system for filtering water, unlike the current systems on the ISS. Astronaut D added that the FLARE suit could use different types of water: waste water, cooling water, and drinkable water. However, he cautioned against using drinkable water due to the risk of contamination from the suit's materials, which could make it unsafe for reuse. He recommends creating a system that connects to waste water for the early stages of the Lunar Gateway, when water recycling will not be available.

4.2.3.4 Operationability of the FLARE Suit The astronauts provided various insights on the operational design of the FLARE suit. Astronaut D stressed the importance of anchoring during donning, mentioning that the secured belt is handy to prevent the suit from floating away in microgravity. He also appreciated the prototype for minimizing loose components, which reduces the risk of entanglement. Astronaut A supported this by highlighting the need for an intuitive and symmetrical design to ensure astronauts can don the suit quickly, especially in emergencies. He emphasized that quick removal is also vital in life-threatening situations, like fires or leaks, where maneuverability is essential. Astronaut B added that visibility should be maintained during the donning of the vest and also emphasized the need for the suit to accommodate toilet use during solar storms, either by allowing quick removal or by enabling the use of diapers underneath. Both Astronaut A and Astronaut B agreed on the importance of designing the suit to facilitate simultaneous use of the suit and a diaper while ensuring easy access to the toilet on the ISS. Astronaut C contributed by suggesting the attachment of shoulder coverage directly to the undergarment with Velcro for improved maneuverability. He also noted the significance of considering the suit's weight during donning in microgravity, as a heavy suit could create momentum that moves the astronaut toward the suit rather than the other way around. He stressed that teamwork should be expected, allowing one astronaut to assist another during donning while ensuring the design permits solo donning with some effort. Lastly, Astronaut C proposed incorporating pangolin scales in the back of the suit to enhance flexibility and reduce the risk of leaks, supporting the idea that segmenting the back bladder could improve safety and comfort. Astronaut A also pointed out the necessity for testing and verification to ensure the suit is compact enough for maneuvering in confined spaces, such as the Pressurized Mating Adapter (PMA) and other docked vehicles. He raised concerns about the potential for bulky designs to hinder movement in tight quarters like the Orion module.

4.2.3.5 Suit Attachment: Straps The group presents mixed suggestions about the attachment methods of the suit to the body. In general, they agree that flexibility (giving options to the astronaut) is ideal to account for different astronaut preferences. Astronaut A positively reviewed the idea of using Velcro on an elastic strip, noting that this approach could accommodate multiple body sizes

and keep the vest close to the body, which he hadn't seen in previous designs. Astronaut A further stressed the need for the vest to fit closely to the body and have minimal edges to avoid accidental disconnections of cables and equipment, a common challenge in microgravity. Astronaut B echoed the idea of offering astronauts choices in the design, allowing them to select the attachment method that works best for them. Astronaut D concluded that flexibility in suit attachment methods is essential, as different crew members will have varying preferences and needs, similar to how people use different setups on Earth. Astronaut B emphasized the importance of elastic attachments to the legs or belt, highlighting that suits floating upwards in microgravity can limit visibility and maneuverability. She pointed out that astronauts often experience this issue with their T-shirts and trousers on the ISS. While she acknowledged that attaching the suit to the legs might be uncomfortable for male astronauts, she recommended providing options for both leg and belt attachments.

4.2.3.6 Additional FLARE Features: Adding Tools and Pockets The group provided input on practical features for tools and personal items to improve the FLARE suit. Astronaut A recommended incorporating Velcro strips and hooks for attaching tools, suggesting that the soft side of the Velcro should be on the suit's exterior to prevent snagging on spacecraft surfaces. He also advised that if a hook-and-loop system is used, the loop side should be attached to the suit to avoid accidental entanglement in confined spaces. Astronaut A emphasized the need for a dedicated pocket for personal dosimeters, as these items are specific to each astronaut and should be kept separate from the one-size-fits-all suit to prevent confusion about data ownership. Astronaut D supported the idea of tool attachment, suggesting pockets as a possible solution, while Astronaut C agreed that using Velcro for storing tools and equipment is a valuable addition to the suit's functionality. Astronaut B cautioned against elastic Velcro attachments getting caught on racks and items within the space station

4.2.3.7 Color Coded Add-On Water Bladders The astronauts agree that color coding the add-on water bladders would enhance clarity and efficiency during donning.

4.2.3.8 Adding a Helmet to the FLARE Suit The astronauts collectively agree on the importance of adding head protection to enhance the safety of the FLARE suit. Astronaut A expressed the need for a detachable helmet to provide essential brain protection while addressing potential issues with reduced situational awareness and compatibility with standard emergency masks used on the ISS. He noted that these masks cover the nose, mouth, and chin, suggesting that the helmet should detach easily, possibly through Velcro strips. Astronaut B agreed with these remarks. Given that the design for the Lunar Gateway's mask is still under consideration, she highlighted the necessity of accommodating multiple mask options in the suit design.

4.2.3.9 FLARE Suit Materials The discussion about suit materials reveals a mix of concerns and suggestions, each centered around the balance between comfort and durability. Astronaut C suggested exploring self-healing materials to minimize risks from punctures, which would enhance the suit's durability. Astronaut A emphasized that the fabric of the suit should strike a balance between comfort and practicality. He highlighted the trade-offs astronauts face on the ISS, such as choosing comfortable cotton trousers that are easily stained versus Teflon trousers that are more

practical but less comfortable. Although the FLARE suit is intended for emergency use and will not be frequently replaced, Astronaut A stressed the need for materials that provide comfort during prolonged wear, especially during Solar Particle Events, while also being easy to clean.

4.2.3.10 Radiation Protection Above Comfort The astronauts unanimously express to prioritize radiation protection over comfort in the suit design, though the tolerance for discomfort decreases when the suit has to be worn over an extended period of time. Astronaut A emphasized that the highest level of protection against radiation should take precedence, even if it sacrifices some comfort features. He noted that although comfort is less important for a survival suit, how long it is worn plays a significant role. Astronauts might be fine with a bulky suit when they are to wear it for a short time, but it could become increasingly restrictive during longer wear. Astronaut D supported this perspective by stating that movement limitations are acceptable for short-term use, arguing that comfort is not a priority in survival situations. Astronaut C added that astronauts would likely adapt to the vest over time, drawing parallels to the 10 kg lead-lined gowns used in surgical settings for radiation protection. He noted that wearing protective gear is manageable, and astronauts might find familiarity with the vest. Additionally, Astronaut A mentioned that while the high water content of the suit contributes to increased momentum, he believes astronauts will be able to manage this effectively.

4.2.4 Key Takeaways from Feedback Testing

To integrate astronaut feedback into FLARE suit design, several key decisions are influenced directly by their insights. In summary, the addition of an undergarment for moisture and heat management was induced by feedback from Astronaut A, whose experience with the Astrorad suit showed the importance of breathable materials like Merino wool to prevent thermal discomfort from sweat buildup. Next, concerns about a one-size-fits-all vest will lead to a more flexible approach in the second FLARE prototype, with a base layer in multiple sizes to be added before the SPE, and colour-coded water bags of different sizes to be added in the Orion module during sheltering. The use of elastic Velcro-based attachments, as Astronaut A and Astronaut B agreed on, help ensure the suit is even more adaptable to various astronaut sizes. Addressing water reclamation and purification needs, Astronaut A and Astronaut D both stressed the importance of developing a suit which is able to reuse waste water in the suit, especially during the early stages of the Lunar Gateway. This will remain a key consideration in further development of the suit.

Operational design improvements, such as reliable anchoring during donning and intuitive, symmetrical design for quick removal, will be guided by the suggestions of Astronaut D, Astronaut A, and Astronaut B. Additional valuable suggestions for the second iteration prototypes include and testing the suit's compactness to ensure ease of movement in confined spaces like the Orion module, and adding practical features like Velcro strips for tool attachment and a dedicated pocket for personal dosimeters to enhance the functionality of the suit. Lastly, astronaut feedback also agreed on the addition of a detachable helmet for head protection, which was already pre-identified as a next step of the FLARE project.

Figure 45: ”End-user” astronaut Matthias Maurer with two FLARE suit 1/4-scaled prototypes at hand.

The goal of astronaut testing was to ensure the suit could withstand the demands of space travel while remaining functional, comfortable, and user-friendly. These sessions allowed to catch potential flaws early and optimize the vest's usability for a range of real-world scenarios the astronauts may face.

As such, astronaut testing is essentially an iterative process of collaboration, which aims to bring designers to a closer understanding of the unique needs of the astronaut end-users. This is an integral part of the systems engineering mindset, and in particular of human-centered design. Human-centered principles were applied throughout this testing phase, focusing on direct collaboration with astronauts rather than viewing them as passive contributors. Not only did their feedback on comfort, flexibility, and practicality inform the design, but their experiences with other suits helped shape the features of FLARE to avoid past mistakes.
And yet, the challenge remains in balancing the variety of preferences — after all, ”If you ask five astronauts for feedback, you can get ten different answers!” (per Samantha Cristoforetti during a feedback session). If balanced right, this diversity of opinions can enrich the iterative process. The end result will be a more adaptable and functional suit, designed with astronaut needs at the forefront.

4.3 Radiation Geant4 Simulation Testing

In this phase of testing, the radiation shielding capabilities of the FLARE vest prototype were evaluated using Geant4 simulations. During the initial development stage of the FLARE vest, Geant4 simulations had already been performed to gain a technical basis for the vest topography, focusing on the different vest thicknesses required for each organ (Section 3.1.3). These simulations were realized by Dr. Sylvain Blunier and its outcome served as the basis for the first FLARE prototype.

To maintain consistency with the earlier simulations, the current testing phase made use of the same environmental setup. In this setup, the human phantom was again chosen as the ICRP-145 meshed phantom, which provides a highly detailed anatomical representation. This phantom was exposed to radiation conditions replicating the October 22, 1989 Solar Particle Event, one of the most significant solar events to be recorded, while placed inside the European-built I-HAB module of the Lunar Gateway. The I-HAB module was again chosen as it provides a realistic spacecraft environment in which astronauts are expected to spend considerable time. The module was again simulated on 1/3-scale as an aluminum cylinder with an external diameter of 1.1 meters, a length of 2 meters, and a thickness of 4 mm.

The simulated radiation environment used to describe the energy spectrum and fluence of protons during the SPE of 22 October 1989, was obtained from the Xapsos et al. (2000) model available on the ESA SPENVIS platform. Protons in this spectrum were modeled to be isotropically beamed onto the human phantom, as to mimick a realistic space radiation environment during a Solar Particle Event, without the protective effects of Earth's magnetic field.

Through simulation, the effective dose reduction of the FLARE radiation shielding vest is found to be **36.7** $\pm$ **4.45 %**, compared to the no-vest shielding case.

Figure 46: 3D simulation setup, including the I-HAB module (dark grey), FLARE prototype vest (blue), and human phantom.

4.4 Stratospheric Balloon Testing

As final testing phase, a stratospheric balloon flight experiment was conducted. Instead of directly flying the FLARE vest into stratospheric environment, a small IoT device called SensorConfetti was tested to evaluate its ability to communicate real-time environmental data to ground [84]. This technology demonstration serves as a precursor to a future campaign in which the FLARE prototype is to be tested alongside a dosimeter, with real-time data transfer enabled by the SensorConfetti device.

The stratospheric balloon testing was organized with the help of the **Royal Meteorological Institute (RMI)** of Belgium, based near its capital in Uccle. The RMI is the main Belgian federal organization dedicated to scientific research in meteorology, known in particular for its ozone research and climate projections (Figure 47) [85].

The RMI is a particularly strong partner due to its decade-long experience in stratospheric balloon flights and as it holds the required licenses to launch in Europe's highly regulated environment for stratospheric flights. The RMI has furthermore decades of experience with weather balloon launches, particularly through its long-running ozonesonde program. In this programme, the RMI has carried out three ozonesonde launches per week since 1969, resulting in the Uccle ozonesonde dataset, one of the most densest and longest-standing records of its kind worldwide [86].

The point of contact during the arrangement and execution of the stratospheric ballooning for this thesis was Roeland Van Malderen, Senior Researcher at Royal Meteorological Institute.

Figure 47: On the left, picture taken from the top of the Royal Meteorological Institute, showing the grass field from where stratospheric balloons are launched. On the right, a stratospheric weather balloon with ozonesonde payload is transfered to the main grass field for launch, a procedure which the RMI has carried out three times a week since the year 1969.

4.4.1 The Aim of Stratospheric Balloon Testing

Stratospheric ballooning is the most cost-effective and accessible method for simulating space environment including a complex radiation spectrum with cosmic radiation.
In addition to the stratosphere as model for space radiation environment, it also holds potential as a model for space's low temperatures and pressures. For example, NASA's Compton Spectrometer and Imager (COSI) mission was first flown on long-duration balloon missions before committing to a satellite mission. The cold temperatures and low pressures in the stratosphere helped simulate the thermal and vacuum conditions of space, allowing scientists to assess how well the instrument would perform in space.
Lastly, stratospheric ballooning has the advantage of allowing for an iterative testing process, meaning instrument performance data from iterative balloon flights can be compared to sequentially optimize the instrument design, and reduce mission risk of a final space mission.

In light of the FLARE project, a stratospheric balloon test was executed on a small IoT device called SensorConfetti to assess and validate its ability to transmit real-time environmental data to the ground. Developed by Jacopo Carra and Diogo Ferreira within the Spaceship EAC student team at the European Astronaut Center, SensorConfetti is originally designed to be deployed across wide areas and to form an adaptive Ad-Hoc network, which is capable of large-scale environmental monitoring and data transmission on the lunar surface (Figure 48) [84]. This stratospheric test is a preparatory step for a future campaign with larger stratospheric balloon, where the FLARE prototype can be tested alongside a dosimeter, for which SensorConfetti enables real-time data transfer.

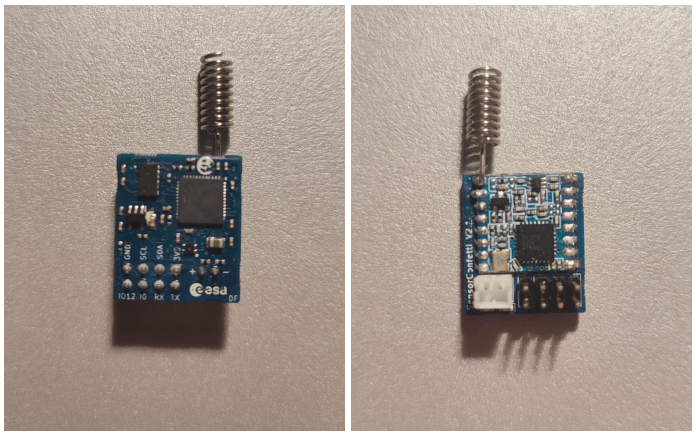

Figure 48: Front and back of the SensorConfetti devices integrated in the stratospheric payload.

The stratospheric balloon testing phase did not directly incorporate the FLARE vest into its mission payload due to the mass constraints posed on the stratospheric balloon payload. For the type weather balloons operated by the Royal Meteorological Institute, a total payload constraint of maximally 2.5 kg exists (including all measurement devices). This is mainly because of (1) more severe authority restrictions for stratospheric balloons with payload above 3 kg, and (2) vastly more expensive ballooning equipment needed for heavier payloads.

This payload mass constraint limited the option to include the FLARE vest directly in the testing phase. The water mass needed for a scientifically valuable test on the stratospheric balloon would exceed this available mass, even under the lowest-volume experimental configuration. Such low-volume setup would involve enclosing a dosimeter within a spherical water shield as mock-up for the FLARE vest, and comparing the mixed-field radiation dose measured inside this sphere to that of a free-floating dosimeter on the same payload. In this way, the experiment would assess how effectively a water shield attenuates the incoming stratospheric mixed-field radiation. To stay within the 2.5 kg payload limit, the maximally possible radius for the water sphere is 7 cm. However, this experiment size is too small to provide meaningful results.

Model calculations suggest a dose increase of about 5% for 5 cm of water shielding and 10% for 10 cm, due to Galactic Cosmic Rays at altitudes of 30-35 km. Data from a previous DLR balloon flight showed a statistical uncertainty of around 4% at the 1-sigma level for a two-hour flight. Although this flight will be at lower magnetic shielding, this effect may be offset by the lower Galactic Cosmic Ray intensity during the solar maximum. Therefore, the effect is expected to be detectable only for the 10 cm shielding, but not for 7 cm. Additionally, the observed effect would differ from the desired outcome for the FLARE vest, as the additional shielding would lead to an increase in dose, rather than a decrease, as expected during a Solar Particle Event. While such experimental measurement is valuable for the improvement of current atmospheric models, it does not directly support the objectives of the FLARE suit.

4.4.2 Characterization of the Stratospheric Radiation Environment

At the time of launch, in September 2024, the solar cycle approaches a maximum, as indicated by the publicly available solar cycle progression data (`https://www.swpc.noaa.gov/products/solar-cycle-progression`). During solar maximum, the increased number of sunspots leads to a significant reduction of approximately 40% in galactic cosmic ray intensity compared to solar minimum conditions, as is shown in Figure 49. Therefore, the galactic cosmic ray intensity is expected to be close to its cycle minimum during the balloon flight experiment [87].

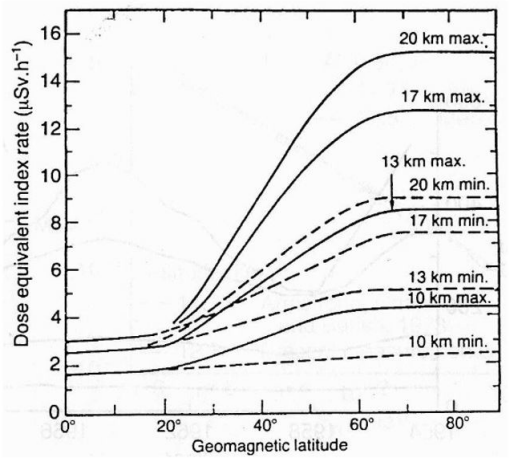

Figure 49: The highest and lowest galactic dose equivalent rates based on geomagnetic latitude at various altitudes. Source: [88]

The website https://predict.sondehub.org/ can be used in the days prior to balloon launch in order to calculate its estimated landing spot and the time of landing. This website operates using most recent European weather forecasts, up to 10 days in advance. For launch at RMI's site in Uccle (Belgium), the following parameters can be used: Latitude/Longitude: 50.797984940591626 / 4.35833785987734, Launch altitude: 100m, Ascent Rate: 5 m/s, Burst/Float Altitude: 30 000m.

The nominal float phase of the weather balloon is approximately two hours, reaching an altitude of about 30 km. Based on Figure 49, the total dose equivalent rate during the float phase is expected to range between 9 and 16 µSv/h. This corresponds to an estimated total dose equivalent of 18-32 µSv over the course of a stratospheric flight.

4.4.3 Summary of the Experimental Testing Activities

During the stratospheric balloon flight experiment, one SensorConfetti device was positioned in a 3D-printed holder on the outside of a Styrofoam box. This device was programmed to send a message downward every second to another identical device on ground. This device on ground serves to collect these messages and check if the first device in stratospheric environment is operating as intended. The total experimental payload includes:

- 1 SensorConfetti device: 23 g
- 1 Space Camera: 70 g (https://www.stratoflights.com/en/shop/space-cam/)
- 1 Battery pack: 88 g (https://www.stratoflights.com/en/shop/batterypack/)
- 1 Styrofoam box

Figure 50: On the left, the SensorConfetti payload is shown before flight, after attachment to the ozonesonde payload of the RMI (white box). On the right, the flight path with altitude label of the payload is shown. The stratospheric balloon was launched in Uccle and landed near the city of Venlo.

The total payload of SensorConfetti weighed 312.2 grams and was attached before flight to the ozone radiosonde payload of the Royal Meteorological Institute, as is shown in the left picture of Figure 50. The flight trajectory is shown on the right of the same Figure 50, visualizing a flight path from its launch site in Uccle (Belgium) to a field near the city of Venlo (the Netherlands).

During flight, the device has been exposed to harsh conditions: risks include potential radiation interference, temperature or variations in pressure, data loss due to EMF interference in the signal path, or the devices being too far away to communicate effectively. This allows the stratosphere as an ideal analogue to verify the robustness of SensorConfetti devices. Furthermore, it allows to evaluate the devices' communication range in an open environment free from obstructions.

The balloon reached an altitude of **34 064 m** and total flight time of **2:36:03 h**, with maximal speed of 180 km/h measured at 30 010 m altitude an and average ascent speed of **5.03 m/s** and decent speed of 12.25 m/s. Figure 51 shows the altitude, environmental and sensor profiles in greater detail. More characteristics of the stratospheric flight can be found in the archives of the websites `https://radiosondy.info` and `https://sondehub.org`, using the flight identifier 'V3641576'.

Figure 51: On the top left, the altitude profile over time of the stratospheric flight is shown. On the top right, the air humidity, external temperature and atmospheric pressure profiles are shown. On the bottom left, the ascent speed profile is shown. The sharp drop around 13:20 corresponds to the burst of the balloon and the period of free fall that follows. As the parachute opens, the descent speed stabilizes again. On the bottom right, the ascent speed is shown to be around 5 m/s during the ascent of the balloon. Source: Sondehub.

Figure 52: A picture taken near peak altitude ($\approx$ 30 km) of the SensorConfetti device with stratosphere background.

4.4.4 Key Takeaways from Stratospheric Testing

The stratospheric balloon flight demonstrated the effectiveness of SensorConfetti as a reliable data-transfer device, capable of mid- to long-range communication, even under the challenging conditions of the stratosphere. The device achieved a communication range 2–3 times longer than originally estimated. For the in-depth analysis of the SensorConfetti's performance in this stratospheric experiment, is referred to the dedicated study of Diogo et al. in [84].

Beyond its technological achievements, the flight also captured remarkable video footage viewing Earth from the stratosphere, as shown in Figure 52. The complete video of this stratospheric balloon flight can be viewed at `https://www.youtube.com/watch?v=qw5uFksBiBY`.

This experiment is a valuable step for the FLARE project, as SensorConfetti helps enable future stratospheric testing of the FLARE suit in a larger stratospheric balloon. In such upcoming missions, the FLARE prototype is to be tested in a payload including dosimeters, with real-time data transfer provided by SensorConfetti. Such mission will give a cost-effective way to simulate space conditions, including a mixed-field radiation with GCRs, low temperatures, and pressures, and allow for potential iterative testing to optimize design and reduce mission risks.

5 Conclusion

The FLARE suit has been developed in the context of this thesis within Spaceship EAC, a research team of ESA based in the European Astronaut Center which is actively involved in low-level technology development and concept demonstration. The FLARE suit is a personal radiation shielding system designed for wearable use by astronauts within intravehicular microgravity environment. Its primary purpose is to shield astronauts from high-energy charged particles during Solar Particle Events (SPEs), which are sporadic bursts of radiation of which on average 3 to 5 per year are sufficiently intense to crew health to impact space missions. Potential risks include acute radiation sickness, increased cancer risk, and serious internal organ damage.

The topic of radiation shielding has become increasingly pressing among international space agencies in the latest years. In the past decades, crewed missions were confined to spacecraft in Low Earth Orbit, which on a radiation-level enjoys the natural protection against charged particles by Earth's magnetosphere. However, as international efforts shift towards lunar exploration -through the planned Lunar Gateway Program, Artemis Program, and the Chinese Lunar Exploration Program- the risk of Solar Particle Events resurfaces, after it had largely been set aside when the final Apollo mission last traveled beyond the magnetosphere in 1975. The Apollo missions typically lasted only a few days and, by good fortune, where never impacted by an SPE. However, with planned missions spanning months or even years, the risks of SPEs will this time reoccur with a certainty to impact. To date, no appropriate answer has been developed to withstand their health impact on crew.

The FLARE project is a practical solution to help close the gap in current radiation protection technology. The suit is characterized by the use of water as primary shielding component, which it uses in an intriguing topographic design. Shielding was concentrated on the torso area, particularly over vital organs, which experience the most biological impact from radiation exposure.

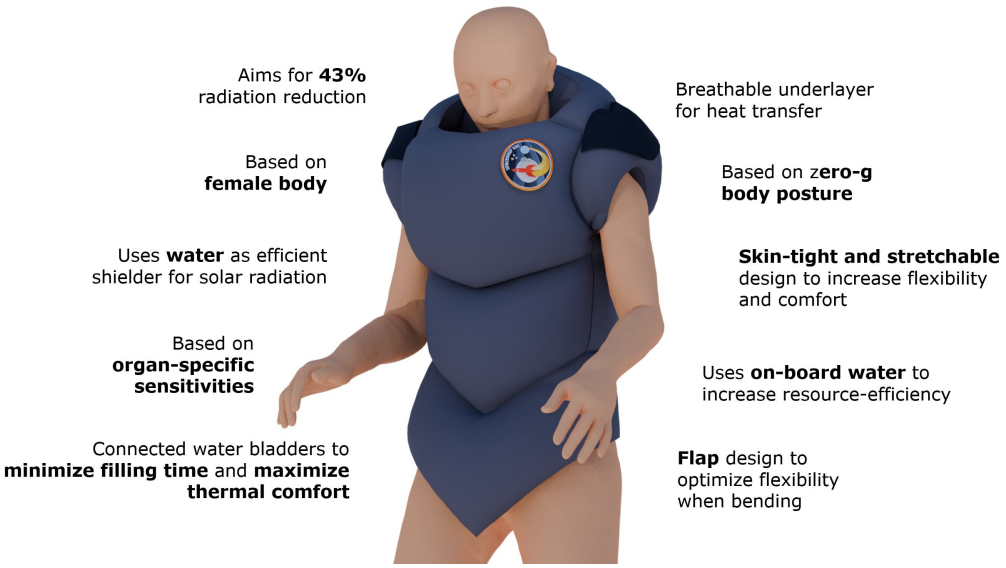

The FLARE first prototype weighs 37 kg when fully equipped and consists of 36 L water contained in interconnected water bags with circuitry and valves. The vest has launch mass of approximately 964 g, which includes only the unfilled garment. The water used is onboard water which can originate from either condensate water, drinking water, or waste water. During a large SPE, the suit reduces the effective dose to the astronaut by 36 % ($\pm$ 4.5 %), which reduces the chances of induced cancer considerably and also immediate effects such as cardiovascular disease and sterility.

Radiation testing at the HollandPTC accelerator facility has confirmed that water and the solid outer layer of FLARE are interchangeable, meaning that the simulation-based water thickness can be partially substituted by the solid material without significant differences in radiation protection. This finding allows to substitute for solid material in the suit areas most prone to external puncture risk.

Two state-of-the-art vest technologies have previously been developed to protect against Solar Particle Events. These include the PERSEO (Italian Space Agency) and Astrorad (Stemrad company) vests. Compared to these vests, FLARE's water-based design enables more flexibility and adaptability for diverse astronaut body types. A breathable undergarment to the suit furthermore overcomes reported issues regarding thermal discomfort for both PERSEO and Astrorad. Astronaut feedback testing confirmed a positive outlook of the intended system for comfort, flexibility, and user-friendliness.

Radiation simulation testing in Geant4 has confirmed that the radiation shielding capability of FLARE (36 $\pm$ 4.5 %) is promising for future missions beyond Earth's magnetosphere. Its capability cannot be compared to the Astrorad vest, since the shielding capability of Astrorad has not yet been publicly reported using dose quantities that can be compared. For the PERSEO vest, only the capability to shield blood-forming organs has been reported. However, since the FLARE suit contains more water (36 liters compared to 22 liters in PERSEO) and has an organ-sensitive optimized design, the radiation shielding capability of FLARE is expected to be higher compared to that of PERSEO.

Overall, the FLARE suit has been developed as a personal radiation shielding system to address the risks posed by Solar Particle Events during long-duration space missions. The suit uses 36 liters of onboard water distributed in a topographic design, with shielding concentrated over vital organs to reduce the effective radiation dose by 36 $\pm$ 4.5%. Comparisons with existing solutions, such as PERSEO and Astrorad, show the FLARE suit's potential for improved operational flexibility and comfort. Accelerator testing has confirmed the interchangeability of water and solid outer layers, enabling material adaptations for puncture-prone areas. While current results are promising, further work is required to validate its performance through full-scale radiation testing, microgravity trials, and iterative design improvements.

6 Recommendations

Future iterations of the FLARE suit should focus on enhancing its radiation shielding capabilities, aiming to improve shielding beyond the current 36 $\pm$ 4.5% dose reduction. This can be done by optimizing the shielding topography, i.e. redistributing water around the body to maximize protection, and by researching alternative materials with superior shielding effectiveness.
In order to quantify and validate the performance of different vest alternatives, iterative radiation simulation testing using Geant4 and proton accelerator experiments at facilities such as HollandPTC will be necessary at each or most iterations.
To complement modeling and accelerator testing, the FLARE vest could be integrated into a stratospheric balloon experiment equipped with dosimeters and real-time monitoring systems such as SensorConfetti. This approach has the advantage of simulating mixed-field radiation conditions, including Galactic Cosmic Rays. Stratospheric testing will present logistical challenges, including payload integration and compliance with atmospheric launch regulations, but the data obtained would provide value as a complement to proton accelerator testing and Geant4 modeling in the assessment of the vest's shielding capabilities.

In addition to improving radiation shielding, future work should focus on optimizing flexibility, thermal comfort, and operational efficiency. To this aim, advanced design concepts explored within this thesis such as dragon-scale patterns and D3O patches require more research and prototyping to assess whether their integration into the suit is feasible.
In addition to materiality research, it will be important to transition from the current 1/4-scale model to a full-scale prototype with functional water bladders and advanced layering. Full-scale testing will allow for optimization of the suit's attachment mechanisms and the overall fit. In addition, full-scale flexibility testing includes assessing whether the suit restricts necessary joint mobility during emergency activities. This assessment may be performed on ground, but is ideally also performed in microgravity environment, such as during a parabolic flight campaign. Apart from flexibility, also the donning and filling procedure can be verified under these circumstances, as well as the vest's ability to meet the targeted 30-minute deployment time during SPE events. During full-scale prototype testing phases, realistic operational scenarios and astronaut feedback will be of large importance.

A final recommendation for future work involves addressing the logistical requirements for the vest's use in the Lunar Gateway. This includes studying the feasibility of repurposing onboard water resources, such as waste water or condensate water, for filling the suit. In later phases, water analysis will be important to confirm water quality after use in the suit and to evaluate potential material degradation from prolonged water exposure. A structured systems engineering workflow can help quantify the suit's usage cycle and align it with Lunar Gateway protocols. Additionally, it will be important to stay informed about updates to the Lunar Gateway mission procedures to maintain the vest's operational relevance.

Figure Credits

Several figures in this thesis were created with the expertise of Noora Archer, a Young Graduate Trainee at ESA in virtual design with particular background in virtual fashion design. Figures marked with a † symbol were created or significantly enhanced by her. Her work helped make the technical aspects of FLARE easier to understand and present. For further information regarding the visualizations, Noora can be contacted at noora.archer@esa.int.

References

[1] National Research Council, Division on Engineering, Physical Sciences, Aeronautics, Space Engineering Board, and Committee on the Evaluation of Radiation Shielding for Space Exploration. Managing space radiation risk in the new era of space exploration. National Academies Press, 2008.

[2] Günther Reitz and Christine E Hellweg. Space radiation and its biological effects. In Applications of Laser-Driven Particle Acceleration, pages 217–236. CRC Press, 2018.

[3] Marco Vuolo, Giorgio Baiocco, Martina Giraudo, Cesare Lobascio, Tom Gheysens, Andrea Ottolenghi, Giorgio Baiocco, Andrea Ottolenghi, and Leopold Summerer. Perseo: Personal radiation shielding for interplanetary missions. Technical report, ESA, 2015.

[4] G De Angelis, FF Badavi, JM Clem, SR Blattnig, MS Clowdsley, JE Nealy, RK Tripathi, and JW Wilson. Modeling of the lunar radiation environment. Nuclear Physics B-Proceedings Supplements, 166:169–183, 2007.

[5] Gregory A Nelson. Space radiation and human exposures, a primer. Radiation research, 185(4):349–358, 2016.

[6] Shaowen Hu. Solar particle events and radiation exposure in space. NASA Space Radiation Program Element, Human Research Program, pages 1–15, 2017.

[7] Sébastien Ruhlmann. The flare suit: A protection against solar radiation in space, 2019.

[8] Guenther Reitz, Thomas Berger, Pawel Bilski, Rainer Facius, Michael Hajek, Vladislav Petrov, Monika Puchalska, Dazhuang Zhou, Johannes Bossler, Yury Akatov, et al. Astronaut's organ doses inferred from measurements in a human phantom outside the international space station. Radiation research, 171(2):225–235, 2009.

[9] Marco Durante and Francis A Cucinotta. Physical basis of radiation protection in space travel. Reviews of modern physics, 83(4):1245, 2011.

[10] Shaowen Hu, Myung-Hee Y Kim, Gene E McClellan, and Francis A Cucinotta. Modeling the acute health effects of astronauts from exposure to large solar particle events. Health physics, 96(4):465–476, 2009.

[11] Francis A Cucinotta and Marco Durante. Cancer risk from exposure to galactic cosmic rays: implications for space exploration by human beings. The lancet oncology, 7(5):431–435, 2006.

[12] FA Cucinotta, FK Manuel, J Jones, G Iszard, J Murrey, B Djojonegro, and M Wear. Space radiation and cataracts in astronauts. Radiation research, 156(5):460–466, 2001.

[13] D A Schauer and O W Linton. Ncrp report no. 160, ionizing radiation exposure of the population of the united states, medical exposure—are we doing less with more, and is there a role for health physicists? Health physics, 97(1):1–5, 2009.

[14] Human Integration Design Handbook (NASA/SP-2010-3407/REV1), 2022.

[15] Lawrence W Townsend, Judy L Shinn, and John W Wilson. Interplanetary crew exposure estimates for the august 1972 and october 1989 solar particle events. Radiation research, 126(1):108–110, 1991.

[16] Francis A Cucinotta, Honglu Wu, Mark R Shavers, and Kerry George. Radiation dosimetry and biophysical models of space radiation effects. Gravitational and Space Biology, 16(2):11–19, 2003.

[17] Robert A English, Richard E Benson, J Vernon Bailey, and Charles M Barnes. Apollo experience report: Protection against radiation. Technical report, NASA, 1973.

[18] Christine E Hellweg and Christa Baumstark-Khan. Getting ready for the manned mission to mars: the astronauts' risk from space radiation. Naturwissenschaften, 94:517–526, 2007.

[19] Joseph F Weiss and Michael R Landauer. Protection against ionizing radiation by antioxidant nutrients and phytochemicals. Toxicology, 189(1-2):1–20, 2003.

[20] Alessandra Menicucci. Radiation environment and effects in planetary exploration, 2023. TU Delft, Planetary Sciences II class, PowerPoint presentation.

[21] SA Washburn, SR Blattnig, RC Singleterry, and SC Westover. Active magnetic radiation shielding system analysis and key technologies. Life sciences in space research, 4:22–34, 2015.

[22] Francis A Cucinotta, Myung-Hee Y Kim, and Lori J Chappell. Evaluating shielding approaches to reduce space radiation cancer risks. NASA Technical Memorandum, 217361, 2012.

[23] CGTN. Mars astronaut radiation shield set for moon mission trial. Video Presentation, March 5th, 2017.

[24] G Baiocco, M Giraudo, L Bocchini, S Barbieri, I Locantore, E Brussolo, D Giacosa, L Meucci, S Steffenino, A Ballario, et al. A water-filled garment to protect astronauts during interplanetary missions tested on board the iss. Life sciences in space research, 18:1–11, 2018.

[25] Saralyn Mark, Graham BI Scott, Dorit B Donoviel, Lauren B Leveton, Erin Mahoney, John B Charles, and Bette Siegel. The impact of sex and gender on adaptation to space: executive summary. Journal of women's health, 23(11):941–947, 2014.

[26] C.C. Ricks, R.C. & Lushbaugh. Radiosensitivity of man: Based on retrospective evaluations of therapeutic and accidental total-body irradiation. Final Unclassified Report. Ridge Associated Universities, 1975.

[27] Marjan Boerma, Vijayalakshmi Sridharan, Xiao-Wen Mao, Gregory A Nelson, Amrita K Cheema, Igor Koturbash, Sharda P Singh, Alan J Tackett, and Martin Hauer-Jensen. Effects of ionizing radiation on the heart. Mutation Research/Reviews in Mutation Research, 770:319–327, 2016.

[28] Scott A England, Elizabeth A Benson, and Sudhakar L Rajulu. Functional mobility testing: Quantification of functionally utilized mobility among unsuited and suited subjects. Technical report, NASA, 2010.

[29] Lisa O Rippy. Nasa human systems integration handbook. Technical report, NASA, 2021.

[30] Engineering Toolbox. Metabolic heat of persons. Website. Accessed on 13/5/2024.

[31] ECSS-E-ST-10-02C. Verification. tech. rep. european cooperation for space standardization, 2018.

[32] ECSS-E-ST-10-03C. Testing. tech. rep. european cooperation for space standardization, 2022.

[33] James Richard Wertz, David F Everett, and Jeffery John Puschell. Space mission engineering: the new SMAD. Microcosm Press, 2011, 2011.

[34] Blender Foundation. Blender - a 3d modelling and rendering package. `https://www.blender.org/`, 2023. Version 3.6.2, Open Source Software.

[35] National Aeronautics and Space Administration (NASA). Lunar electric rover concept. PDF document, 2008. NASA Facts, NF-2008-10-464-HQ, Universities Space Research Association, Lunar and Planetary Institute.

[36] Guy André Boy. Human-centered design of complex systems: An experience-based approach. Design Science, 3:e8, 2017.

[37] Adult reference computational phantoms. icrp publication 110., 2009.

[38] Radiological Protection. The 1990 recommendations of the international commission on radiological protection. icrp publication 60. Ann ICRP, 21(1-3):2, 1990.

[39] Radiological Protection. The 2007 recommendations of the international commission on radiological protection. icrp publication 103. Ann ICRP, 37(2-4):2, 2007.

[40] European Space Agency. Spenvis. `https://www.spenvis.oma.be/`. Accessed: 2024-08-07.

[41] S. Agostinelli, J. Allison, K. Amako, J. Apostolakis, H. Araujo, P. Arce, M. Asai, et al. Geant4 - a simulation toolkit. Nuclear Instruments and Methods in Physics Research Section A: Accelerators, Spectrometers, Detectors and Associated Equipment, 506(3):250–303, 2003.

[42] Marco Vuolo, Martina Giraudo, R Musenich, V Calvelli, F Ambroglini, WJ Burger, and R Battiston. Monte carlo simulations for the space radiation superconducting shield project (sr2s). Life sciences in space research, 8:22–29, 2016.

[43] ICRP. Adult mesh-type reference computational phantoms. Annals of the ICRP, 49(3), 2020.

[44] Han Sung Kim, Yeon Soo Yeom, Thang Tat Nguyen, Chansoo Choi, Min Cheol Han, Jai Ki Lee, Chan Hyeong Kim, Maria Zankl, Nina Petoussi-Henss, Wesley E Bolch, et al. Inclusion of thin target and source regions in alimentary and respiratory tract systems of mesh-type icrp adult reference phantoms. Physics in Medicine & Biology, 62(6):2132, 2017.

[45] Arcangela Maldera, Marina Sutto, Alessandra Gaeta, Michele Maddalo, PE Colombo, and Alberto Torresin. Estimate organ dose from ct examination: a software comparison. Physica Medica: European Journal of Medical Physics, 32:82, 2016.

[46] M Zankl, Janine Becker, Choonsik Lee, Wesley Emmett Bolch, Yeon Soo Yeom, and Chan Hyeong Kim. Computational phantoms, icrp/icru, and further developments. Annals of the ICRP, 47(3-4):35–44, 2018.

[47] Michael Anthony Xapsos, JL Barth, EG Stassinopoulos, Edward A Burke, and GB Gee. Space environment effects: Model for emission of solar protons (esp): Cumulative and worst case event fluences. Technical report, Goddard Space Flight Center, 1999.

[48] Thom Richardson. The introduction of plate armour in medieval europe. Royal armouries yearbook, 2(1):40–45, 1997.

[49] Joe Gieck and Frank C McCue III. Fitting of protective football equipment. The American Journal of Sports Medicine, 8(3):192–196, 1980.

[50] Bin Wang, Wen Yang, Vincent R Sherman, and Marc A Meyers. Pangolin armor: overlapping, structure, and mechanical properties of the keratinous scales. Acta biomaterialia, 41:60–74, 2016.

[51] Prashant Rawat, Deju Zhu, Md Zillur Rahman, and Francois Barthelat. Structural and mechanical properties of fish scales for the bio-inspired design of flexible body armors: A review. Acta biomaterialia, 121:41–67, 2021.

[52] Praburaj Venkatraman and David Tyler. Applications of compression sportswear. Materials and technology for sportswear and performance apparel, 195, 2015.

[53] Praburaj Venkatraman and David Tyler. Applications of compression sportswear. Materials and technology for sportswear and performance apparel, 195, 2015.

[54] Dava J Newman, Marita Canina, and Guillermo L Trotti. Revolutionary design for astronaut exploration—beyond the bio-suit system. In AIP Conference Proceedings, volume 880, pages 975–986. American Institute of Physics, 2007.

[55] Pierre J Bertrand, Allison Anderson, Alexandra Hilbert, and Dava J Newman. Feasibility of spacesuit kinematics and human-suit interactions. 44th International Conference on Environmental Systems, 2014.

[56] Brand Norman Griffin. Design guide: the influence of zero-g and acceleration on the human factors of spacecraft design. NASA Johnson Space Centre, 1978.

[57] Frances E Mount, Mihriban Whitmore, and Sheryl L Stealey. Evaluation of neutral body posture on shuttle mission sts-57 (spacehab-1). Technical report, NASA, 2003.

[58] K Han Kim, Karen S Young, and Sudhakar L Rajulu. Neutral body posture in spaceflight. In Proceedings of the Human Factors and Ergonomics Society Annual Meeting, volume 63, pages 992–996. SAGE Publications Sage CA: Los Angeles, CA, 2019.

[59] David A Holmes. Waterproof breathable fabrics. Handbook of technical textiles, 12:282, 2000.

[60] Yadie Yang and Hong Hu. Spacer fabric-based exuding wound dressing–part i: Structural design, fabrication and property evaluation of spacer fabrics. Textile Research Journal, 87(12):1469–1480, 2017.

[61] Yanping Liu and Hong Hu. Compression property and air permeability of weft-knitted spacer fabrics. The Journal of the Textile Institute, 102(4):366–372, 2011.

[62] Yanping Liu, Hong Hu, Li Zhao, and Hairu Long. Compression behavior of warp-knitted spacer fabrics for cushioning applications. Textile Research Journal, 82(1):11–20, 2012.

[63] VK Kothari. Polyester and polyamide fibres–apparel applications. In Polyesters and polyamides, pages 419–440. Elsevier, 2008.

[64] Dana Křemenáková, Jiří Militkỳ, Mohanapriya Venkataraman, and Rajesh Mishra. Thermal insulation and porosity—from macro-to nanoscale. Thermal Physics and Thermal Analysis: From Macro to Micro, Highlighting Thermodynamics, Kinetics and Nanomaterials, pages 425–448, 2017.

[65] Mohanapriya Venkataraman, R Mishra, and J Militky. Comparative analysis of high performance thermal insulation materials. J. Text. Eng. Fash. Technol, 2(3):401–409, 2017.

[66] Sibel Kaplan and Bilge Yilmaz. Thermal comfort performances of double-face knitted insulation fabrics. Fibers and Polymers, pages 1–9, 2022.

[67] Wang Wei. A summary of the research status and development trends of protective clothing for the elderly. In Journal of Physics: Conference Series, volume 1790, page 012024. IOP Publishing, 2021.

[68] Nihal Sarier and Emel Onder. The manufacture of microencapsulated phase change materials suitable for the design of thermally enhanced fabrics. Thermochimica acta, 452(2):149–160, 2007.

[69] Dounia Benmoussa, Kolos Molnar, Hassan Hannache, and Omar Cherkaoui. Development of thermo-regulating fabric using microcapsules of phase change material. Molecular Crystals and Liquid Crystals, 627(1):163–169, 2016.

[70] Understanding spacer fabrics: Breathability, cushioning, and more. Monofabrics Blog, 2020. Accessed: 2024-10-21.

[71] Xiuming Qin, Bo Wang, Xin Zhang, Yutao Shi, Shihang Ye, Yuezhan Feng, Chuntai Liu, and Changyu Shen. Superelastic and durable hierarchical porous thermoplastic polyurethane monolith with excellent hydrophobicity for highly efficient oil/water separation. Industrial & Engineering Chemistry Research, 58(44):20291–20299, 2019.

[72] A Boubakri, Nader Haddar, K Elleuch, and Yves Bienvenu. Impact of aging conditions on mechanical properties of thermoplastic polyurethane. Materials & Design, 31(9):4194–4201, 2010.

[73] Yadie Yang and Hong Hu. Spacer fabric-based exuding wound dressing–part i: Structural design, fabrication and property evaluation of spacer fabrics. Textile Research Journal, 87(12):1469–1480, 2017.

[74] Sayyed Bijan Jia, Mohammad Hadi Hadizadeh, Ali Asghar Mowlavi, and Mahdy Ebrahimi Loushab. Evaluation of energy deposition and secondary particle production in proton therapy of brain using a slab head phantom. Reports of practical oncology and radiotherapy, 19(6):376–384, 2014.

[75] Martina Giraudo, Christoph Schuy, Uli Weber, Marta Rovituso, Giovanni Santin, John W Norbury, Emanuele Tracino, Alessandra Menicucci, Luca Bocchini, Cesare Lobascio, et al. Accelerator-based tests of shielding effectiveness of different materials and multilayers using high-energy light and heavy ions. Radiation Research, 190(5):526–537, 2018.

[76] Peter Kuess, Nina Sejkora, Anna Klampfer, Sarah Madlener, Peter Weiss, Sibylle Schmied, Dietmar Georg, Seda Özdemir-Fritz, Gernot Grömer, and Albert Hirtl. Characterising potential space suit textiles in proton beams using radiotherapy-based dosimetry. Advances in Space Research, 70(7):1925–1934, 2022.

[77] Celebrity F Groenendijk, Marta Rovituso, Danny Lathouwers, and Jeremy MC Brown. A geant4 based simulation platform of the hollandptc r&d proton beamline for radiobiological studies. Physica Medica, 112:102643, 2023.

[78] Rui Zhang and Wayne D Newhauser. Calculation of water equivalent thickness of materials of arbitrary density, elemental composition and thickness in proton beam irradiation. Physics in Medicine & Biology, 54(6):1383, 2009.

[79] Wayne Newhauser, Jonas Fontenot, Nicholas Koch, Lei Dong, Andrew Lee, Yuanshui Zheng, Laurie Waters, and Radhe Mohan. Monte carlo simulations of the dosimetric impact of radiopaque fiducial markers for proton radiotherapy of the prostate. Physics in Medicine & Biology, 52(11):2937, 2007.

[80] Steven Michiels, Ana Maria Barragán, Kevin Souris, Kenneth Poels, Wouter Crijns, John A Lee, Edmond Sterpin, Sandra Nuyts, Karin Haustermans, and Tom Depuydt. Patient-specific bolus for range shifter air gap reduction in intensity-modulated proton therapy of head-and-neck cancer studied with monte carlo based plan optimization. Radiotherapy and Oncology, 128(1):161–166, 2018.

[81] S Handley, Y Chen, and S Ahmad. Su-gg-t-430: Normalized bragg peak curves for various proton energies in a cylindrical water phantom: A simulation with mcnpx and geant4 monte carlo codes. Medical Physics, 37(6Part22):3285–3285, 2010.

[82] Marco Vuolo, Giorgio Baiocco, Sofia Barbieri, L Bocchini, Martina Giraudo, Tom Gheysens, C Lobascio, and A Ottolenghi. Exploring innovative radiation shielding approaches in space:

a material and design study for a wearable radiation protection spacesuit. Life Sciences in space research, 15:69–78, 2017.

[83] Genevation Aircraft Ltd. Innovative structural material research and manufacturing study for passive radiation protection for future space mission tn2 based on ccn1 (tn7). 2024.

[84] A. Cowley D. Ferreira, J. Carra. Sensor confetti: A compact iot device for lunar large-scale environmental monitoring and data transmission. European Astronaut Centre, European Space Agency (ESA), 2024.

[85] Royal Meteorological Institute of Belgium. Research at rmi, 2024. Accessed: 2024-11-28.

[86] Roeland Van Malderen, Dirk De Muer, Hugo De Backer, Deniz Poyraz, Willem W Verstraeten, Veerle De Bock, Andy Delcloo, Alexander Mangold, Quentin Laffineur, Marc Allaart, et al. 50 years of balloon-borne ozone profile measurements at uccle, belgium: short history, scientific relevance and achievements in understanding the vertical ozone distribution. Atmospheric Chemistry and Physics Discussions, 2020:1–38, 2020.

[87] Balázs Zábori, Attila Hirn, Tamás Pázmándi, Péter Szántó, Sándor Deme, István Apáthy, Antal Csoke, and László Bodnár. Environmental dosimetry with the pille tl space dosimetry system during the bexus-12 stratospheric balloon flight. In 13th International Congress of the International Radiation Protection Association Conference Paper, Paper P, volume 2, page 231, 2012.

[88] Advisory Committee for Radiation Biology Aspects of the SST. Final report, cosmic radiation exposure in supersonic and subsonic flight. Aviat. Space Environ. Med., 53:808–10 817, 1982.